Aeromagnetic Interpretation and Petroleum Prospectivity Assessment - Offshore Canning Basin, Western Australia

For: Geoscience Australia

Date: February 2008

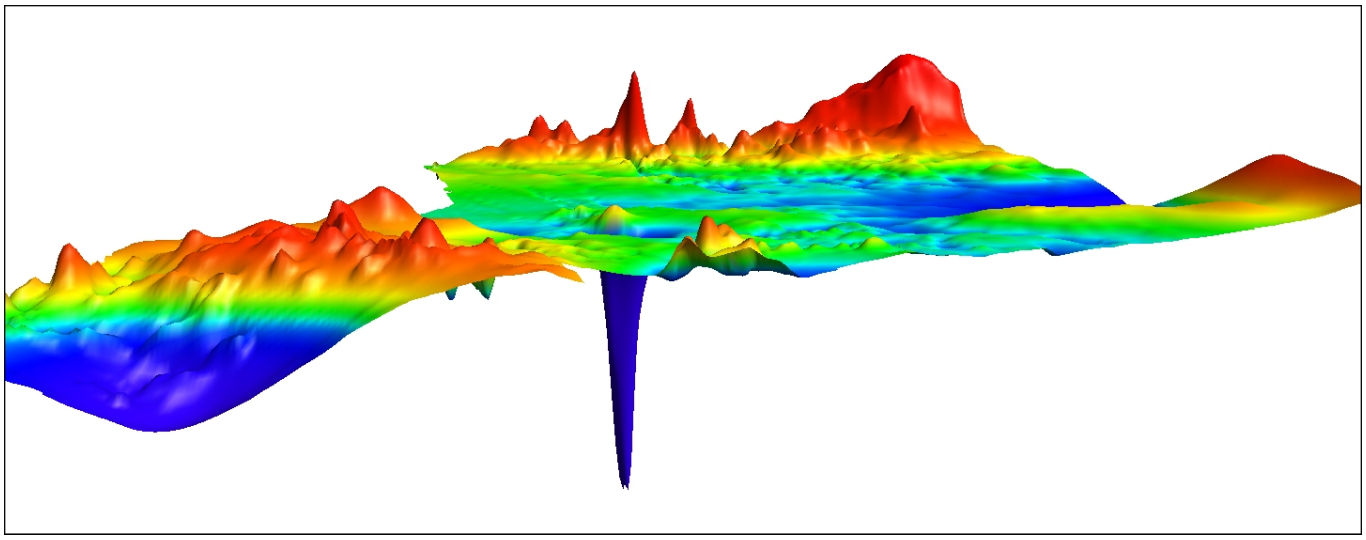

encom advanced realities

Head Office
Level 1/123 Walker Street
North Sydney NSW 2060 Australia
T +61 2 9957 4117 F+61 2 9922 6141

Melbourne
Level 1/469 Glenhuntly Road
Elsternwick VIC 3185 Australia
T +61 3 9523 0033 F+61 3 9523 2296

Perth
Level 2/1050 Hay Street
Perth WA 6005 Australia
T +61 8 9226 0101 F+61 8 9226 0102

Europe
59-60 Thames Street, Berkshire
Windsor SL4 1TX United Kingdom
T +44 1753 272332 F+44 1753 272334

Report Prepared by:

Clive Foss
Principal Consultant
Encom Technology
Level 1/123 Walker St
North Sydney NSW 2060 Australia
T +61 2 9957 4117
Email: Clive.Foss@encom.com.au

Wayne Stasinowsky
Manager Geophysical Research
Encom Technology
Level 1/123 Walker St
North Sydney NSW 2060 Australia
T +61 2 9957 4117
Email: Wayne.Stasinowsky@encom.com.au

Vic Ziolkowski
Oil Exploration Consultants
PO Box 584 Kenmore
QLD Australia 4069
T: +61 7 33742470
Email: wrenworth@bigpond.com

Disclaimer

Magnetic and gravity models indicating depth and position should not be used as absolute solutions. Rather they should be viewed as one of many possible solutions that could fit the data.

The seismic interpretation was performed on limited regional data and its accuracy cannot be assured. The illustrated potential play types are not intended to represent definitive leads or prospects and Encom Technology Pty Limited and OEC Pty Ltd accept no liability in any case where these data are otherwise misconstrued.

NOTE: Many of the figures in this report may be difficult to read at normal scale (100%) but have been provided at higher resolution so that they can be zoomed to a higher scale (200%). To reduce file size, many of the seismic figures have been saved as 8-bit figures which gave a slight degradation of the colour depth.

Table of Contents

Table of Figures

Summary

Geoscience Australia has acquired new high-resolution magnetic data across current Commonwealth offshore Acreage Release Areas W07-12 to 15 in the Offshore Canning Basin, Western Australia. This data was released in October 2007 via Geoscience Australia's geophysical online data delivery system (GADDS). Bids for the release areas close on 17 April 2008.

The expectation for the magnetic field study was that anomalies would predominantly be sourced from basement, and that interpretation of the magnetic field data would provide extrapolation of the basement surface away from those regions where it is reliably imaged on seismic.

However, it has been found that much of the magnetic signal is generated by intrusives within the sedimentary section, many of which are evident on seismic sections and most of which terminate at or below the mapped Late Permian Bedout unconformity. Across much of the survey area these shallow-sourced anomalies mask magnetic field variations from deeper basement.

In some locations very deep magnetic bodies down to 11km are evident, mainly in the western extent of the area. These have been interpreted as coming from deep basement. This is not readily confirmed on the seismic because at these locations basement is below the level reliably imaged by the seismic data.

In many cases faults mapped from the seismic data terminate against anomalies and dislocations mapped from the magnetic field data. In these cases the magnetic features appear to map faults which may not be recognised as significant in interpretation of the sparse seismic coverage.

From the pattern of the faulting it appears that many of these faults may have predominant strike-slip movement, which although consistent with the fault expressions evident on the seismic, would not have been initially interpreted from the sparse 2D seismic coverage alone.

From the interpretation of the seismic and well data, there are a variety of play types evident. Intense structuring in the Late Permian (Bedout unconformity) and Triassic (Fitzroy Movement) has resulted in the formation of large scale folding, inversion and wrenching of the Palaeozoic strata, resulting in numerous structural plays in the Early Permian/Late Carboniferous clastics and Devonian carbonates. Other play types include Devonian carbonate reefs and siliciclastic alluvial fans and fan deltas. In the outboard areas onlapping Mesozoic strata provide opportunity for stratigraphic plays. Early Cretaceous submarine fans also appear to be present in these areas.

These release areas occur in relatively shallow water.

Together, the new magnetic data and interpreted seismic data provide a good indication of the structures within the areas, and interpretation of the two data sets has proven to be complementary to help evaluate the petroleum prospectivity of the release areas.

Introduction

Geoscience Australia has acquired new high-resolution magnetic data across current Commonwealth offshore Acreage Release Areas W07-12 to 15 in the Offshore Canning Basin, Western Australia (see Figure 1). This data was released in October 2007 via Geoscience Australia's geophysical online data delivery system (GADDS).

Bids for the release areas close on 17 April 2008.

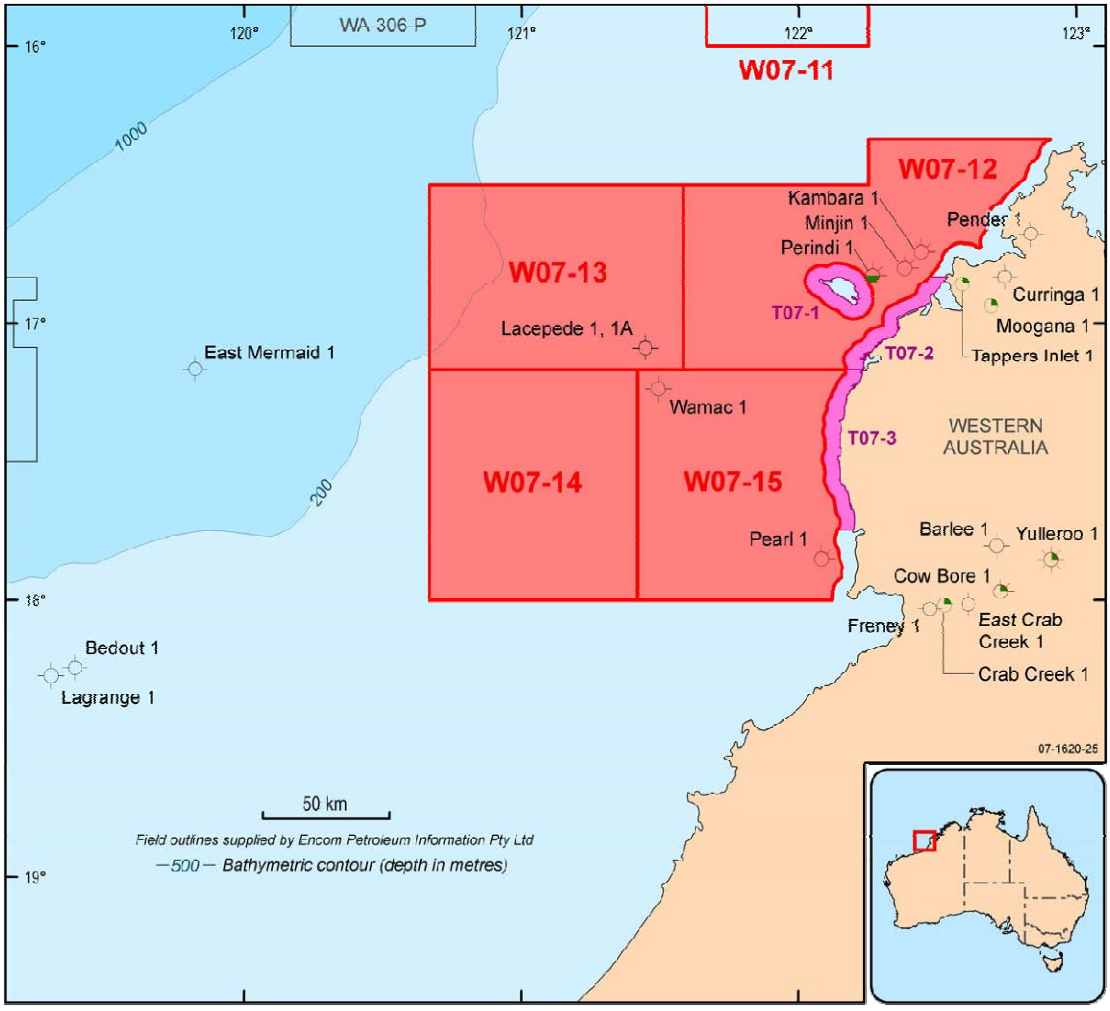

Figure 1 Location of Release Areas W07-12 to W07-15

To assist in assessment of this acreage, Geoscience Australia, under a contract awarded to Encom Technology Pty Limited, has undertaken an integrated magnetic and regional seismic interpretation of these areas

The study is based on interpretation of the new (2007) high-resolution magnetic data across the release areas (see Data Sets below), and has been integrated with interpretation of regional seismic data and well information provided in Geoscience Australia's 2007 Acreage Release Data Package.

Methodology

The interpretation involved the following steps:

- Initial Magnetic Interpretation
  The initial magnetic interpretation involved qualitative interpretation, determining remanent magnetisation, depth estimation to basement and full 3D modelling of depth solutions. It also looked for magnetic expressions of faults and any expressions of hydrocarbon seepage.

- Seismic Review
  The seismic review included reviewing all 2D sections transecting the areas, well completion reports and existing onshore and offshore data and reports. It included looking for potential play styles.

- Combined Magnetic and Seismic Interpretation
  The magnetic and seismic interpretations were combined and modifications made to both to accommodate the combined interpretation.

Initial Objectives

The initial objectives of the project as specified by Geoscience Australia in its tender document (RFT 2007/2855) included:

a) Location, thickness and distribution of magnetic bodies, including volcanic and intrusive bodies within the sediment fill.

b) Structural elements, including basement fabric, depth to basement and total sediment thickness maps.

c) Tectonic history and structural development of the area.

d) Petroleum prospectivity of the area, including structural plays, reef trends and intrusive structures, making use of petroleum systems concepts established and mapped in the adjacent onshore portion of the basin.

e) Any magnetic signature of potential fluid migration and seepage features in the area.

These objectives were to be met within a short time period of three months and completed at the end of January 2008 to allow prospective bidders for Offshore Canning Basin 2007 acreage release areas (W07-12 to 15), time to assess the findings prior to the close of bids on 17 April 2008.

Data Sets

Data sets to be incorporated and integrated in the interpretation include:

a) Levelled and merged magnetic data.

b) Existing regional and satellite gravity data and bathymetry grids.

c) Open file data for exploration wells in the offshore release areas and adjacent onshore portions of the basin.

d) Regional seismic data available in the GA 2007 Acreage Release Data Package.

e) Summaries of the geology and petroleum prospectivity of the offshore Release areas available in the 2007 Release of Offshore Petroleum Exploration Areas CD-Rom (Department of Industry, Tourism and Resources, 2007).

f) Key publications and open file reports on the geology and petroleum systems of the onshore and offshore Canning Basin.

Experience & Key Personnel

Encom has extensive experience with aeromagnetics and regional gravity. The main interpreter of the aeromagnetics and regional gravity was Dr Clive Foss. However, Encom does not have extensive experience in petroleum prospectivity and seismic interpretation so this was subcontracted to Oil Exploration Consultants with Vic Ziolkowski performing these functions.

Encom's Wayne Stasinowsky acted as project manager and acted as reviewer of the magnetic and seismic interpretations.

Geoscience Australia personnel, primarily John Kennard and Edward Bowen, also reviewed and assisted in the interpretation during review and knowledge exchange meetings.

Regional Setting

Figure 2 shows the Offshore Canning 2007 Release Areas overlain on a schematic of the major structural elements. Figure 3 shows a slightly different view of the same and comes from a section of the "Structural Elements of the Canning Basin" map by Shaw et al (1994).

The Canning Basin has a general northwest-southeast trend. The section of the basin underlying the study area is an extension of the Fitzroy Trough, which has a width of approximately 100 km and is bounded by basement highs of the Broome Platform to the south, and the Leveque Shelf to the north.

Structuring of the basin fill occurred during wrenching and inversion in the Late Triassic-Early Jurassic (Fitzroy Movement). Crustal thinning during extension of the basin is believed to have reached about 50%, with crustal thicknesses of 35 to 20 km beneath the basin. Drummond (1991) also reports structuring within the sediments developed in association with partial inversion of the basin in the Jurassic.

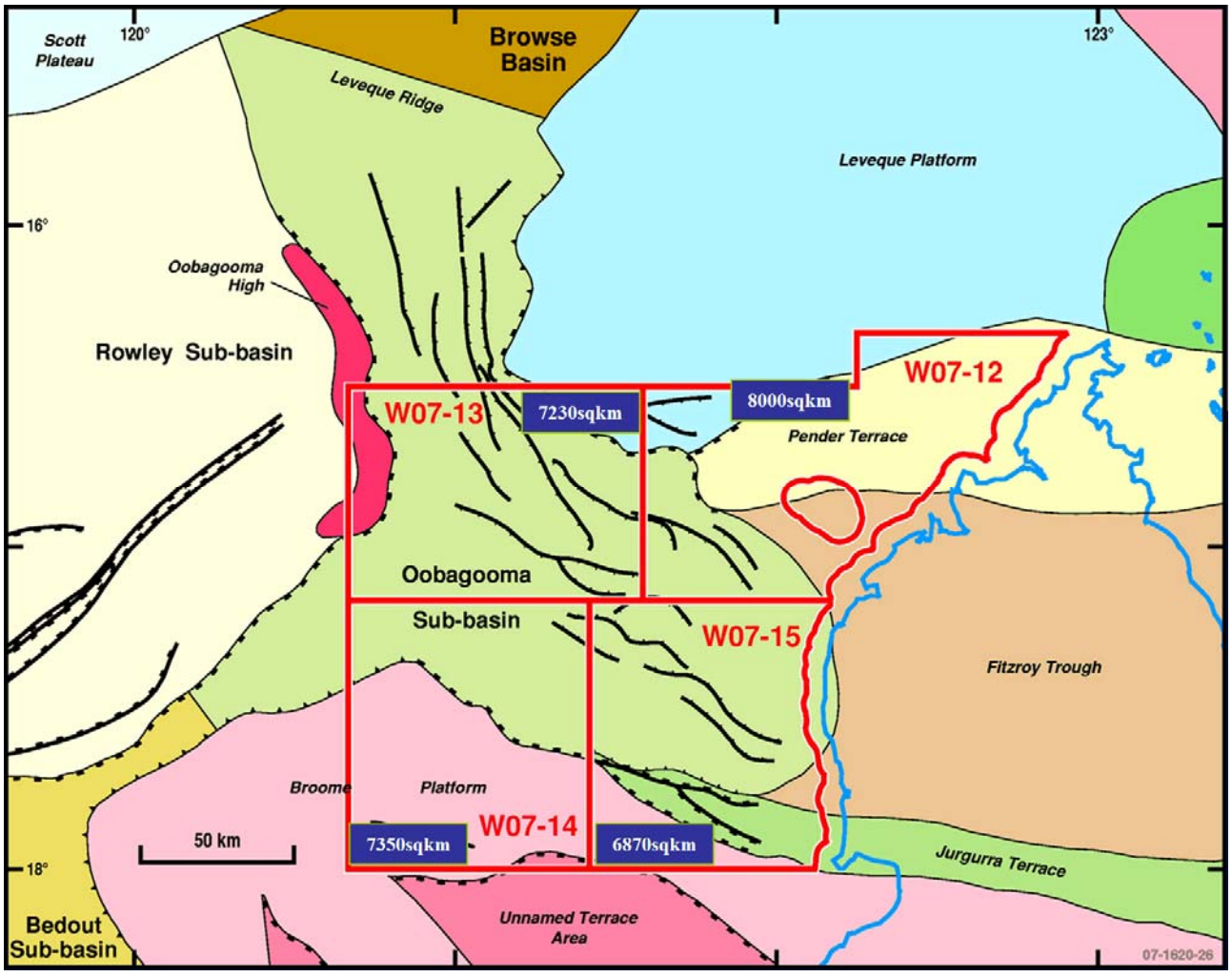

Figure 2 Offshore Canning 2007 Release Areas

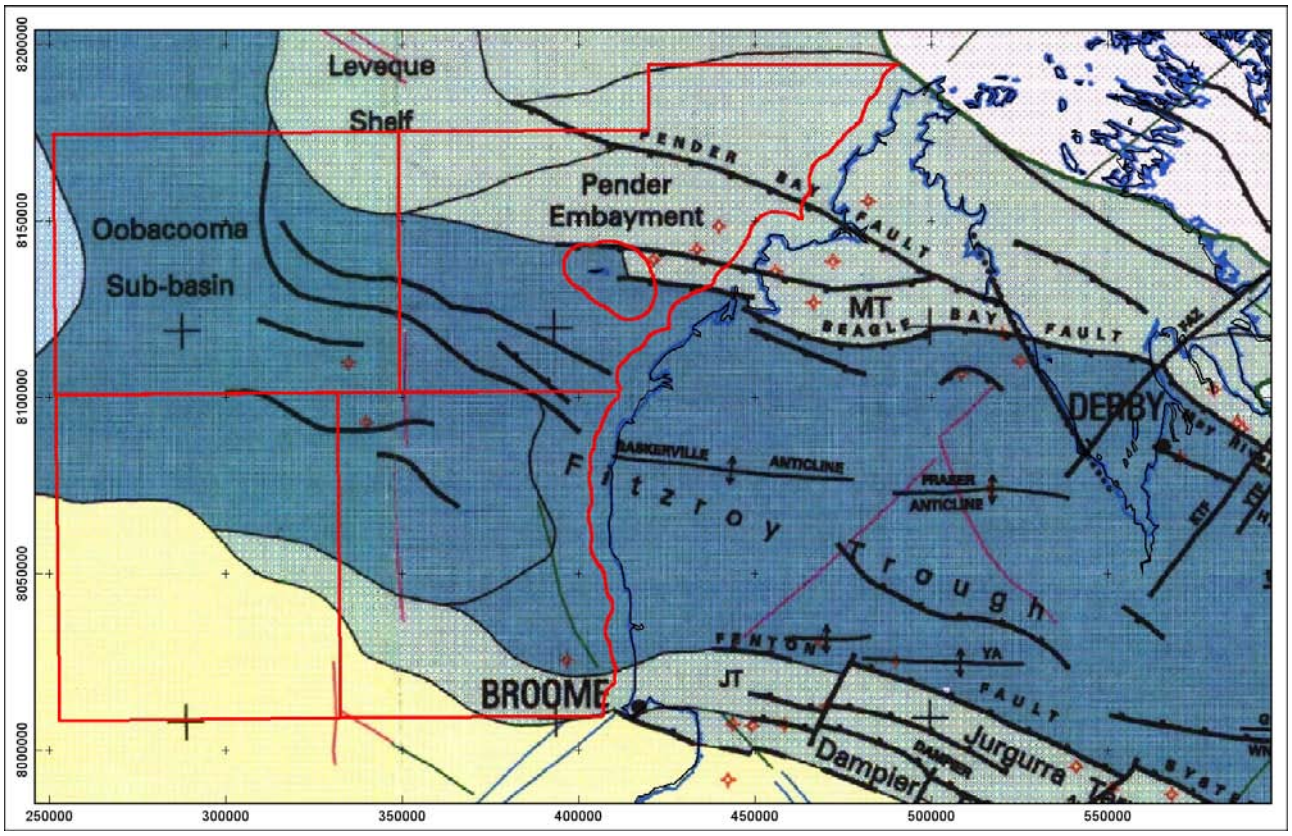

Figure 3 Section of the Regional Structural Elements map by Shaw et al. (1994)

The regional gravity expression of the Canning Basin includes many linear features parallel to the NW-SE tectonic trend. (Figure 4), but individual features do not continue offshore. The coastline roughly coincides with the western margin of a SW-NE trending onshore gravity low, developed perpendicular to the main Fitzroy Trough trend. The Leveque Shelf offshore is marked by a gravity high (which continues southward of the shelf edge). In contrast, the Broome Platform is marked by a gravity low, indicating there are major differences in crustal composition and/or thickness between these two bounding basement highs.

The distribution of gravity stations is plotted in Figure 4. While the onshore coverage is quite detailed, there is only sparse gravity coverage in the near offshore. This gap of sparse data extends across the easternmost blocks WO7-12 and WO7-15.

A map of basement for the whole of Australia, broadly consistent with this study, has been developed by Frogtech (http://www.frogtech.com.au/download.aspx?file=ozseebase_gis.zip). The major difference between the Frogtech study and the current interpretation is in the transition between the Oobagooma Sub-basin and the Broome Arch. The Frogtech study interprets a sharp edge, whereas we have interpreted a more gradual transition, possibly across a series of lesser faults.

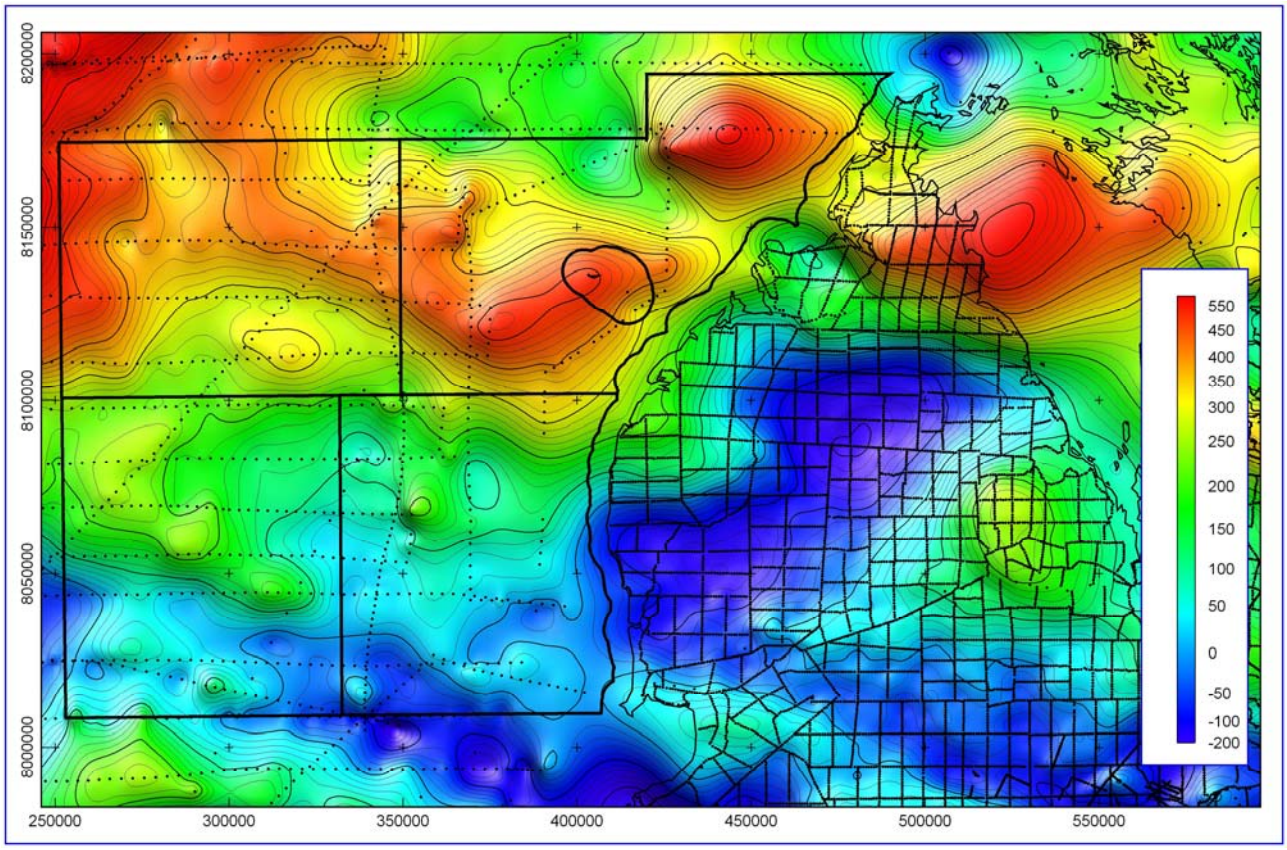

Figure 4 Regional Bouguer gravity image (density = 2.67) generated from data downloaded from GADDS

The corresponding regional magnetic field coverage of this area is shown in the reduced-to-pole (RTP) image of Figure 5. The onshore area is covered with aeromagnetic surveys with line spacings of 400 to 1500 metres. This detailed coverage extends offshore over the easternmost blocks WO7-12 and WO7-15, with the previous 1500 metre line spaced data incorporated in this data mosaic. However, this regional magnetic image only includes sparse ship-track magnetic data over the westernmost blocks WO7-13 and WO7-14. The regional data shows high amplitude, sharp magnetic field variations over the near-shore sections of the Leveque Shelf and Broome Platform, and also several magnetic lows, which have no equivalent in the immediately adjacent onshore.

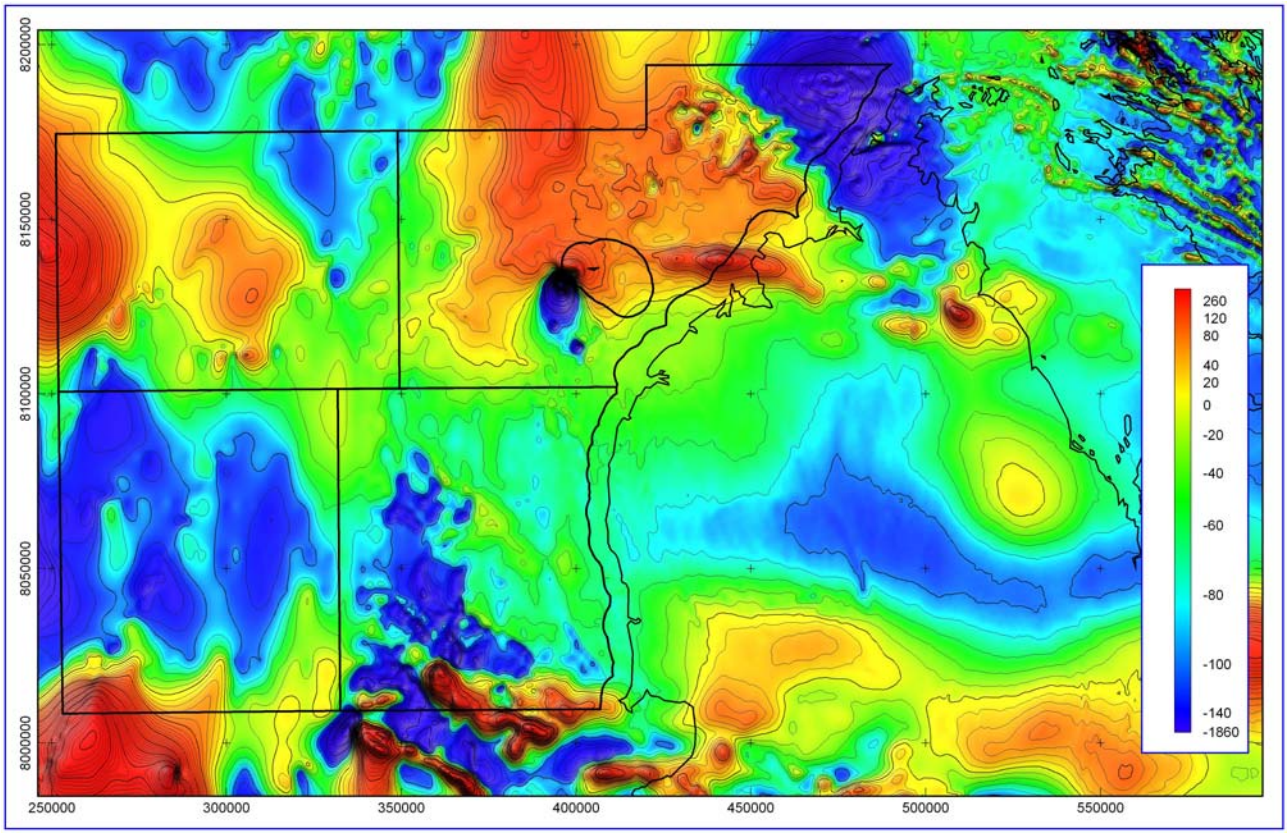

Figure 5 Regional Reduced to Pole image of a TMI grid downloaded from GADDS

To better relate the regional gravity and magnetic field variations to geological structure, a series of enhancements were applied to the regional gravity and magnetic data.

An overlay of the Structural elements map on the tilt filter of Bouguer gravity (Figure 6) highlights clear correspondence between the gravity field and shallow crustal structure over the on-shore Canning Basin, particularly along both the northern and southern margins of the Fitzroy Trough. Unfortunately the sparse offshore data may not be sufficient to reliably support this enhancement, and any interpretation of off-shore crustal structure from the gravity field is speculative.

The tilt filter enhancement was also applied to the reduced-to-pole TMI grid, as shown in Figure 7. There is continuity in features and trends across the coastline to the north and south of the Fitzroy Trough, but this filter highlights a texture zone over the off-shore Fitzroy Trough (block WO7-15), which does not continue across the coastline, revealing that there is a discontinuity in shallow magnetic structures between the on-shore and off-shore areas.

The north-south trending features over the western blocks WO7-13 and WO7-14 are derived only from sparse marine ship-track data, but these trends are confirmed by the new detailed airborne survey.

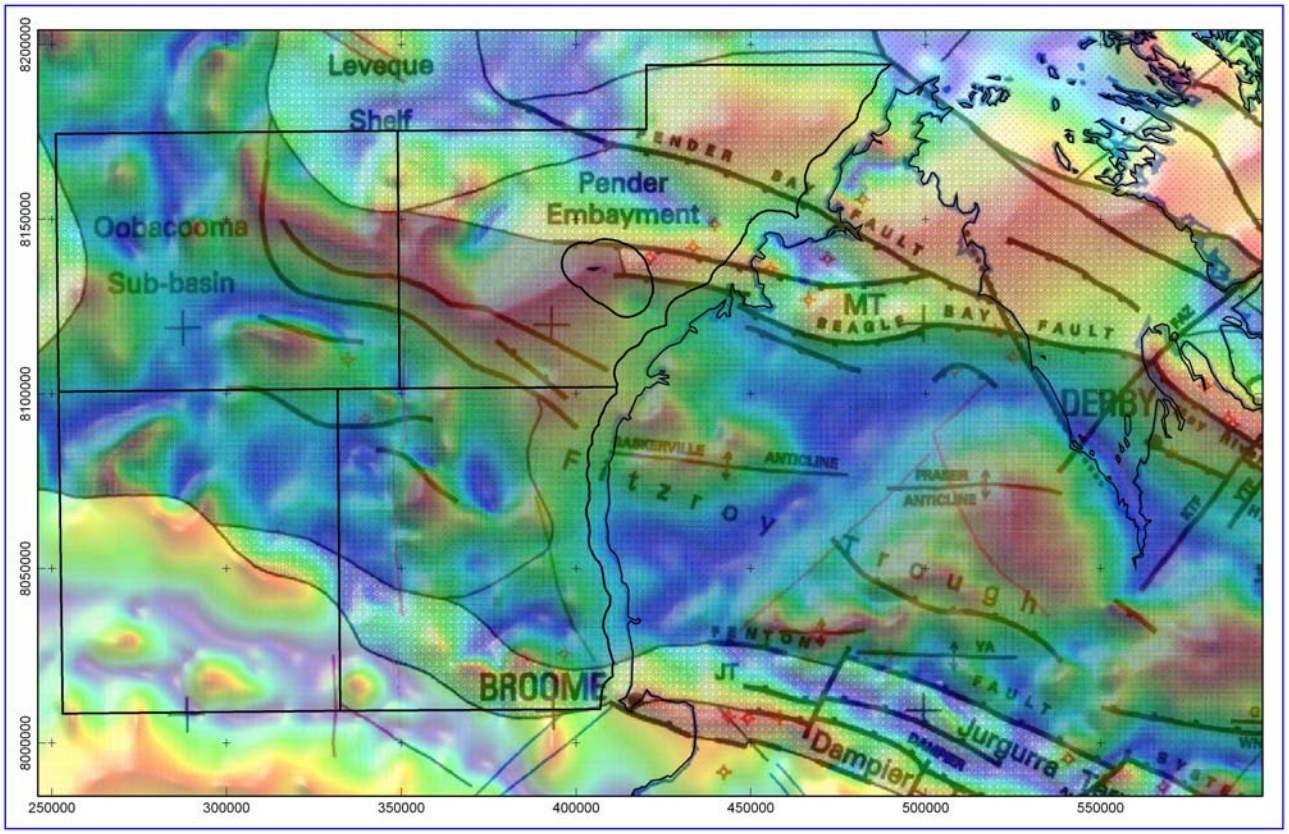

Figure 6 Overlay of the structural elements map on a tilt filter enhancement of Bouguer gravity

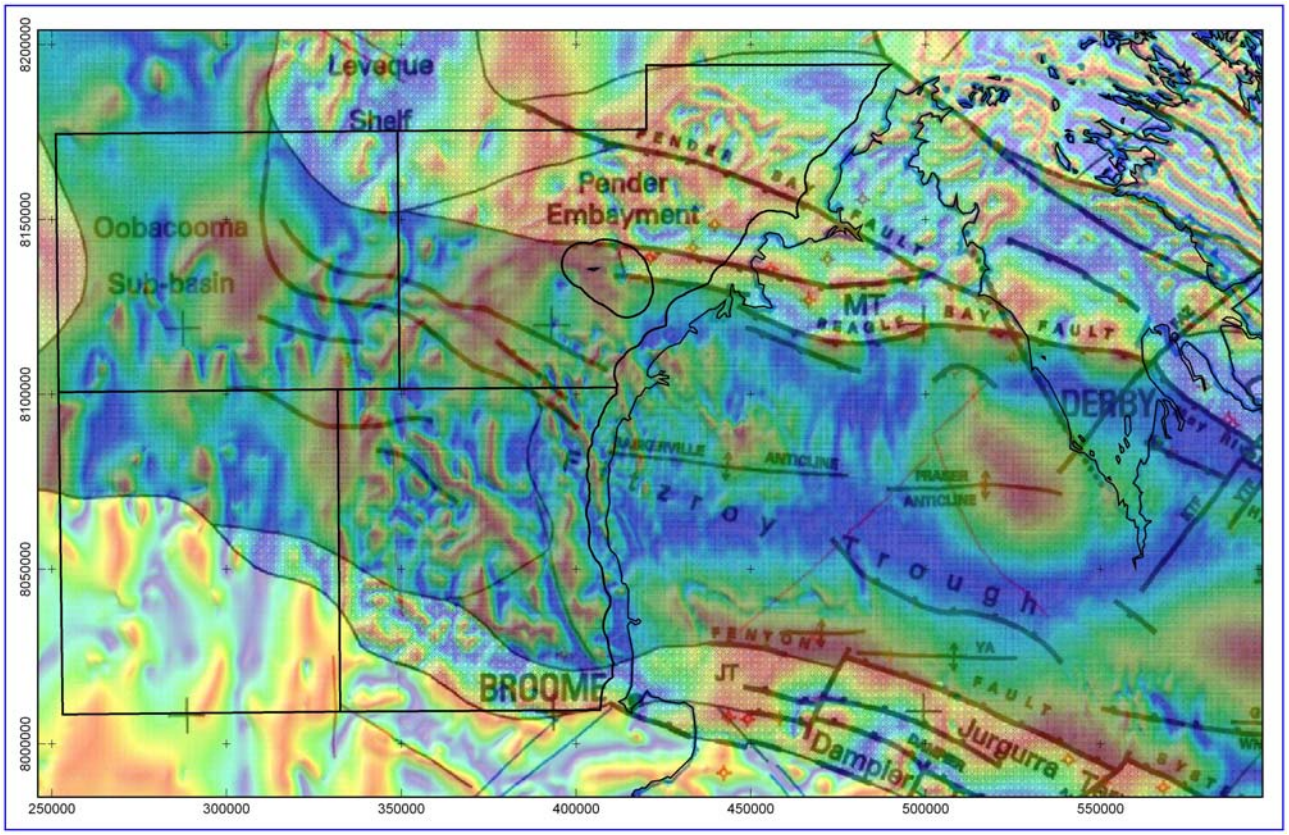

Figure 7 Overlay of the structural elements map on a tilt filter enhancement of RTP TMI

Magnetic Interpretation

Geoscience Australia commissioned a new aeromagnetic survey of the Offshore Canning Basin. The eastern half of this survey (blocks WO7-12 and WO7-15), in-filled an existing survey with line spacing of 1500 metres. The remaining area was flown at 750 metre line spacing. Together with the existing data, this resulted in the whole area having 750 metre line spacing(see Figure 8).

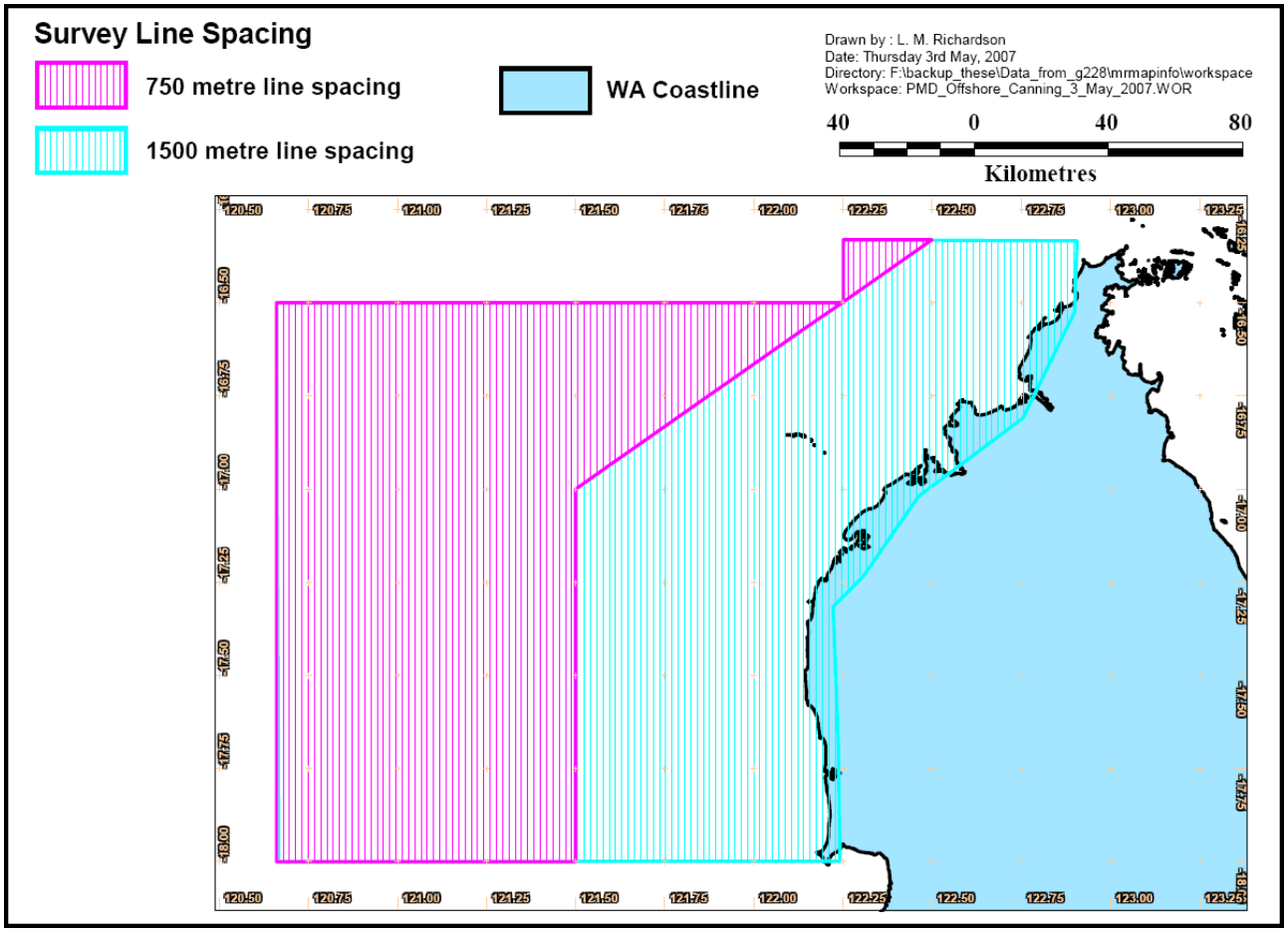

Figure 8 Aeromagnetic Survey Flown in 2007(Figure modified

The survey also covers adjacent State Water Acreage Release Areas (T07-1 to 3), and ties to existing onshore and offshore magnetic survey data (Canning Basin [Yampi, Pender, Broome] WA, Magnetic 1988/89 – P537).

The Survey data covers an area of approximately 31,770 square kilometres and consists of a total of 56,504 line kilometres, comprising 44,633 line kilometres new data (flying height of 60 m asl) and 11,871 line kilometres of previous data. Geoscience Australia, under a contract awarded to Fuguro provided levelled and processed data merged with pre-existing magnetic data to achieve a 750 m line spacing and 3000 metre tie line spacing grid across the release areas.

Interpretation

A TMI image generated from the co-processed old and new data is shown in Figure 9. The sharpest and highest amplitude field variations are mostly in the north-east and southern parts of the area. The smoothest field variations (from deeper sources) are in the north-west.

In several areas the most prominent field variations are negative anomalies (local decreases in field strength) due to predominantly remanent magnetizations of reverse polarity. A 3D display of the TMI grid in Figure 10 shows that a large negative anomaly in the northern section of the area is the highest amplitude feature.

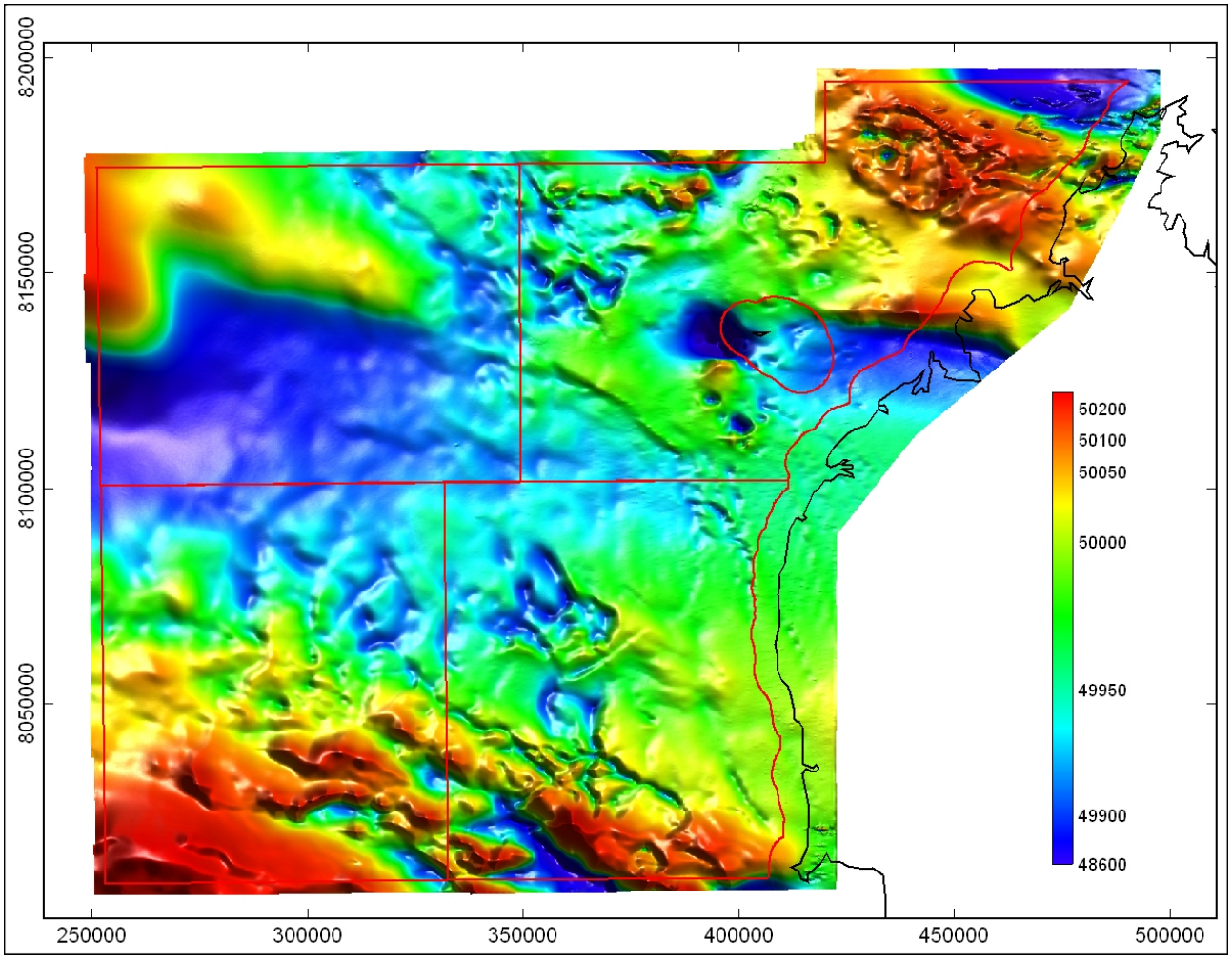

Figure 9 Total Magnetic Intensity (TMI) image of the survey area

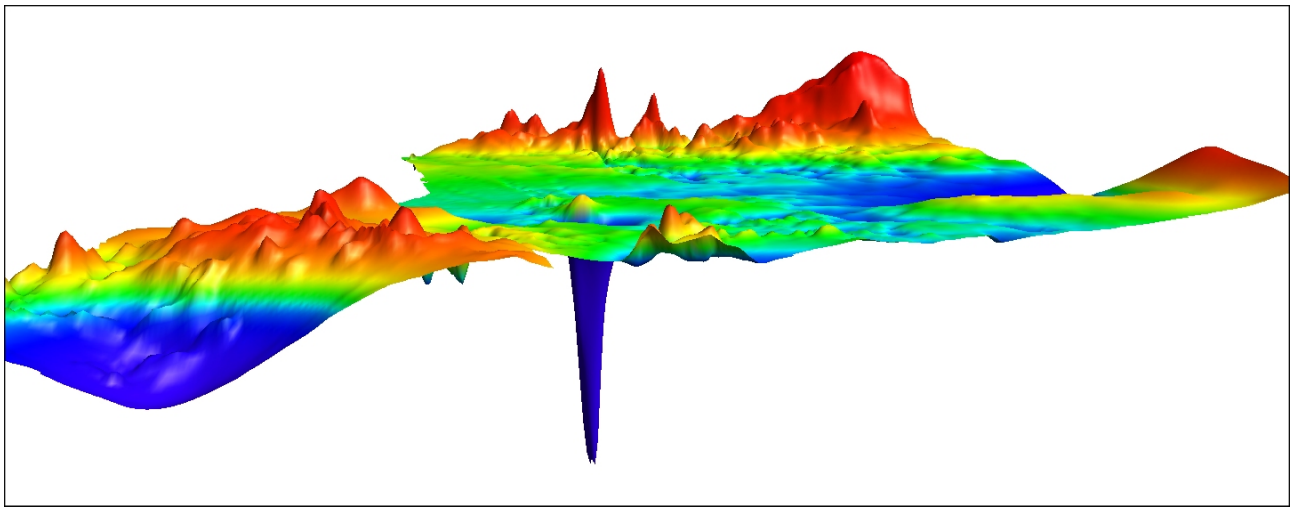

*Figure 10 3D display of TMI (viewed from the north) Colour scale as for Figure ***

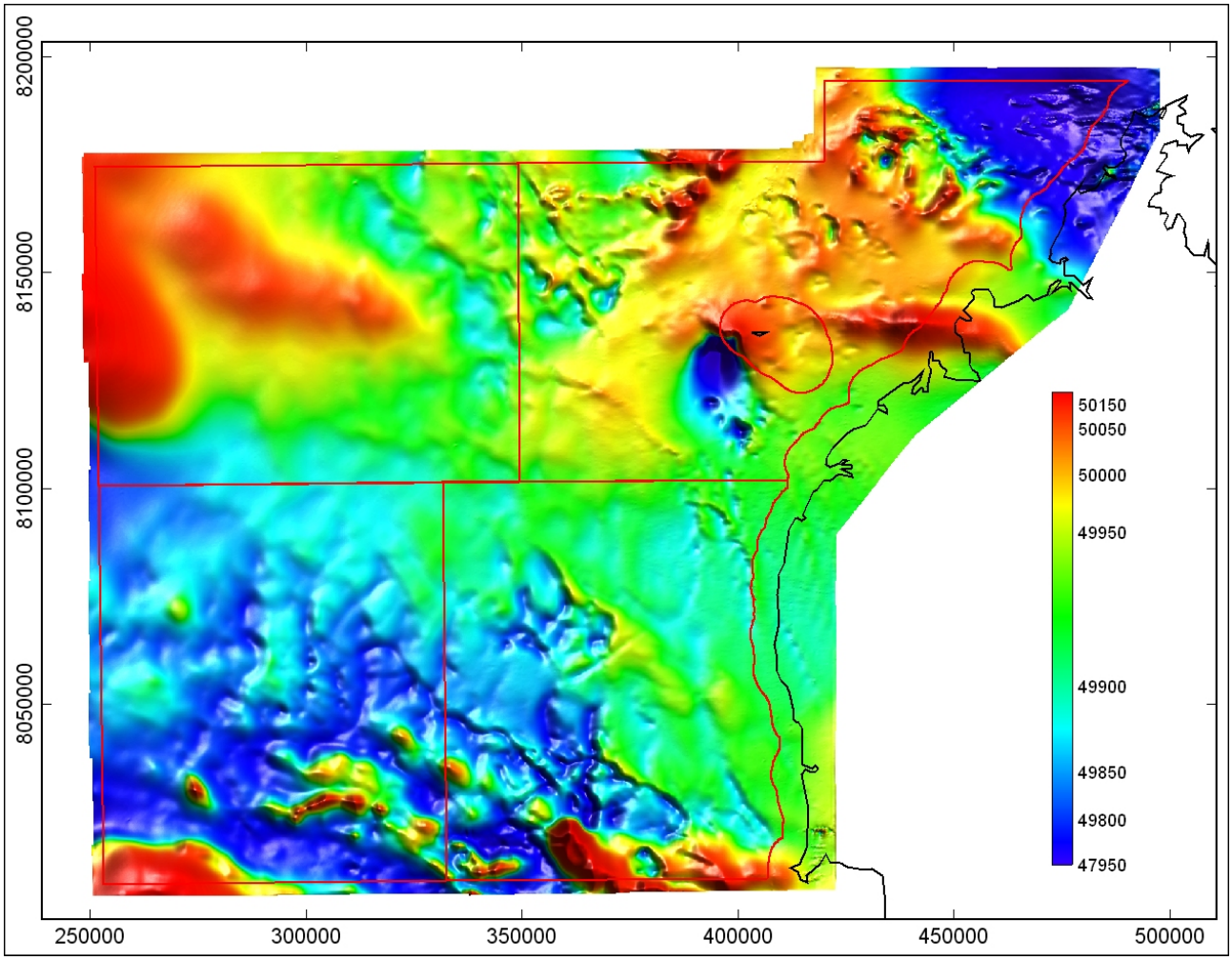

Figure 11 Reduced to pole (RTP) TMI

To simplify the magnetic field variation, and to centre anomalies directly above their source bodies, a reduction to pole (RTP) transform was applied to the data as imaged in Figure 11. This transform does not correctly treat the anomalies due to remanent magnetization, but because that remanence is almost anti-parallel to the present geomagnetic field, the anomalies are not severely distorted (but retain their negative polarity).

To highlight anomalies over shallow sources, with little influence from magnetization direction, an analytic signal transform was applied. The modulus of the analytic signal is imaged in Figure 12. To pre-condition the data for this enhancement a mild upward continuation of 250 metres was applied.

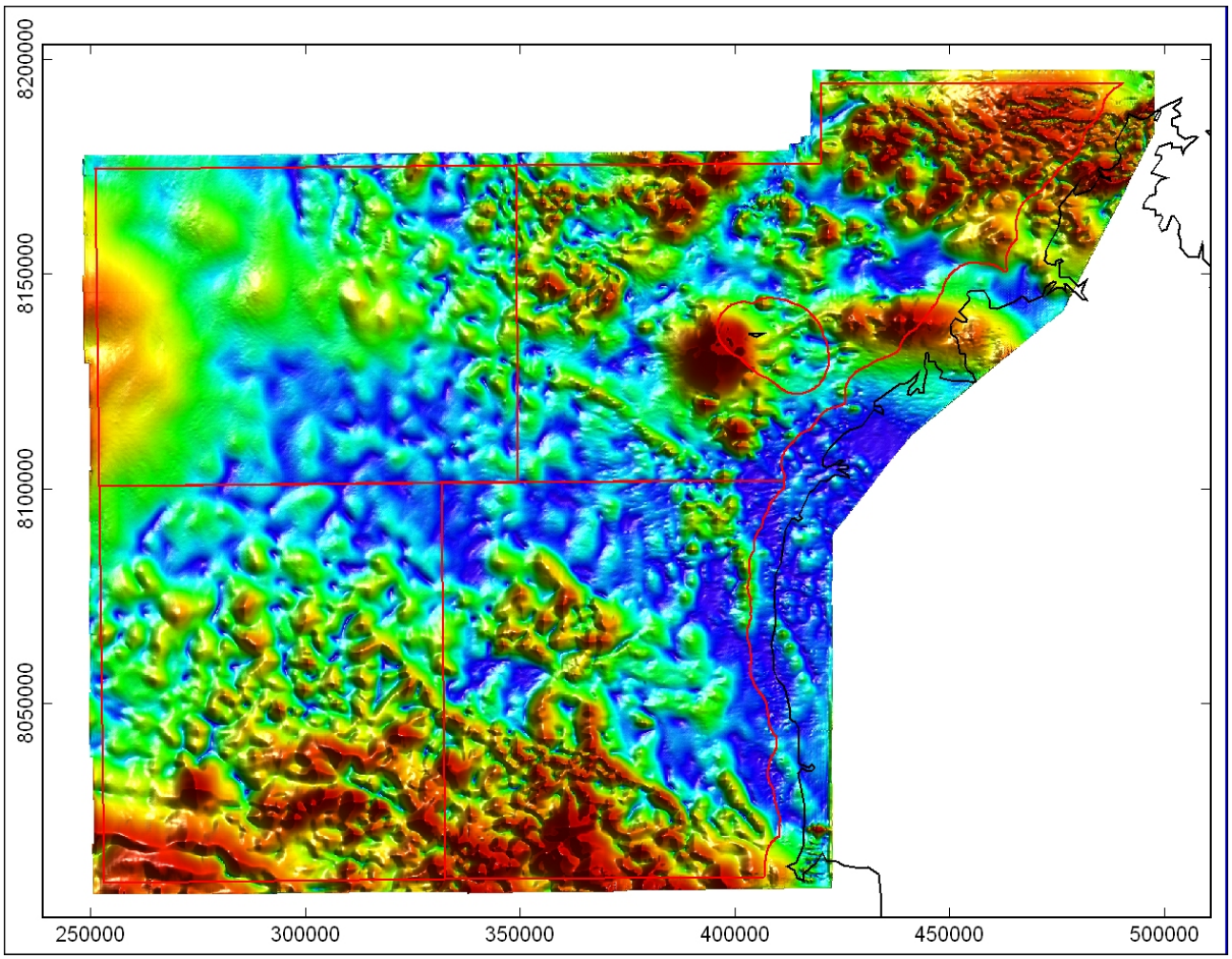

Figure 12 Modulus of the analytic signal of the RTP

Another enhancement of the data which proved useful for recovering trends and dislocations in the magnetic field was the tilt filter (ref Figure 13). This filter reduces the significance of the amplitude of field variations, and accentuates linear trends in the data.

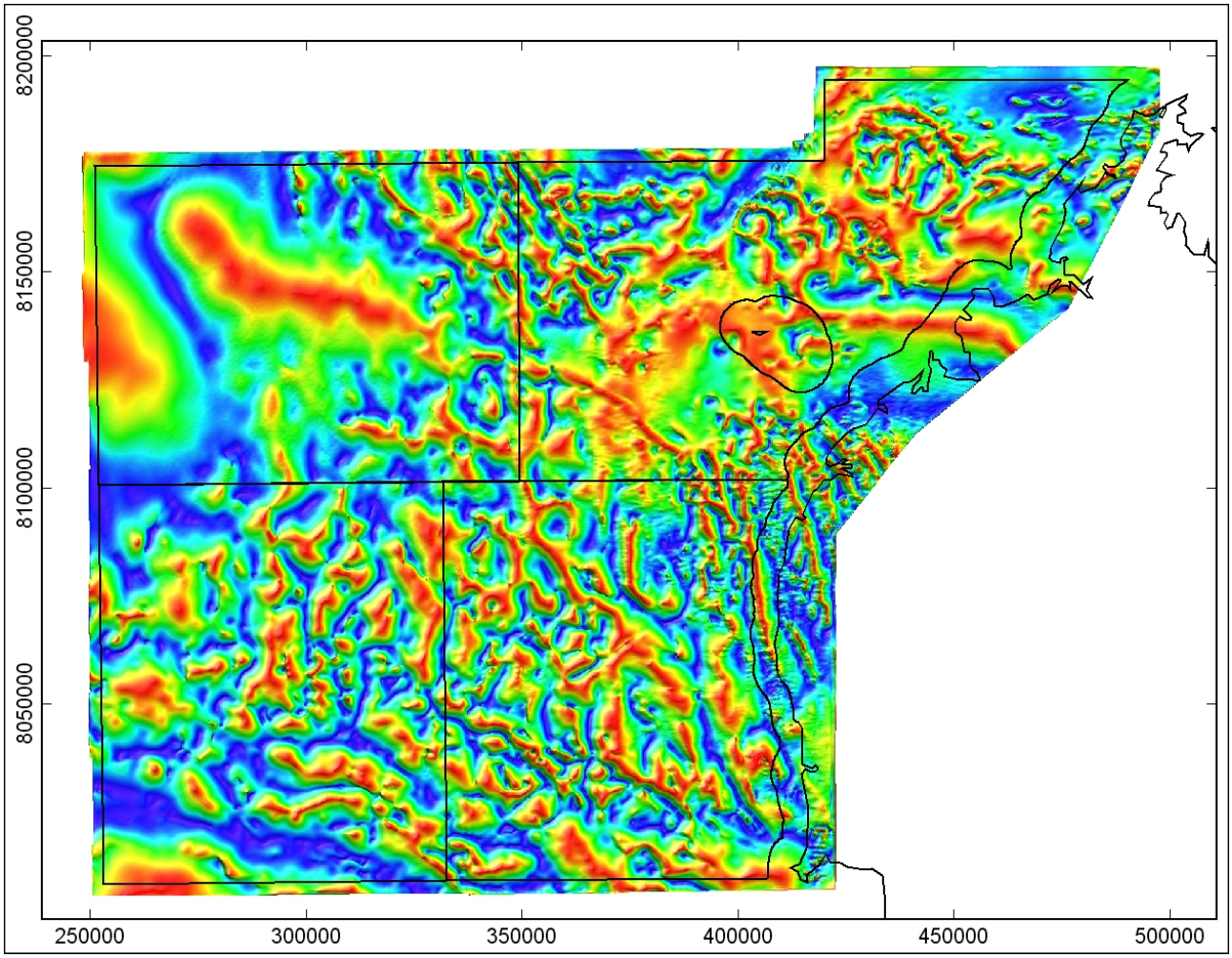

Figure 13 Tilt filter of the RTP

The vertical derivative and tilt filter enhancements of the reduced-to-pole TMI grid were used to trace the axes of linear anomalies, and terminations and displacements in the magnetic field. These linears are plotted over the first vertical derivative (FVD) and tilt filter images in Figure 14 and Figure 15 respectively. There is a complex pattern of trends in the magnetic images, with north-south, northwest-southeast, and southwest-northeast trends, each consistent with known extensional and compressive events over the protracted history of the basin.

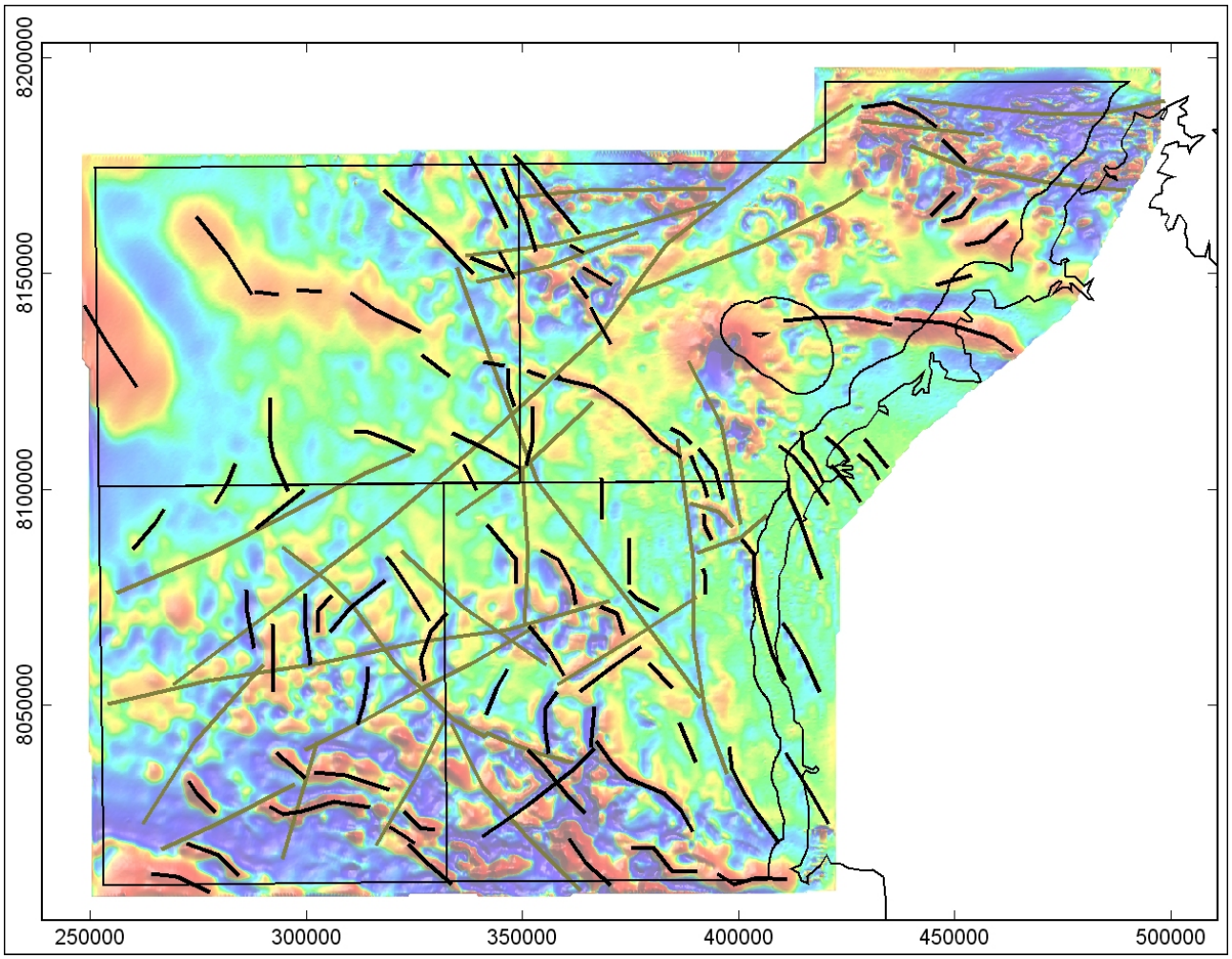

Figure 14 Magnetic anomaly axes and feature terminations and dislocations on image of the FVD of RTP

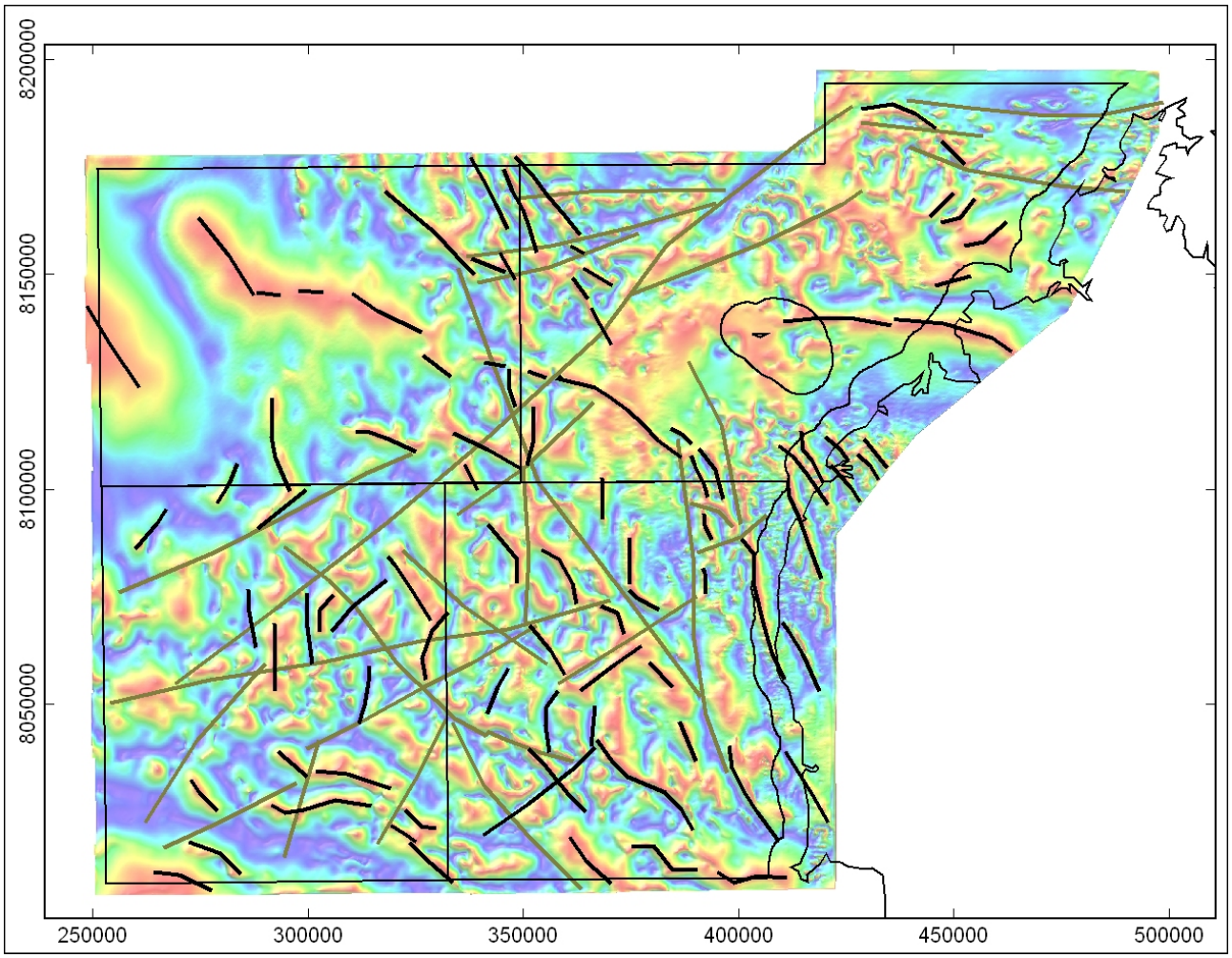

Figure 15 Magnetic anomaly axes and feature terminations and dislocations on image of the Tilt Filter of RTP

Depth to Magnetic Source Estimation

The depth to the top of magnetic source bodies can be estimated from analysis of their magnetic field anomalies. The key indicator of depth is the sharpness in curvature of the field. A greyscale image of the first vertical derivative of the RTP (Figure 16) highlights regional variations in sharpness of curvature.

The sharpest anomalies in the northeast and southeast of the area mark the shallowest magnetic bodies, and the less distinct variations in the northwest of the area mark the deepest magnetic bodies.

There are many methods to derive quantitative depth estimates from magnetic field data, and all require similar assumptions about the geometry of the source bodies. In this study we have used what we believe to be the most reliable technique of inverting selected data using parametric models of depth, magnetization, thickness, dip and depth extent. The inversions are self-adaptive for each source model, but are still bound by the fundamental limitations of non-uniqueness in solution of the inverse problem.

Over sharp, steeply-dipping magnetizations within crystalline basement it is possible to estimate source depth with a confidence of approximately +/-10%, however, many of the magnetic bodies in this study are igneous intrusions into the sedimentary section, as intersected in the Perindi 1 well, and as seen in many of the seismic profiles. These bodies appear to have irregular form. The necessary assumptions about source geometry are less reliable for these sources, resulting in a decrease in confidence in derived depth estimates to possibly +/- 20%.

A more fundamental problem is to then interpret what geological surface a depth estimate applies to. In many cases the intrusives may be terminated at an unconformity surface, but there are several known

unconformities, and furthermore emplacement of bodies within the section can result in bodies located at variable stratigraphic depths, according to local conduits and obstructions for progress of the melt.

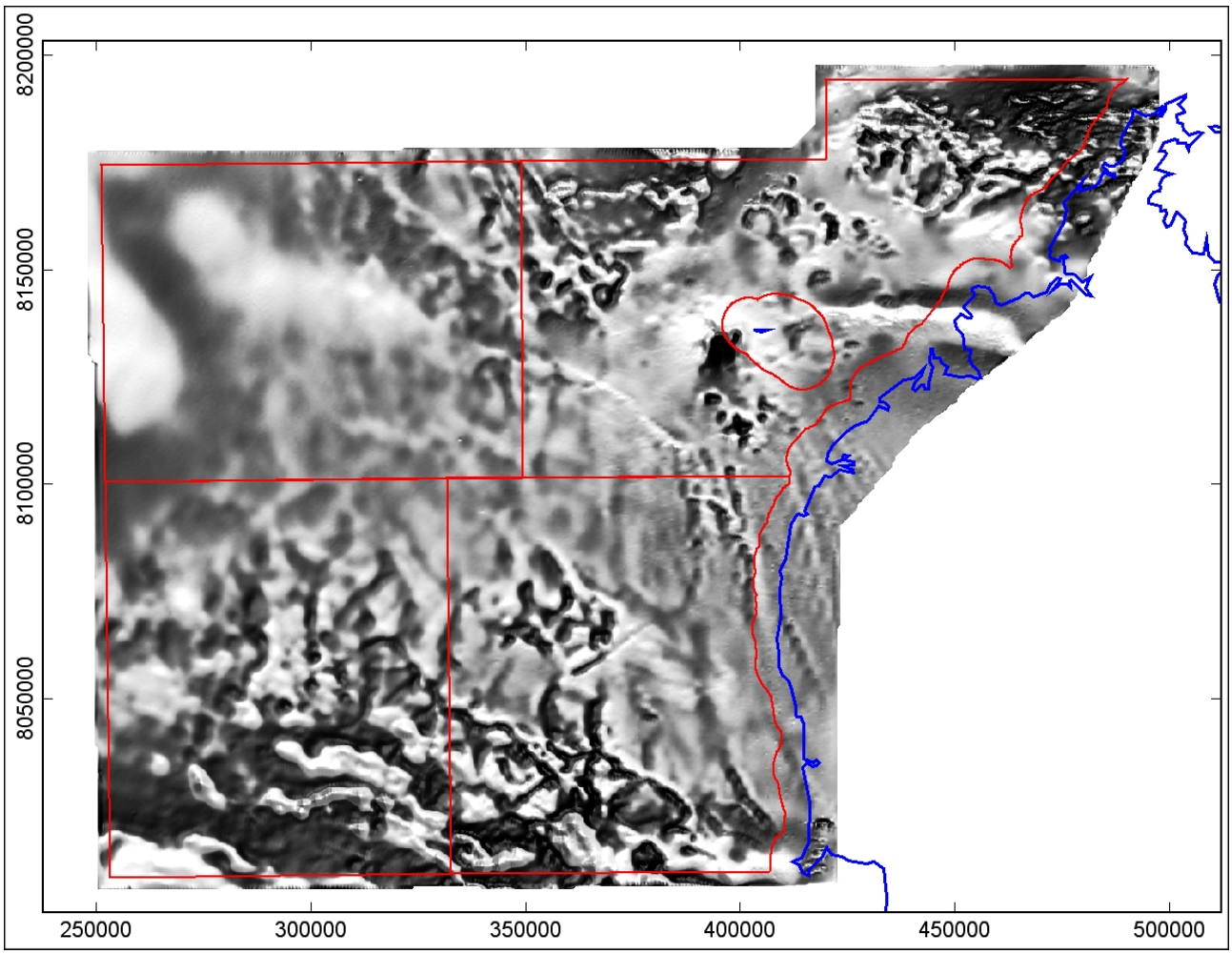

Figure 16 Greyscale image of the first vertical derivative Reduced-to-pole TMI

Figure 17 illustrates derivation of the source depth estimates.

A traverse has been extracted through the TMI grid, passing through the peaks and troughs of local anomalies as perpendicular as possible to the anomaly trends. A series of tabular source bodies is proposed, each with horizontal top and base, and parallel dipping sides. In the area shown there are both positive and negative anomalies. The negative anomalies are due to sources with predominant remanent magnetization of steep positive inclination. For the purpose of depth estimation it is sufficient to represent this remanent magnetization with an induced magnetization of synthetic negative susceptibility.

The location, azimuth and strike extent of the bodies is adjusted in plan view to match the anomaly characteristics. A smooth field is estimated as the background field for the anomalies, and an inversion is run to optimise position along the profile, depth, thickness, apparent susceptibility, and depth extent of the various source bodies, so as to minimise differences between the observed and computed fields.

As shown in the figure, the misfit between observed and computed fields is reduced to almost zero, but unfortunately non-uniqueness does not mean that this proves the validity of the model. In most cases the depths are reasonably robust (+/- 20%), but there is trade-off between the values of most parameters, particularly between size of the bodies and their magnetization. Comparison of the magnetic source bodies with their expression where seen on seismic, suggests that in many cases the bodies may be smaller (and correspondingly of higher magnetization) than derived from the inversions.

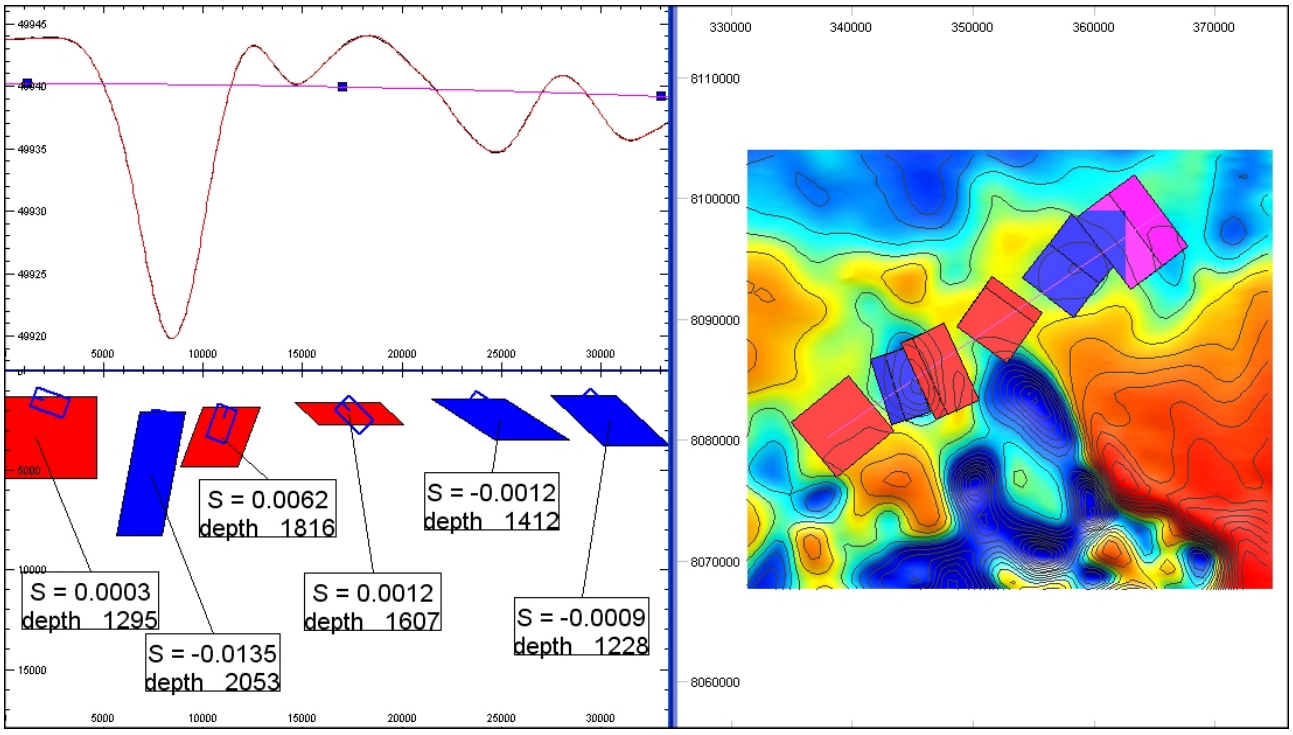

Figure 17 Example magnetic depth estimation traverse

Figure 18 shows the distribution of magnetic source depth estimates made on approximately 250 traverses. Attribution of these depths to their geological sources is discussed in a later section.

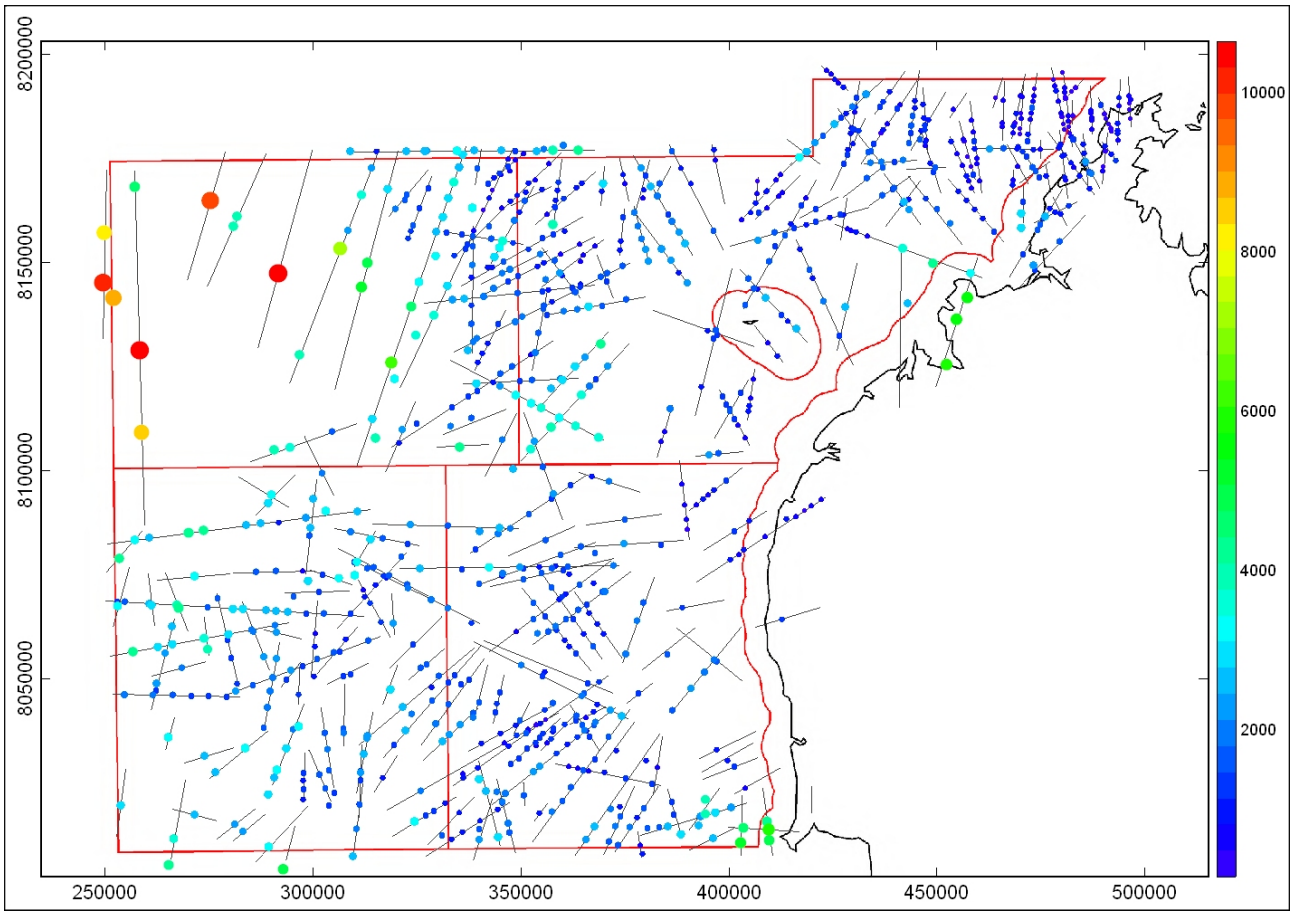

Figure 18 Distribution of magnetic depth estimates (colour and size coded for depth)

Interpretation of Seismic Data

RELEASE AREAS W07-12, 13, 14 & 15

REGIONAL SEISMIC INTERPRETATION

Disclaimer

This seismic interpretation was performed on limited regional data and its accuracy cannot be assured. The illustrated potential play types are not intended to represent definitive leads or prospects and OEC Pty Ltd accepts no liability in any case where these data are otherwise misconstrued.

Introduction

This regional seismic data interpretation was carried out as an adjunct to the Encom Technology Pty Ltd aeromagnetic study of these new release blocks performed on behalf of Geoscience Australia (Figure 2 and Figure 3).

These new areas cover an area that ranges from 8 to 190km offshore. Water depths for the two inboard blocks range from less than 20m to about 80m. The two outboard blocks range from 40m to 300m along the northwestern margin (Figure 19).

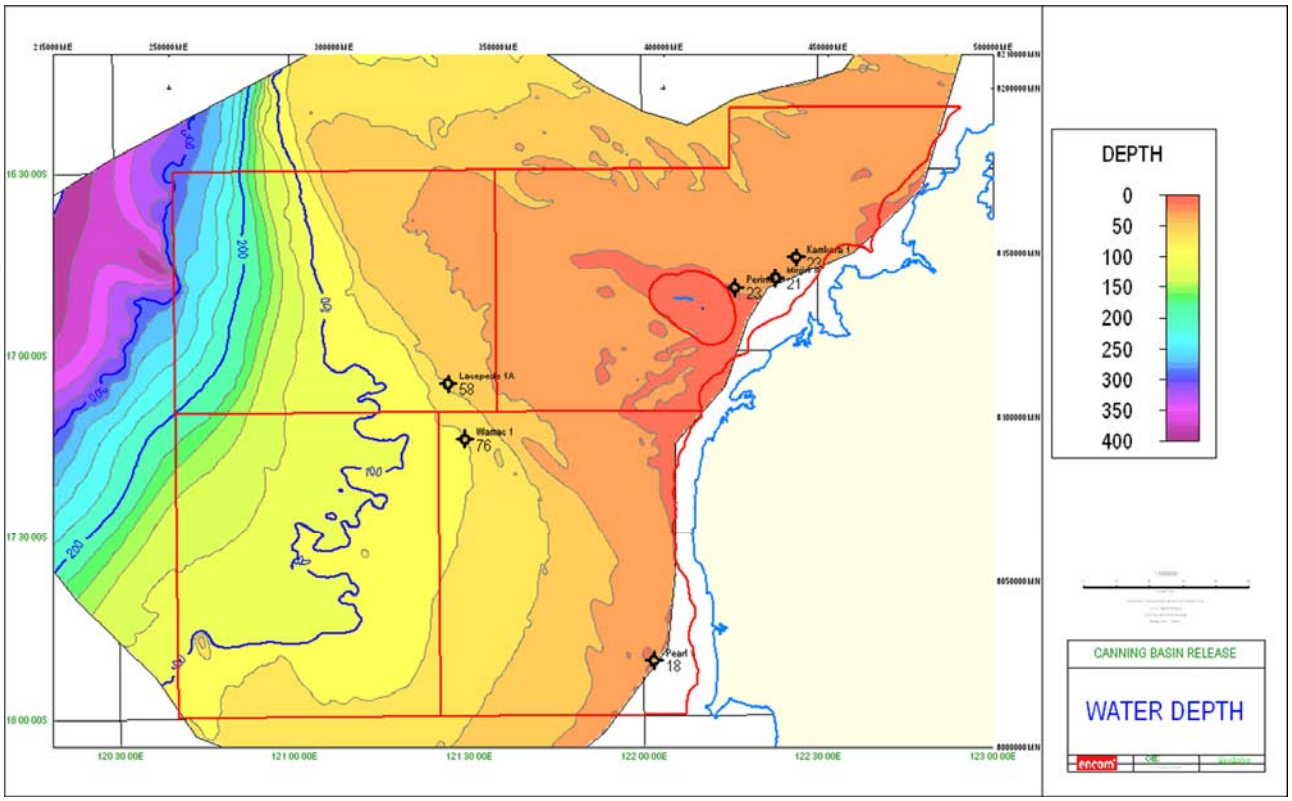

Figure 19 Water Depths

Data Quality and Coverage

The data that were available and used in this interpretation are given at Table 1 and Figure 20.

Table 1 Geophysical Data

VINTAGE	SURVEY	OPERATOR	DISTRIBUTION	TWT	QUALITY
1996	AGSO 175 BROWSE	AGSO	THREE LINES IN W07-12,13	5.5S	GOOD
1993	AGSO 120	AGSO	THREE LINES IN W07-13,14	16S	GOOD
1998	LEVQUE SHELF LS98	GHD GUARDLINE	27 LINES IN W07-12,13 AND EXTREME EAST 15	3.5S	GOOD
1988	SCIENTIFIC MARINE JN88	JAPAN NATIONAL OIL CO	26 LINES W07-13,14 & 15 AND WESTERN 12	5.5S	GOOD TO FAIR

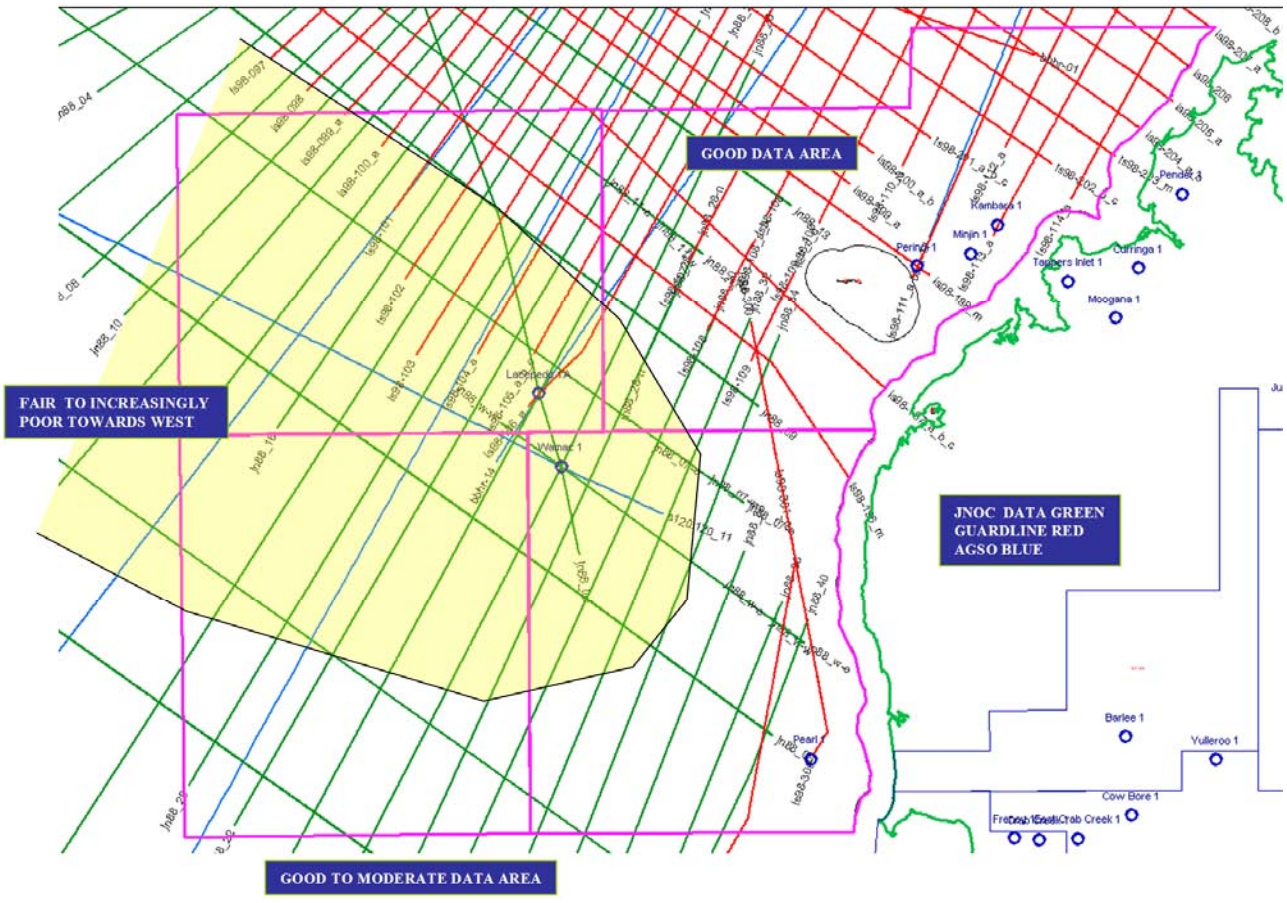

Figure 20 Seismic data distribution and areal quality at the Paleozoic.

Data spacing in the Paleoozoic dip direction varied from 10 to 14km in the southern blocks and 4 to 12 in the northern blocks. In the strike direction the spacing varied from 20 to 30km in the southern blocks and 5 to 40km in the northern ones.

A comparison of the AGSO, Guardline and JNOC surveys is given in Figure 21.

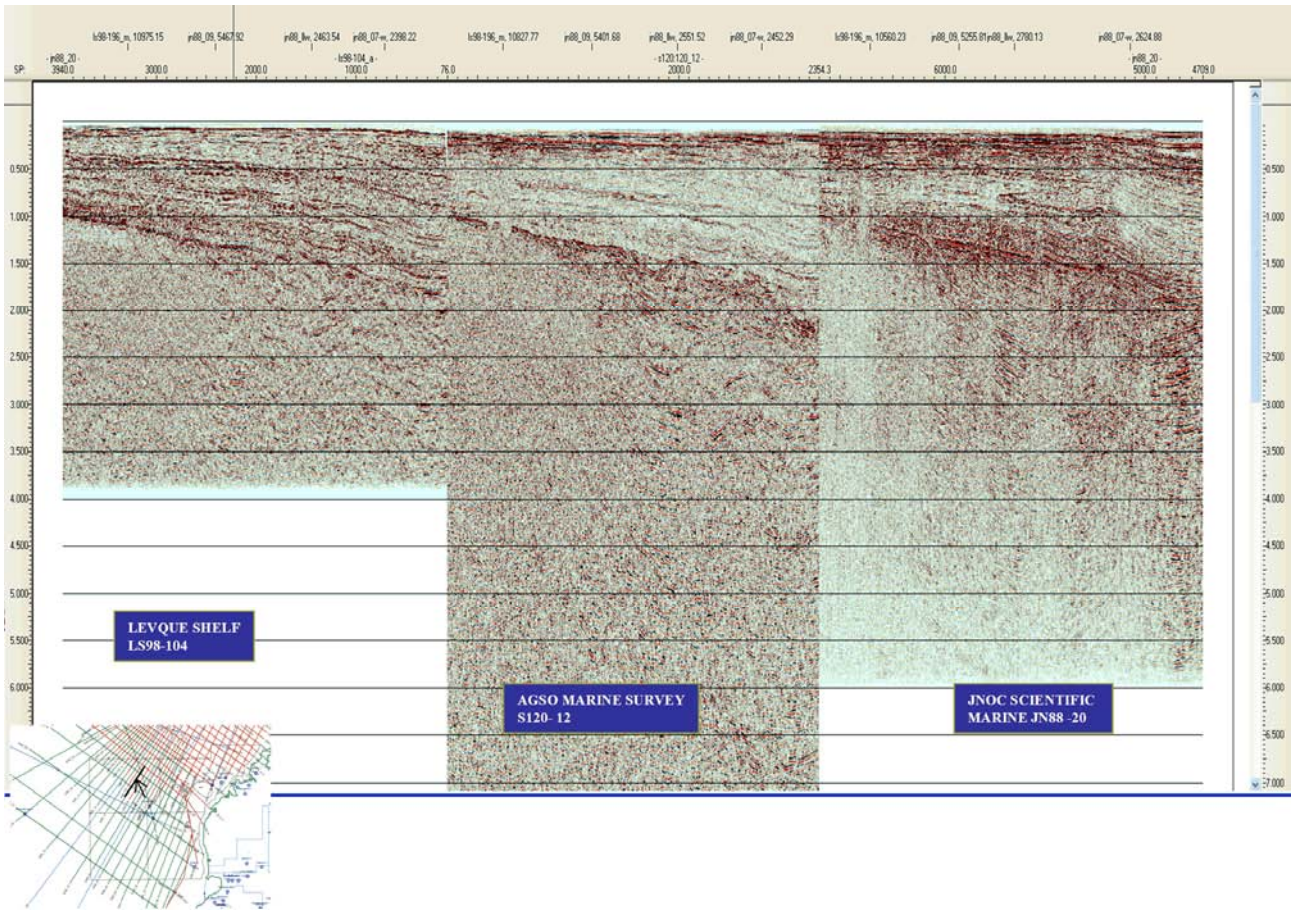

Figure 21 Comparison of adjacent seismic data vintages

Well Ties and Interpreted Horizons

The stratigraphy for these new areas is given in Figure 22 and Figure 23.

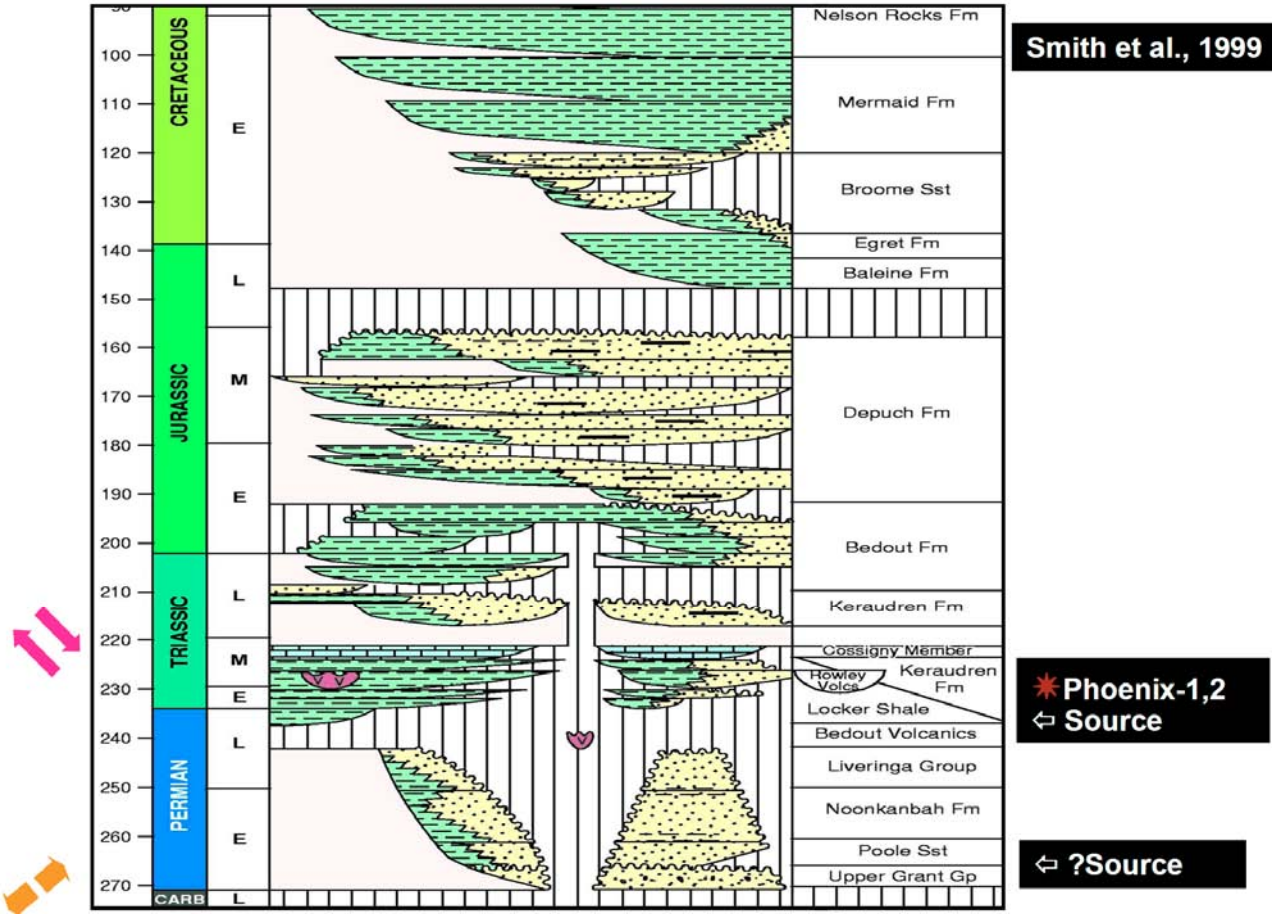

Figure 22 Offshore Canning Stratigraphy part A (refer DITR 2007)

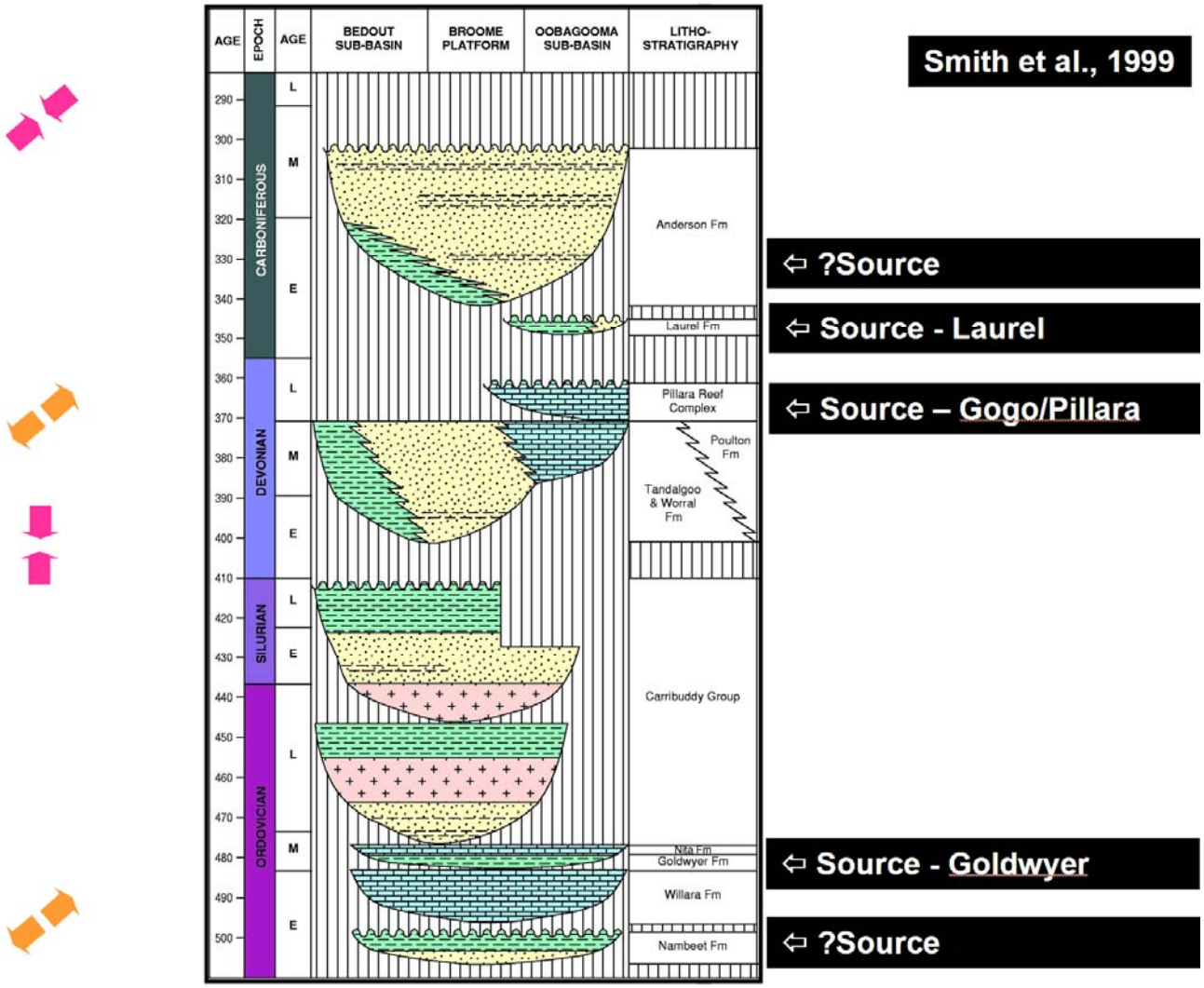

Figure 23 Offshore Canning Stratigraphy part B (refer DITR 2007)

The horizons listed in Table 2 were mapped where possible as they are believed associated with play types that can develop in this area.

Table 2 Interpreted Horizons

Horizon	Area Mapped	Difficulty
Basement *	Entire area	Only on a few deep AGSO lines in graben. Good high impedance reflector where shallow in north. Assumed to be last coherent event on southern platform.
Devonian Horizons	Adjacent to northeastern wells and as high impedence events in cores of some axial inversions	Good discrimination in northeast where strong reflections and rugose terrain associated with carbonate sedimentation is present(block 12).

Horizon	Area Mapped	Difficulty
Base Grant	70% of graben area and all of southern platform	Occasionally angular erosion at base of event. Otherwise difficult to discriminate.
Top Grant *	Entire area where it is deemed to occur. Also carried at base of Bedout U/C where it is considered to outcrop.	Very high impedance reflector on many lines. Occurs at top of group of moderate reflectors. Appears to be onlapped in places.
Top Bedout U/C *	Entire area	Very good event. Unconformity that truncated igneous intrusives. In the vicinity of the new blocks it is coincident with the Fitzroy U/C.
Mid Triassic *	Onlaps western margins of outboard area 13.	Very good event.
Base Jurassic *	Onlaps western half of outboard areas 13 and 14.	Very good event.
Base Cretaceous *	Entire area	Very good event.

***** Denotes horizons for which two-way-time and depth maps were produced.

These horizons are illustrated on line s120;120-11 where the horizons are mapped in that axis of the graben (Figure 24)

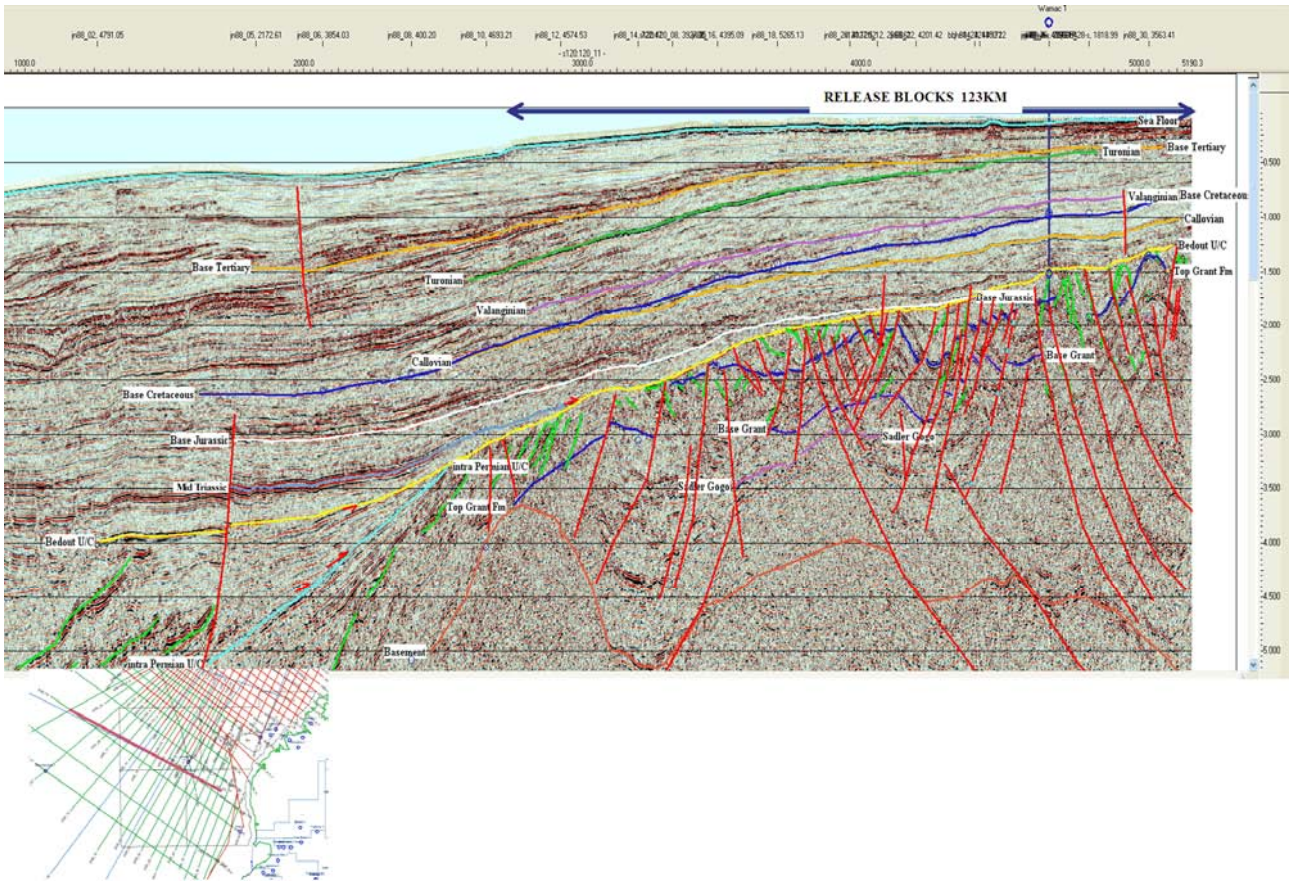

Figure 24 Line s120;120-11 Horizons in axis of graben

Good Paleozoic well ties could be made to the northeastern Kambara 1 and Perindi 1 wells (Figure 25 and Figure 26). Lacepede 1A penetrated Jurassic sediments overlying Early Permian (Asselian) and terminated in Late Carboniferous. Wamac 1 penetrated a similar interval (DITR 2007). Mingin 1 and Pearl 1 are not located on available seismic data. The base Tertiary and the base Cretaceous were also tied to East Mermaid.

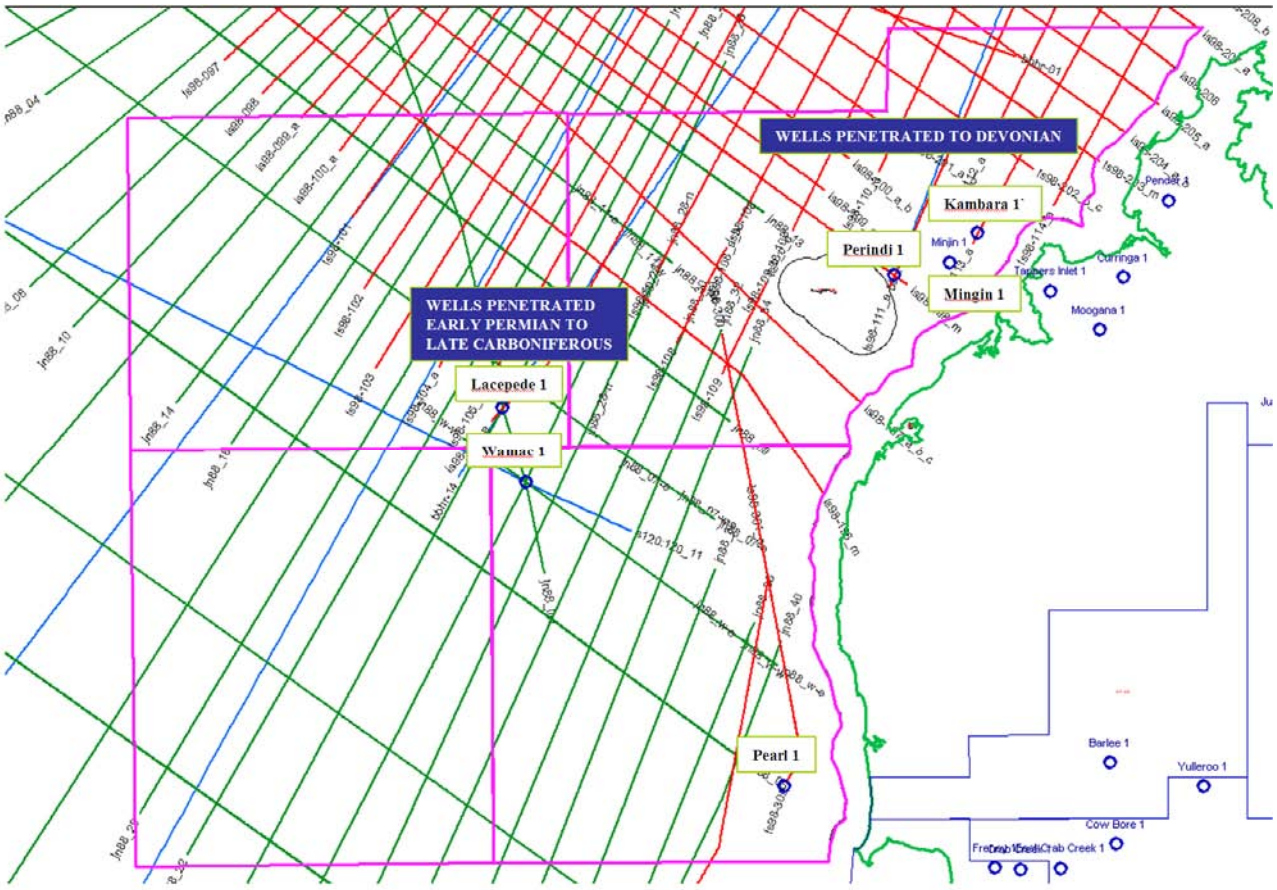

Figure 25 Well Locations

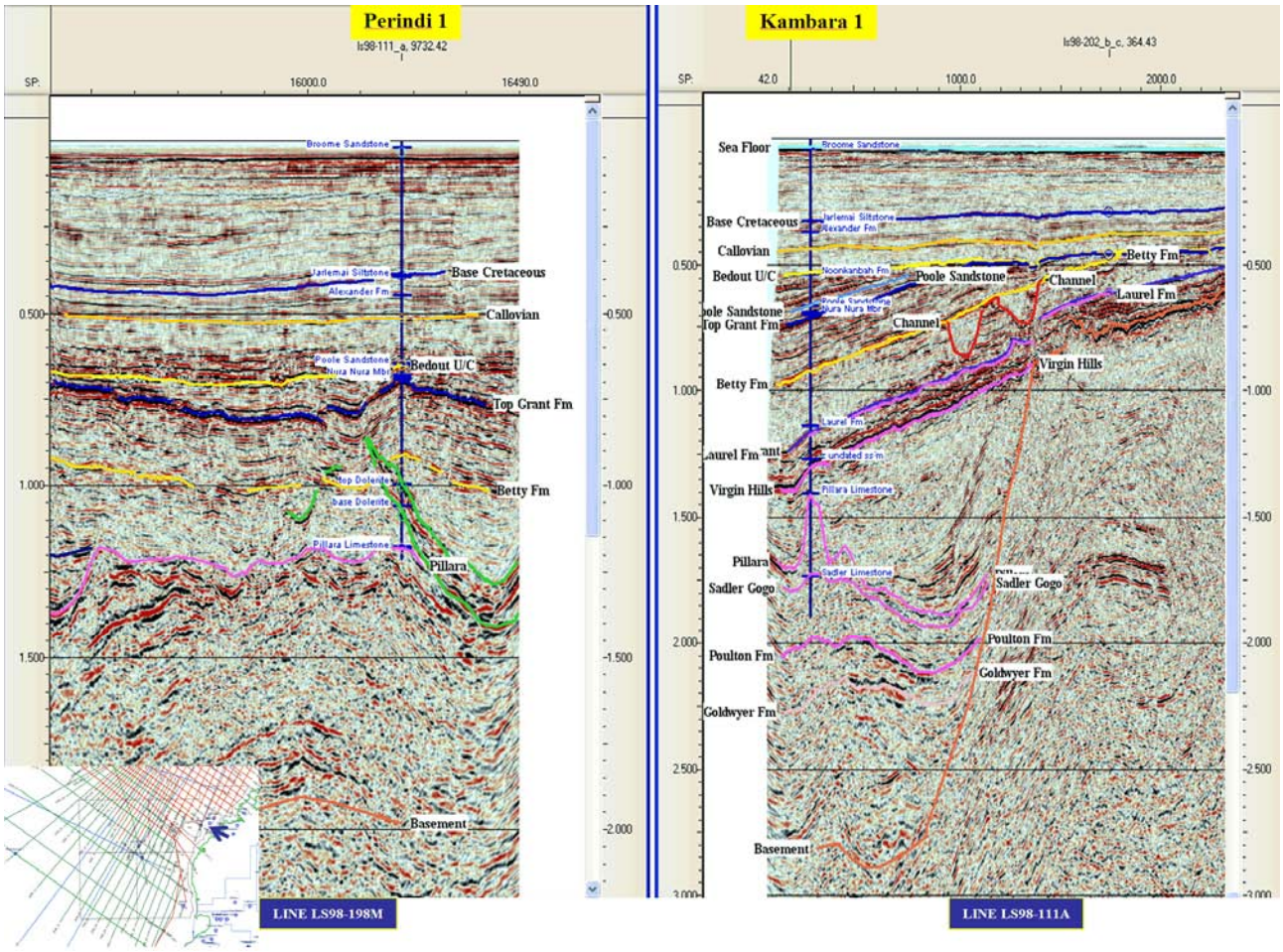

Figure 26 Well ties to Perindi 1 and Kambara 1

Mapping

Two way time maps were constructed for the designated horizons above. Geosciences Australia provided bathymetry data as well as stacking velocities from the JN88 and LS98 seismic surveys. These velocities were converted to interval velocities using Petrosys (DIX method). Depth conversion for each horizon was based on a single interval from sea floor. When tested against well tops errors were less than 5%. Depth maps are given in Figure 19 and Figure 27 to Figure 32.

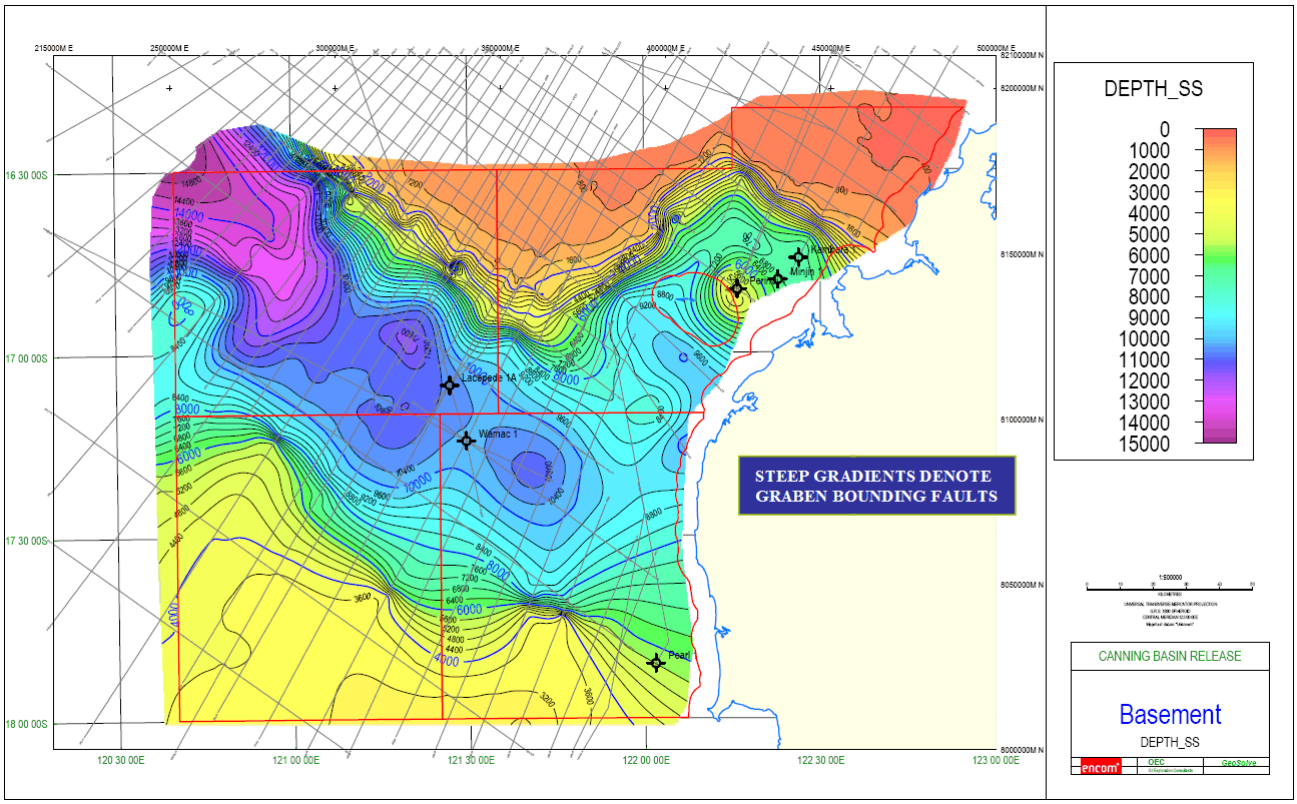

Figure 27 Basement depth structure map CI 400m

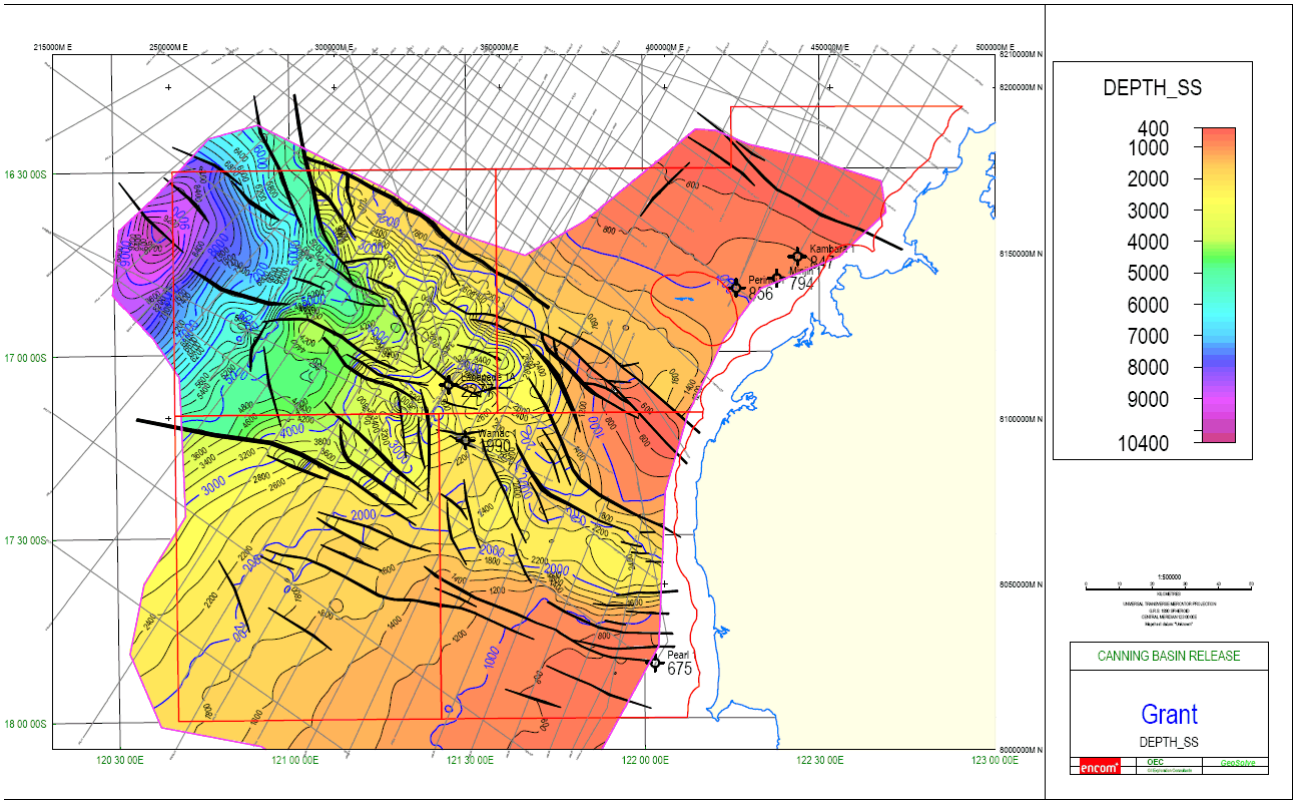

Figure 28 Depth structure near top of or subcropping Grant Fm CI 200m

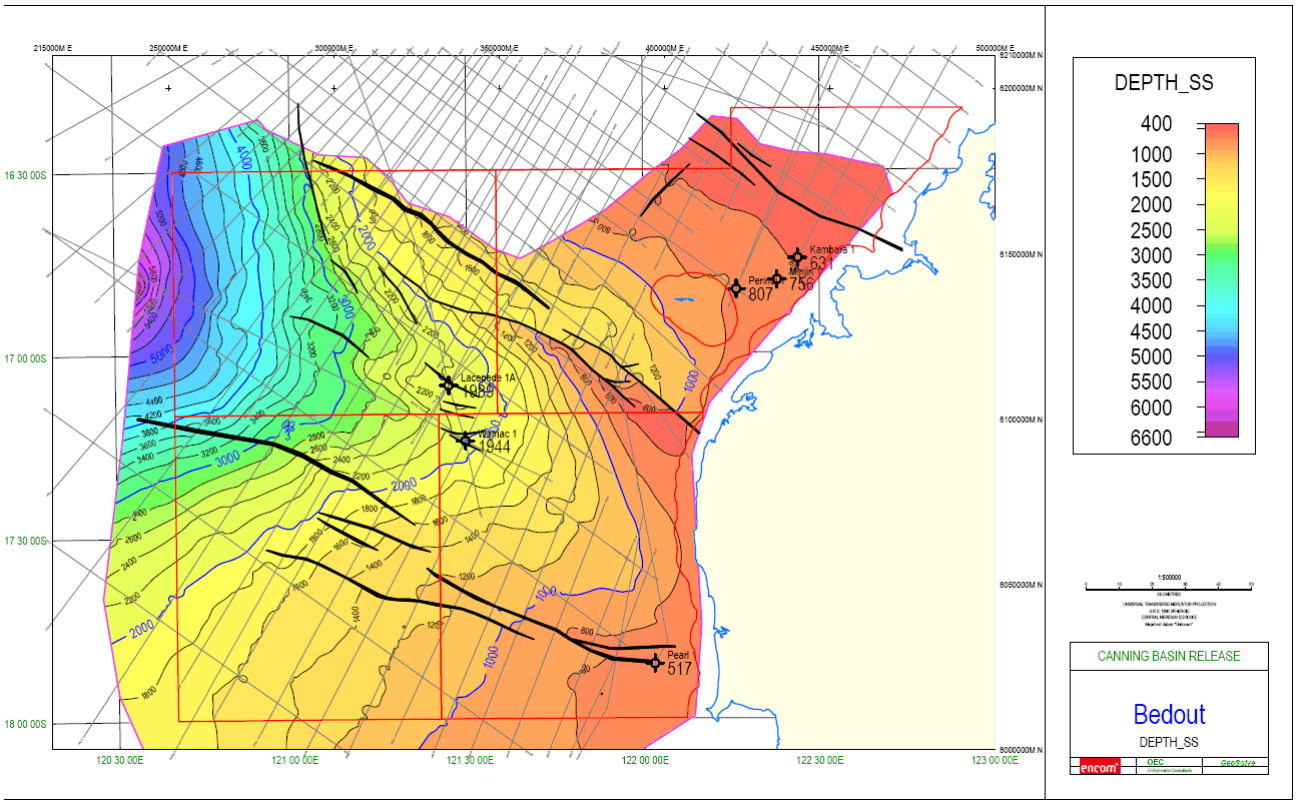

Figure 29 Depth structure Bedout U/C CI 200m

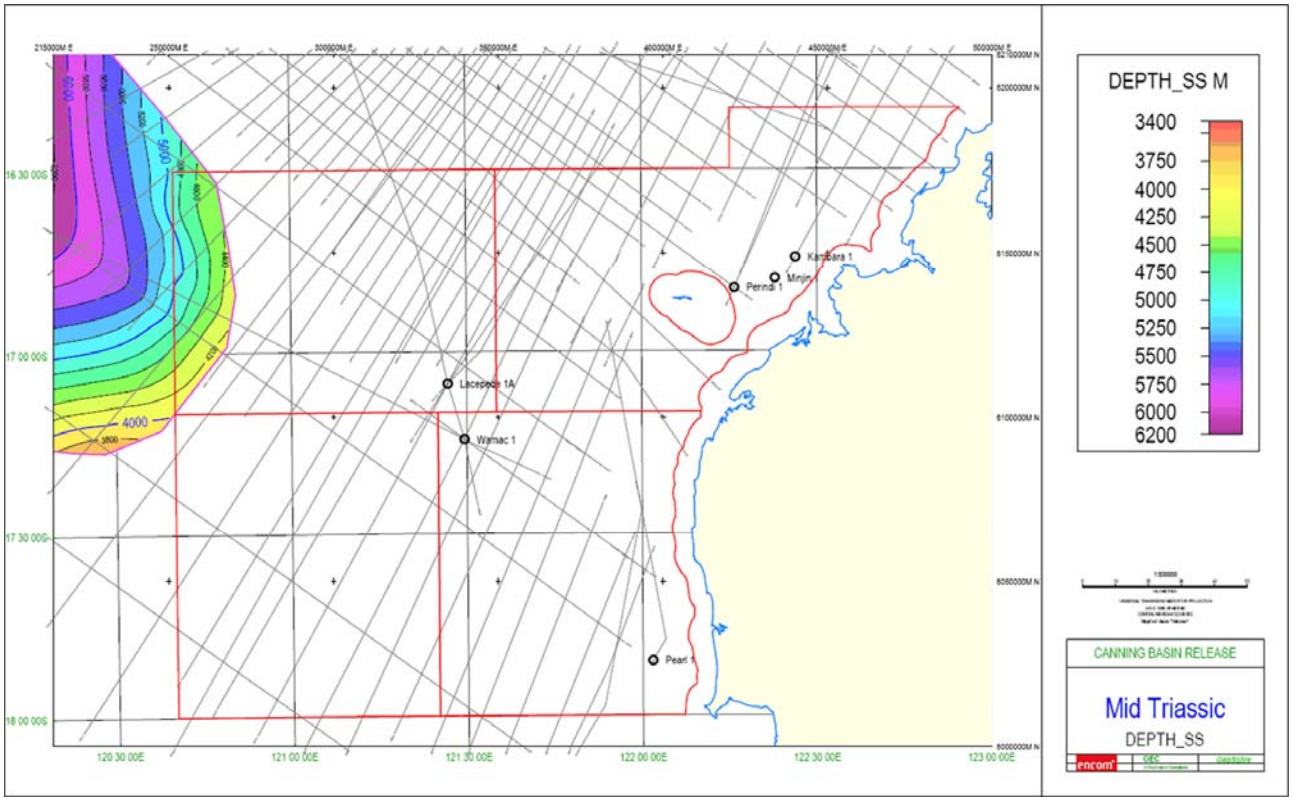

Figure 30 Depth structure Mid Triassic CI 200m

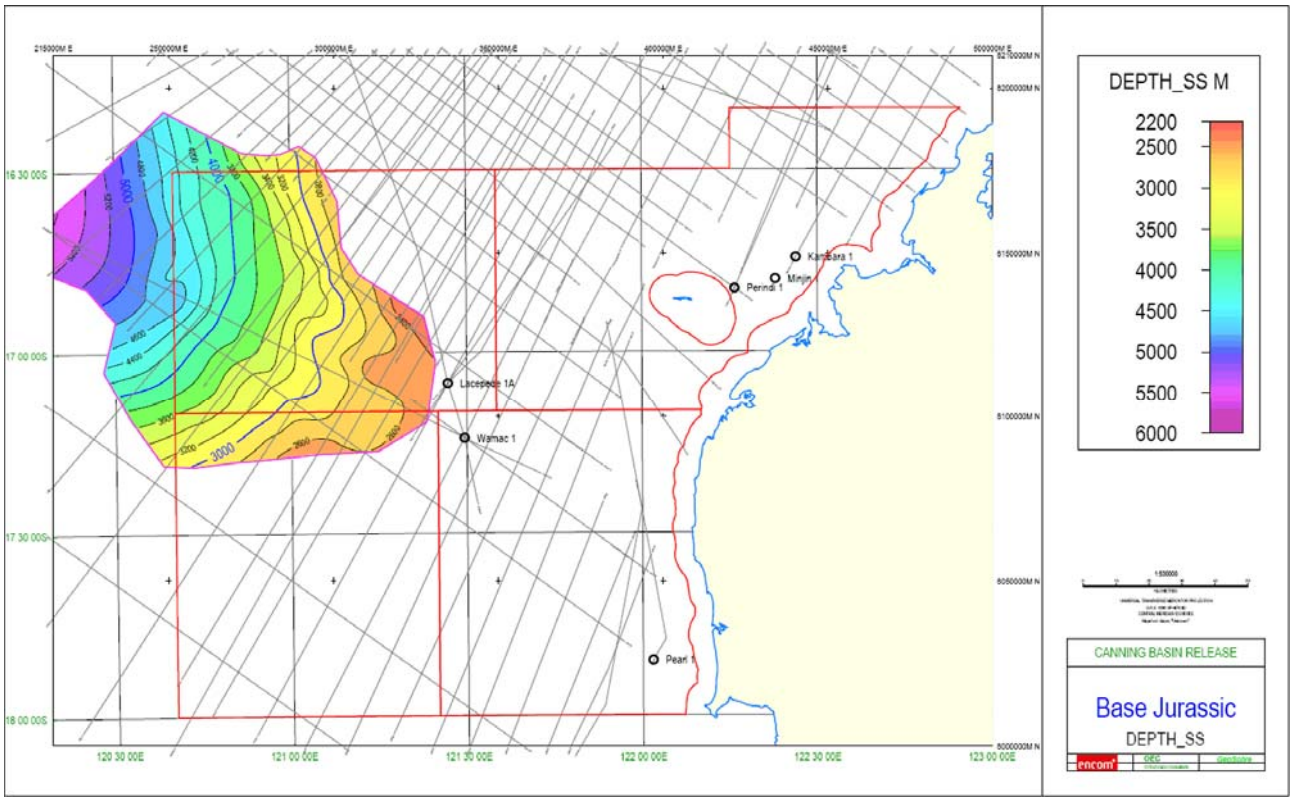

Figure 31 Depth structure Base Jurassic CI 200m

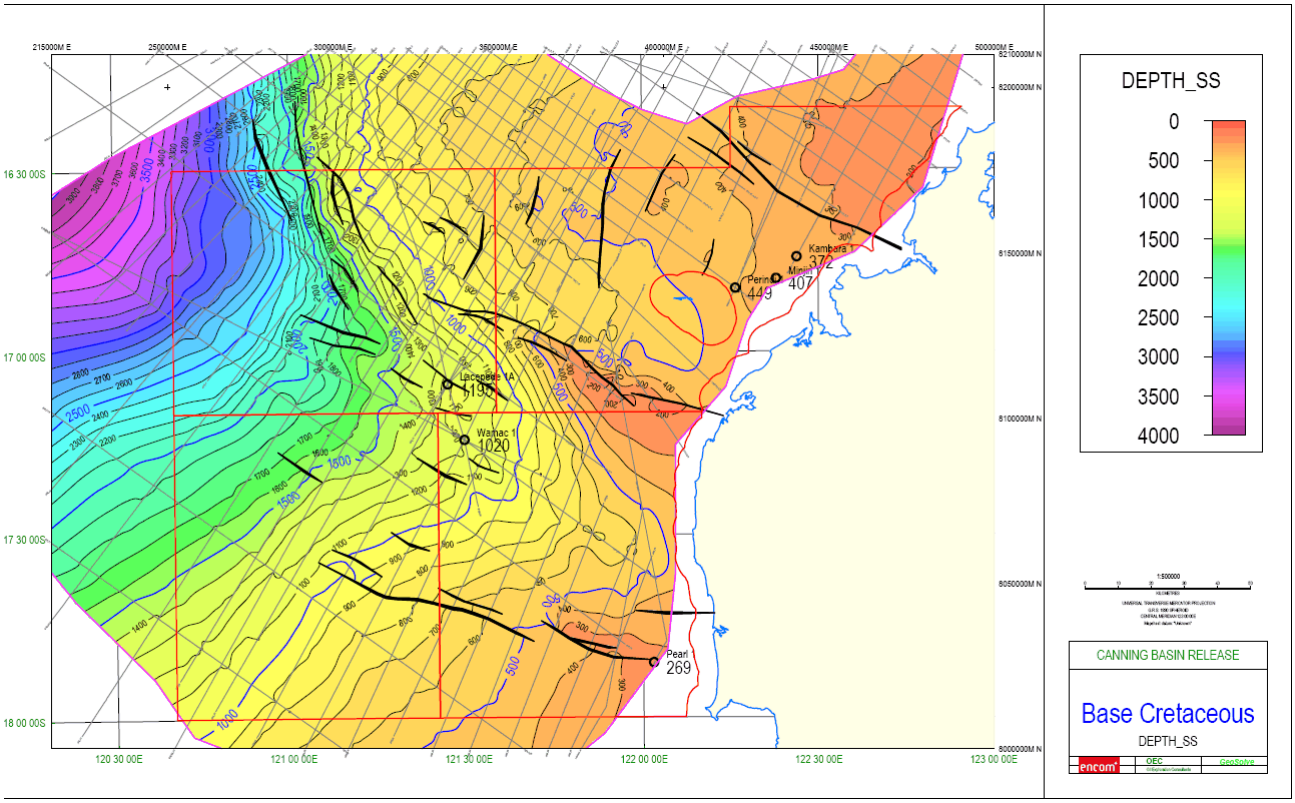

Figure 32 Depth structure Base Cretaceous CI 100m

Structure

The architecture that defines these areas is one of a complex inverted and eroded graben flanked to the north by massive undeformed basement, to the south by the eroded Ordovician Platform and overlain disconformably by folded and thrusted Mesozoics (Figure 33).

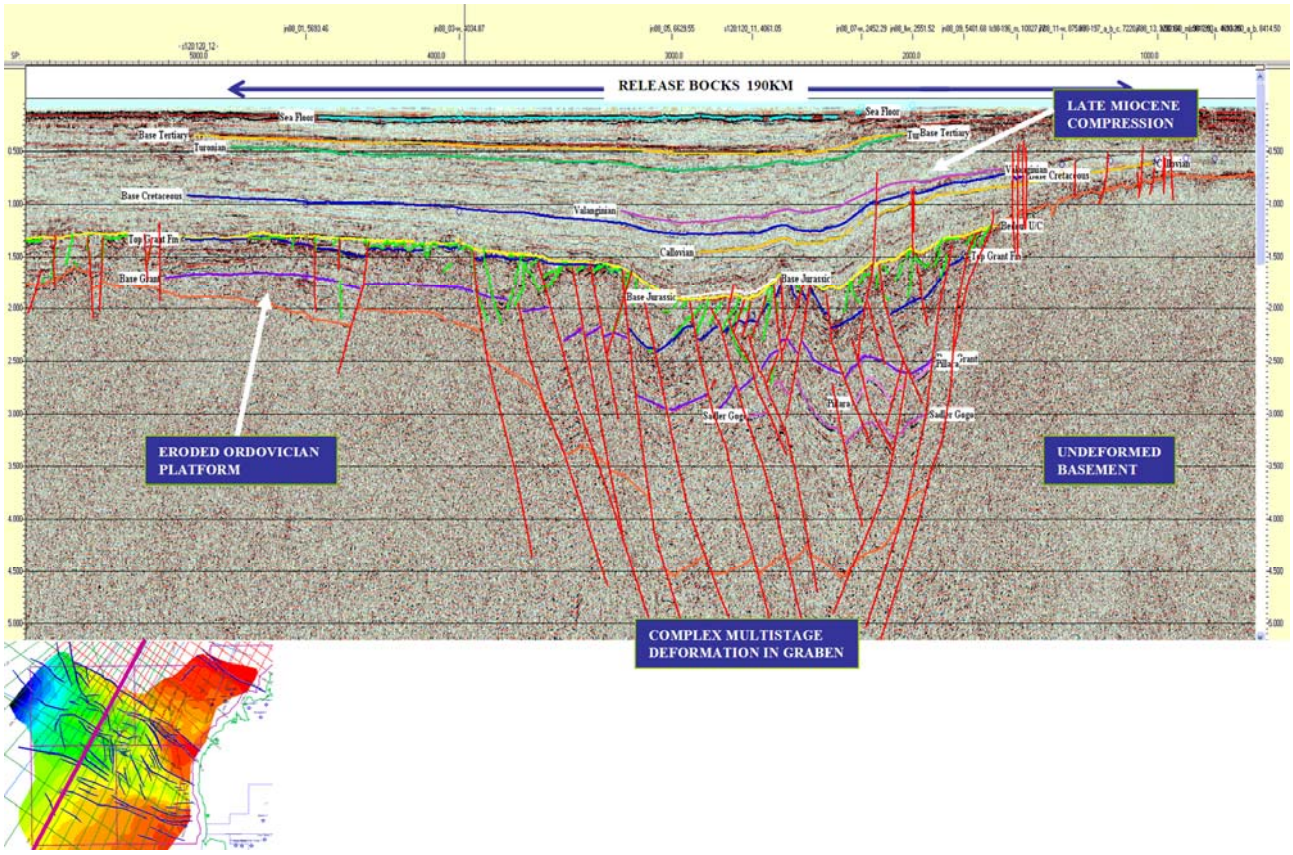

Figure 33 Line s120;120-12 Gross Structure

Seven structural events have been documented in this area (see left margin of stratigraphy diagrams Figure 22 and Figure 23).

Graben fill appears to be very thick. In the inboard axial areas it appears to extend below at least 3.5 seconds or 8 to 10km and early fill may be Silurian/Ordovician and or meta sediments (Figure 34). In deeper seismic data basement is difficult to discern. The graben flanking faults are also poorly imaged suggesting that at least in the north these faults have in part been exposed and eroded as scarps.

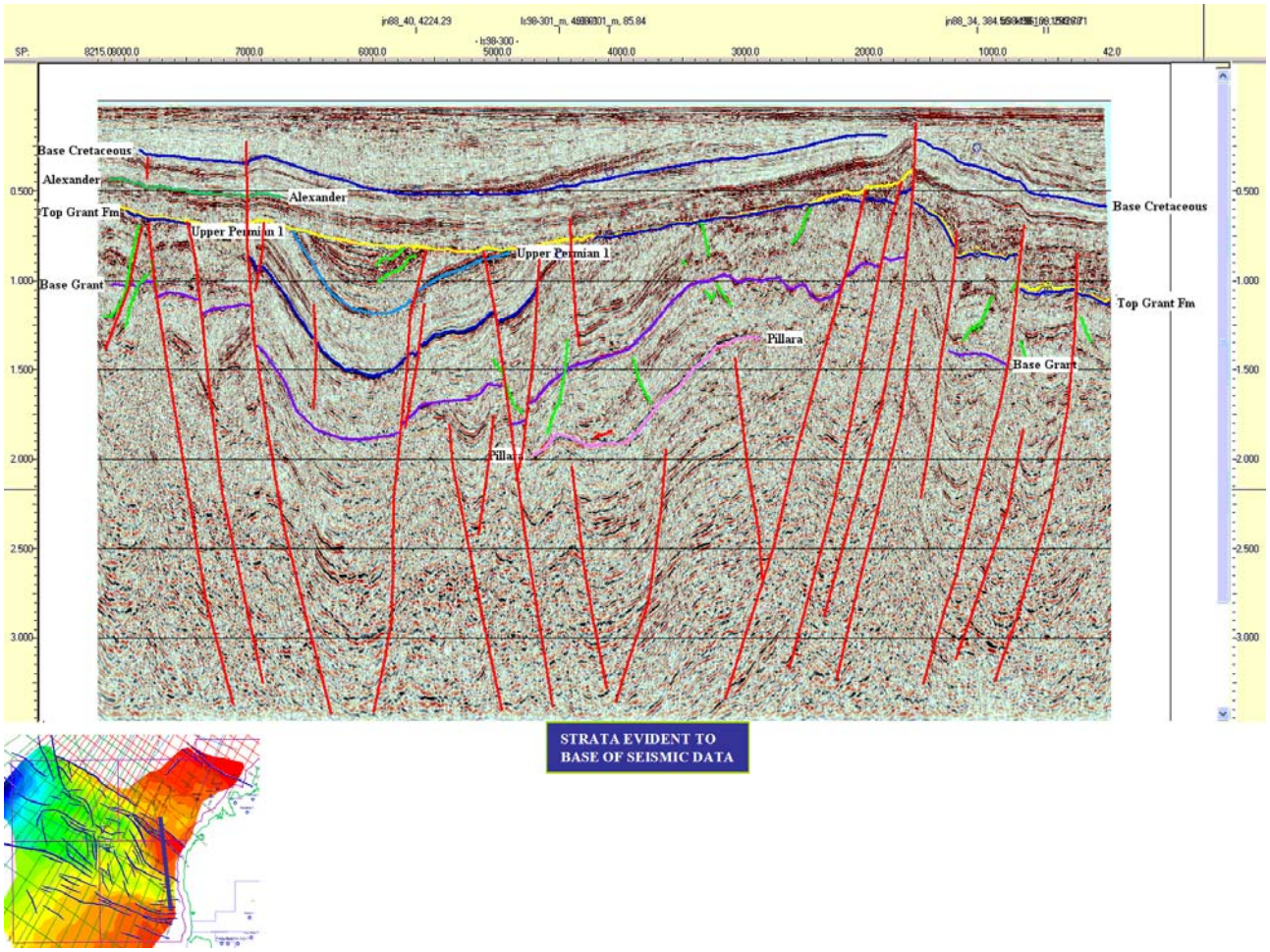

Figure 34 Line LS98-300 Deep Basement?

Evidence for both pre-Late Carboniferous extension and compression are evident in the seismic data (Figure 35).

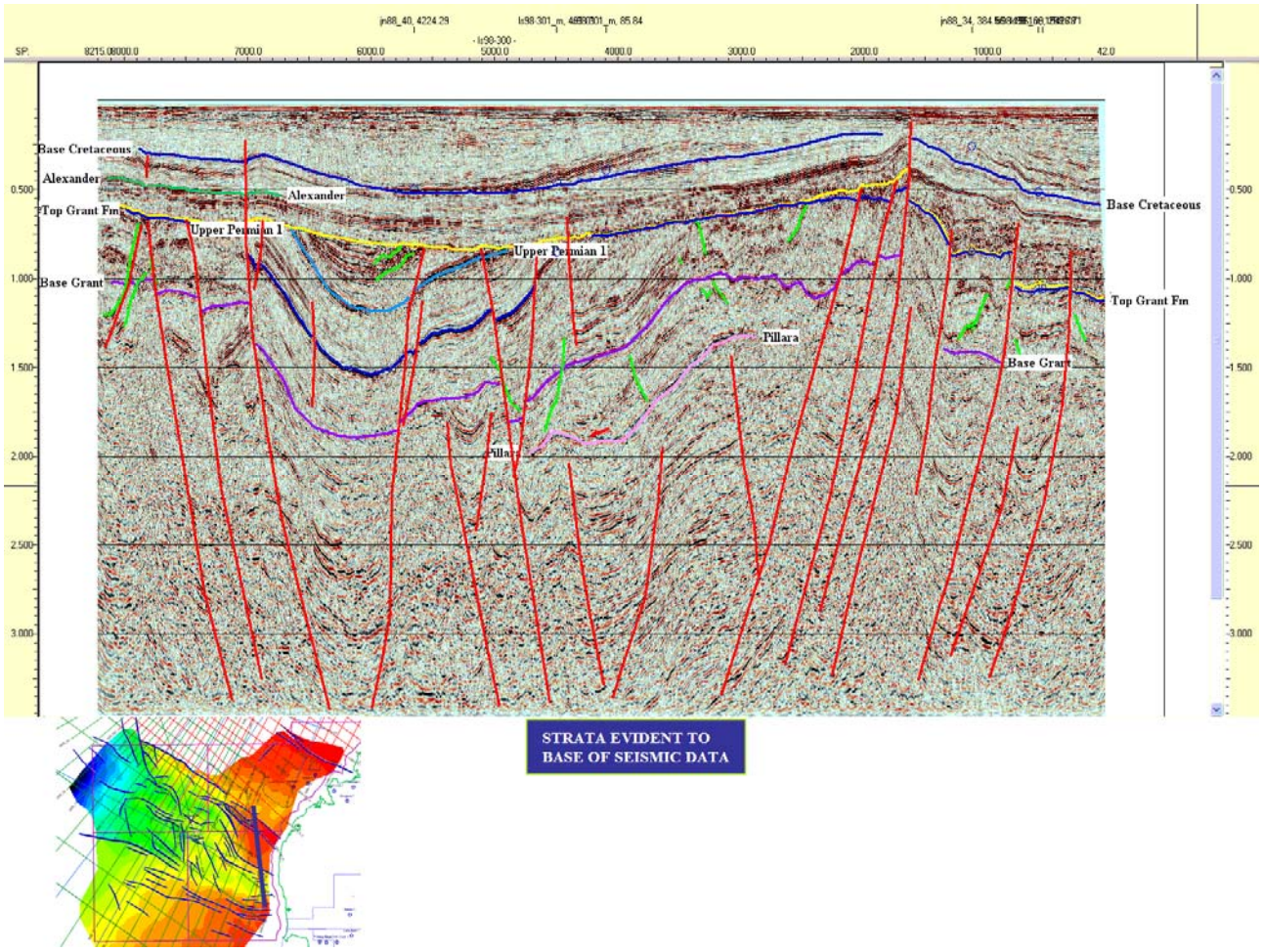

Figure 35 Line LS98-300 Pre-Late Carboniferous extension and compression

Early Permian extension resulted in block faulting. In the Mid Triassic, transpression resulted in very large scale inversion and formation of positive complex flower structures. This Triassic overprinting dominates the current architecture. Compression in the Late Miocene led to reactivation of the major faults (Figure 36 and Figure 37).

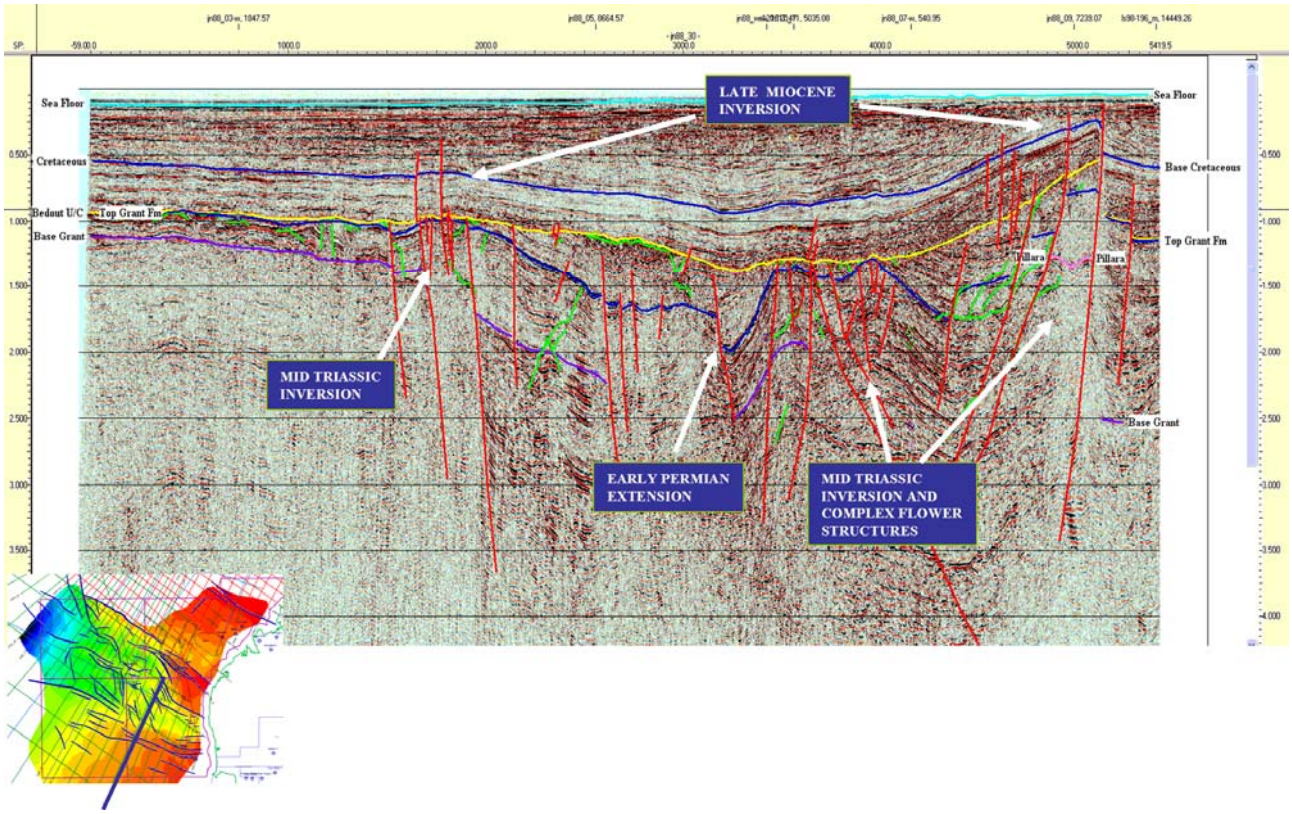

Figure 36 Line JN88-28S Early Permian, Mid Triassic Inversion and transpression and Late Miocene Compression

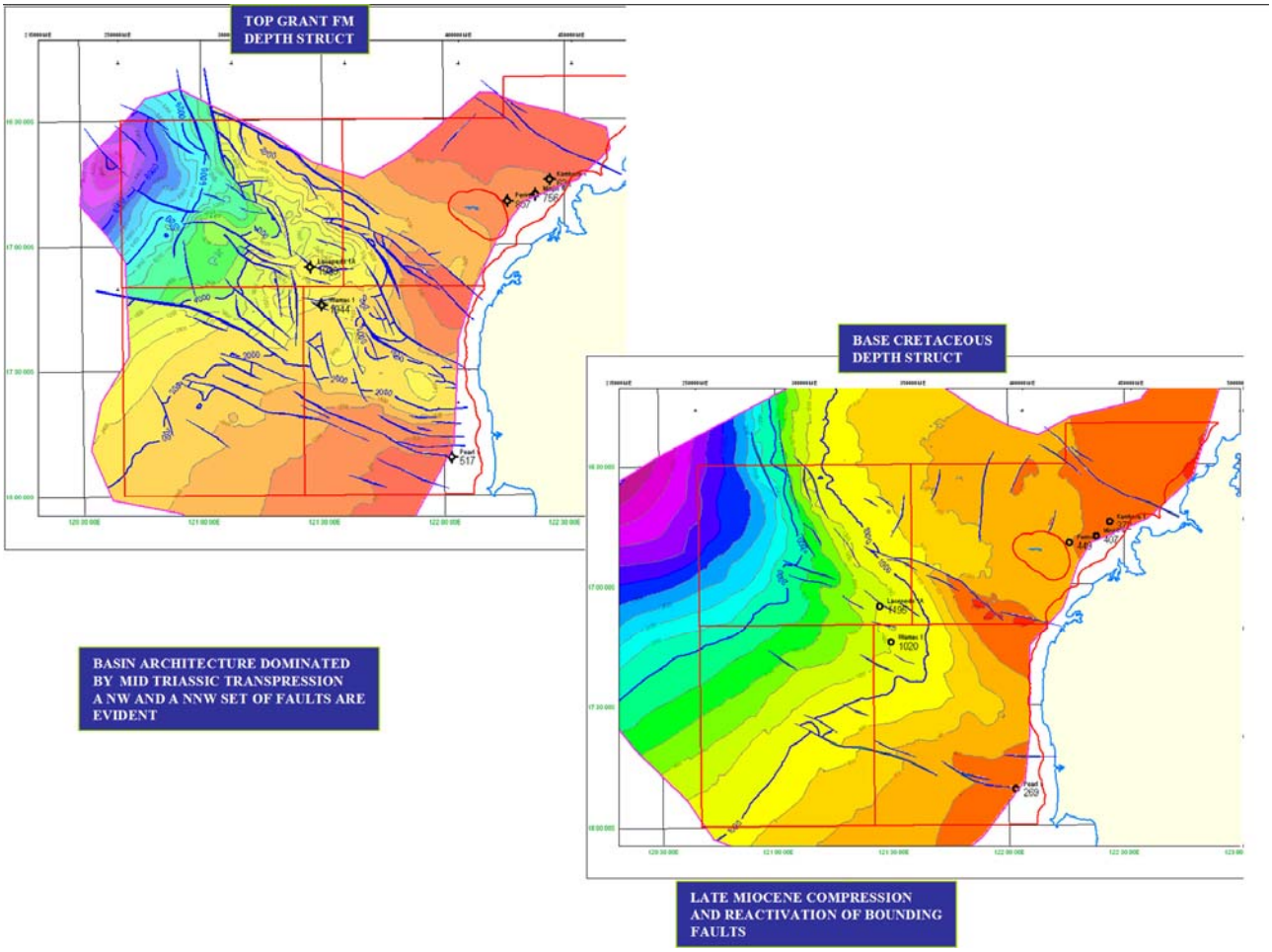

Figure 37 Top Grant Fm and Base Cretaceous surfaces

Small scale Late Miocene wrench faults occur along the northern margin of the graben. These faults are limited to the immediate northern margin, are vertical and probably en echelon. They terminate in the latest Tertiary. They have the appearance of and may be associated with gas chimneys (Figure 38).

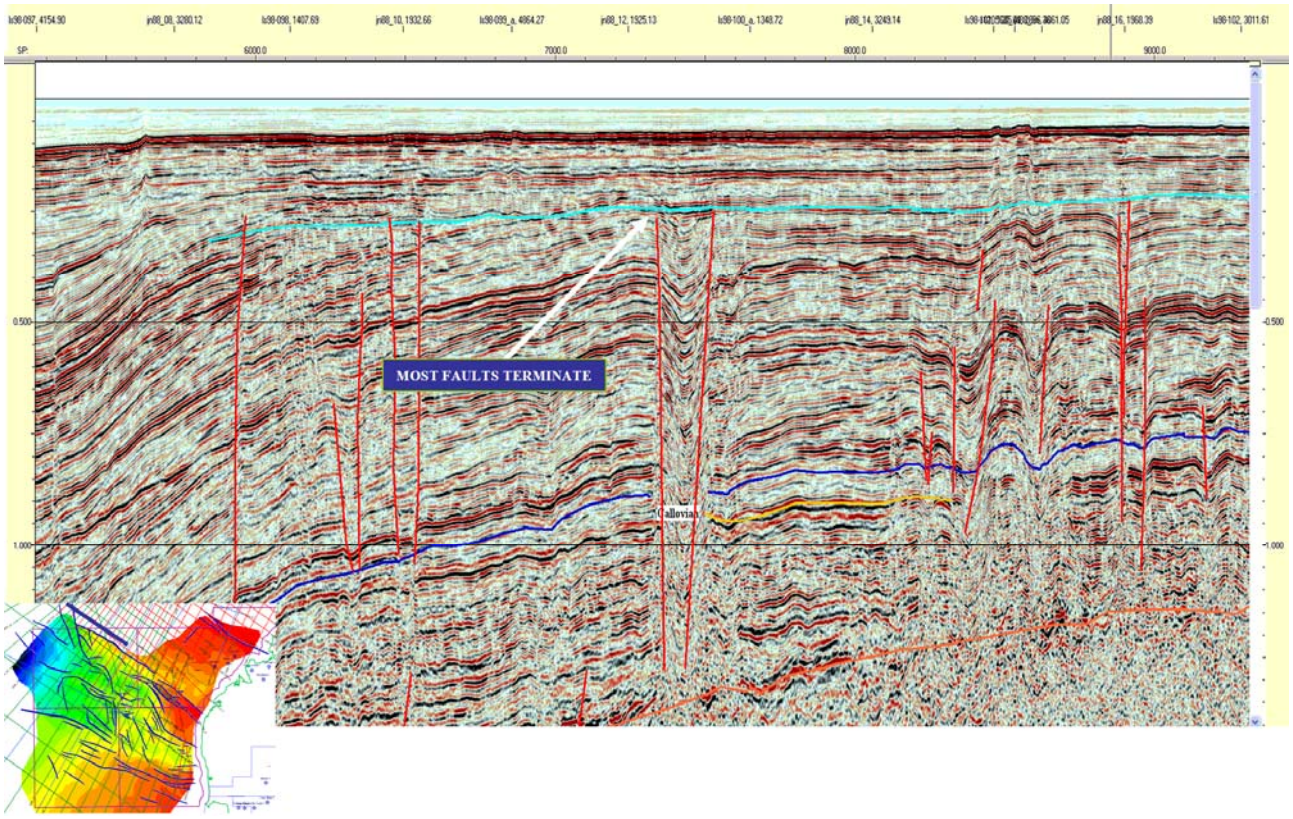

Figure 38 Line LS98-196 Late Miocene compression – small scale wrench faults along northern margin of graben

Igneous Activity

Igneous intrusives are extensive within the Palaeozoic interval (figure 25). Dykes were intersected in Perindi 1 and Wamac 1 (figure 26). These dolerites have intruded reverse and wrench fault planes and suggesting that some of these intrusives are associated with the Fitzroy movement during the Mid Triassic.

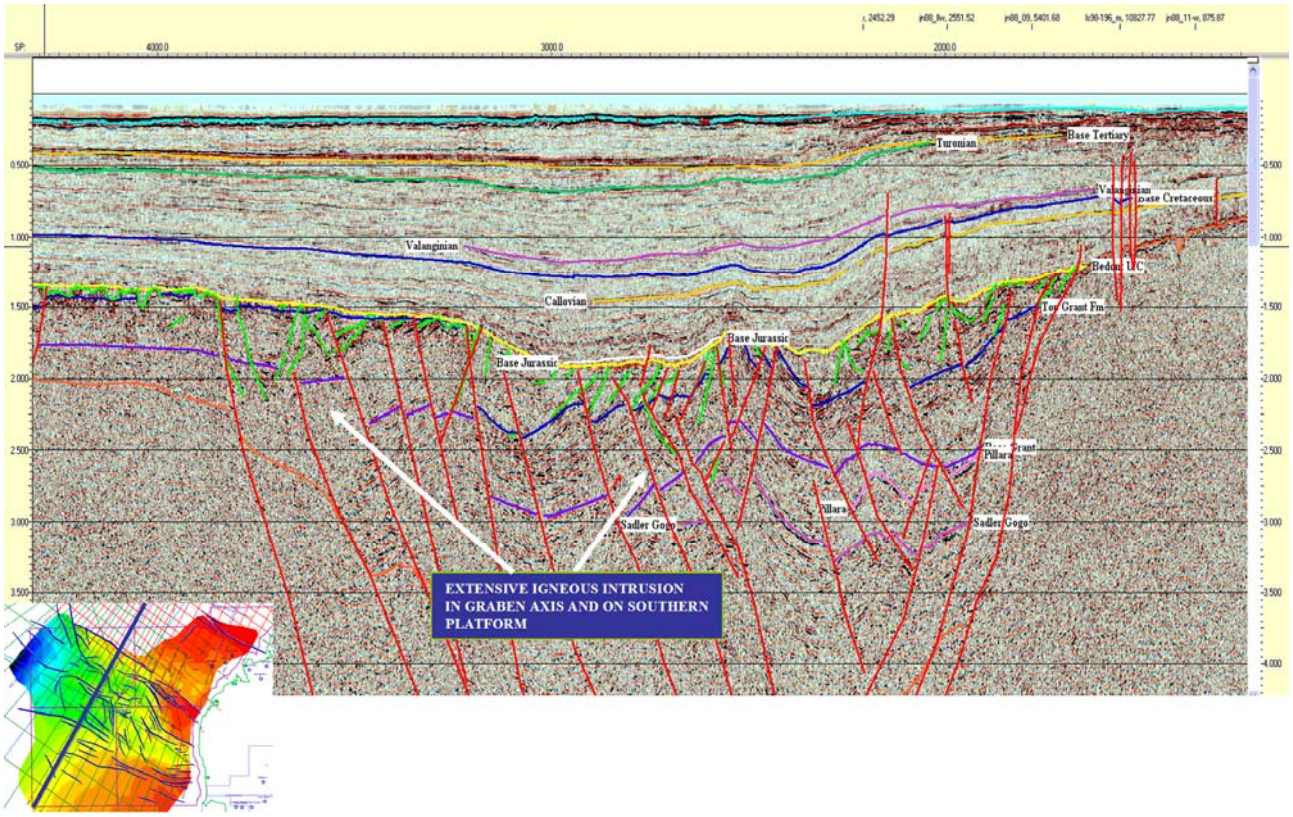

Figure 39 Line s120;120-12 Extensive igneous intrusions terminating at the Bedout U/C

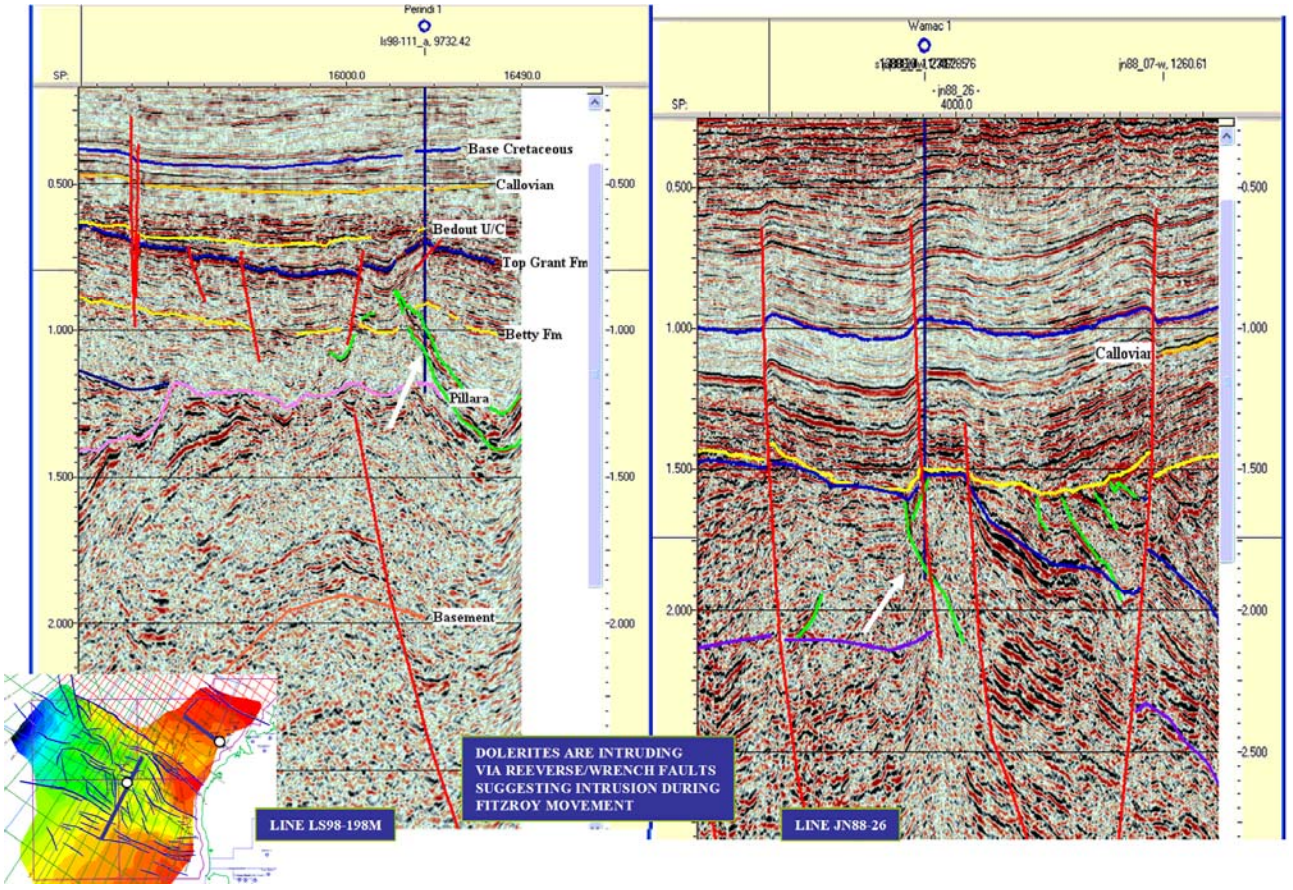

Figure 40 Dolerites intersected by Perindi 1 and Wamac 1

Anomalies

Several anomalies falling into two groups were observed. They have been noted as points of interest and no analyses have been carried out during this interpretation to evaluate these features.

Low Velocity Zones (Gas Chimneys? Lamproites? Wrench Related Brecciation?)

A number of seismic low velocity zones were evident in the vicinity of the northern margin of block W07-13. These were best observed on line LS98-196 (Figure 41).

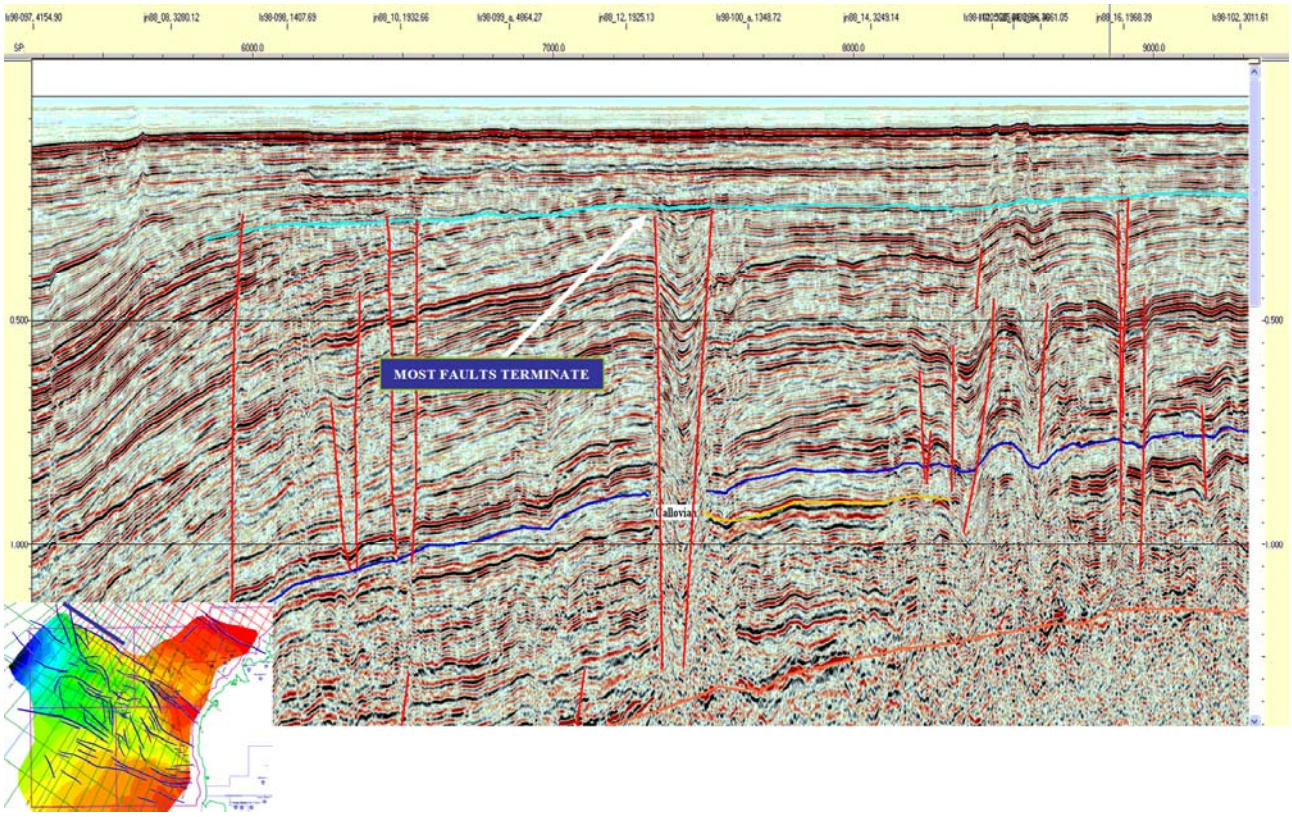

Figure 41 Line LS98-196 Late Miocene small scale wrenching and associated low velocity zones.

The facts as best can be determined are:

- They are low velocity zones as evident by the draw down of seismic events
- The margins are often faulted
- Most do not reach surface (and where they appear to, there is a possibility that this effect was introduced in processing)
- It is difficult to determine whether they intersect basement but in some cases they do not appear to do so.
- They are not undershot and have sharp margins at all depths, indicating they have true vertical extent
- Strata can be seen across the zones (they are not completely disrupted
- They predominantly fall in a zone along the northern margin of the basin where the basement is shallow.

Possible explanations are:

- Gas Chimneys
  - Gas chimneys would produce a low velocity zone
  - However, for the gas to get into the observed locations, it would have to migrate up the northern basin boundary faults to appear over the basement.
  - These features are not evident elsewhere in the basin
- Lamproites
  - The best evidence for these being Lamproites is their similarity to seismic sections shot over the Northern Bonaparte Basin (Gorter and Glikson 2002).
  - Lamproites have also been mapped on shore in the West Kimberly, including “pipes, plugs, sills and dykes” (Jaques and Milligan 2004).
  - In general, they do not have a magnetic signature.
- Wrench Related Brecciation
  - Faulting is evident at the margins of these zones
  - Wrench related faulting is consistent with the structural regime in the area.
  - Seismic lines are too sparse to determine a strike on these features.

The favoured interpretation is that these are zones of brecciation related to wrench faults on the northern margin of the basin. Whether or not they are Lamproites is unclear. It is possible that Lamproites intruded along the zones of weakness caused by the wrench faulting. They would not necessarily have to be magnetic if they had a titanium rich composition (as reported in the Bonaparte Basin by Gorter and Glikson 2002). This would favour the development of Ilmenite rather than magnetite.

The timing of the wrenching is estimated to be late Miocene.

Seismic Brightening

Brightening and an apparent ‘flat spot’ are present over the crest of a structure in the axial zone of the graben (figure 28).

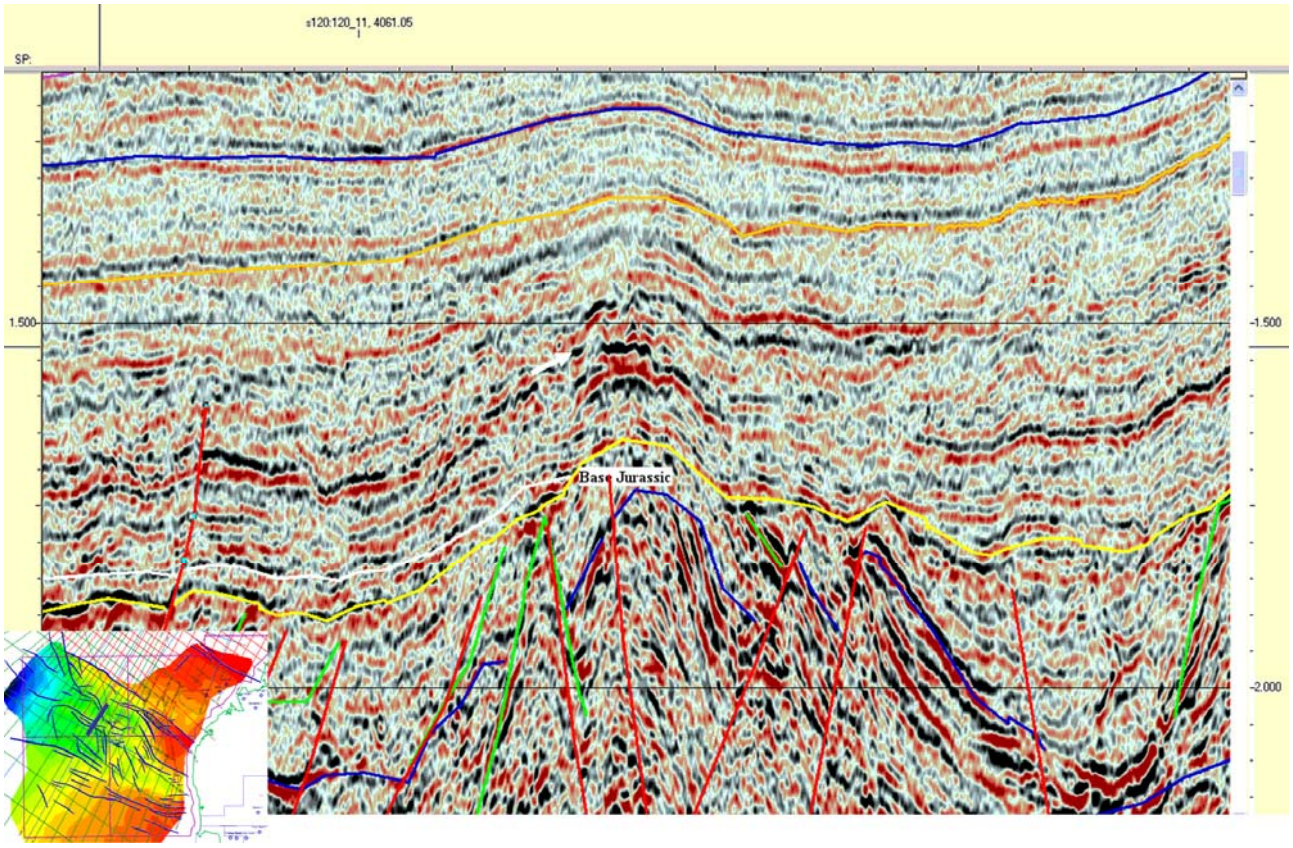

Figure 42 Line S120;120-12 Possible anomaly in Jurassic

Play Types

This section relates to the presence of structural and stratigraphic plays based only on observed seismic geometries. Play types are summarized in table 3.

Table 3 Play Types

Block	Play Types
Block W07-12	Mid and Late Devonian Carbonates both reefal and in structures. Late Devonian fans and fan deltas. Carboniferous and Devonian in large wrenched and inverted fault blocks. **Figure 43 to Figure 46 refer**
Block W07-13	Carboniferous in buttress plays associated with 'gas chimneys'. Carboniferous and Devonian in large wrenched and inverted fault blocks. Onlap and pinchout plays at the base of the Jurassic and Mid Triassic. Early Cretaceous (Berriasian?) submarine fans. **Figure 47 to Figure 56 refer**
Block W07-14	Carboniferous in buttress plays and inverted normal fault blocks. Onlap and pinchout plays at the base of the Jurassic. Early Cretaceous (Berriasian?) submarine fans. **Figure 57 to Figure 59 refer**
Block W07-15	Carboniferous in inverted/wrenched fault blocks and inverted buttresses along southern margin. **Figure 60 to Figure 63 refer**

Block W07-12

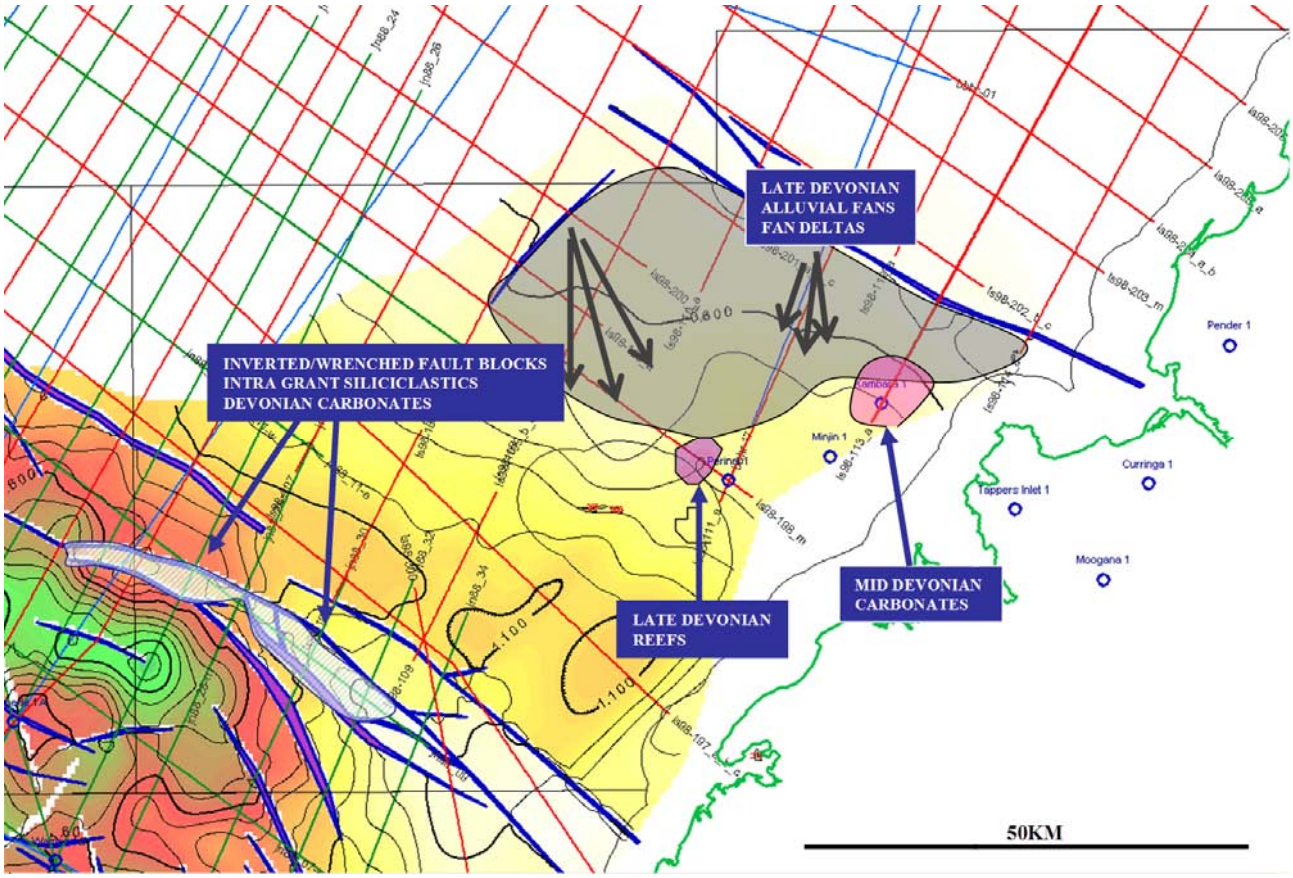

Figure 43 Block W07-12 Play Types (top Grant structure)

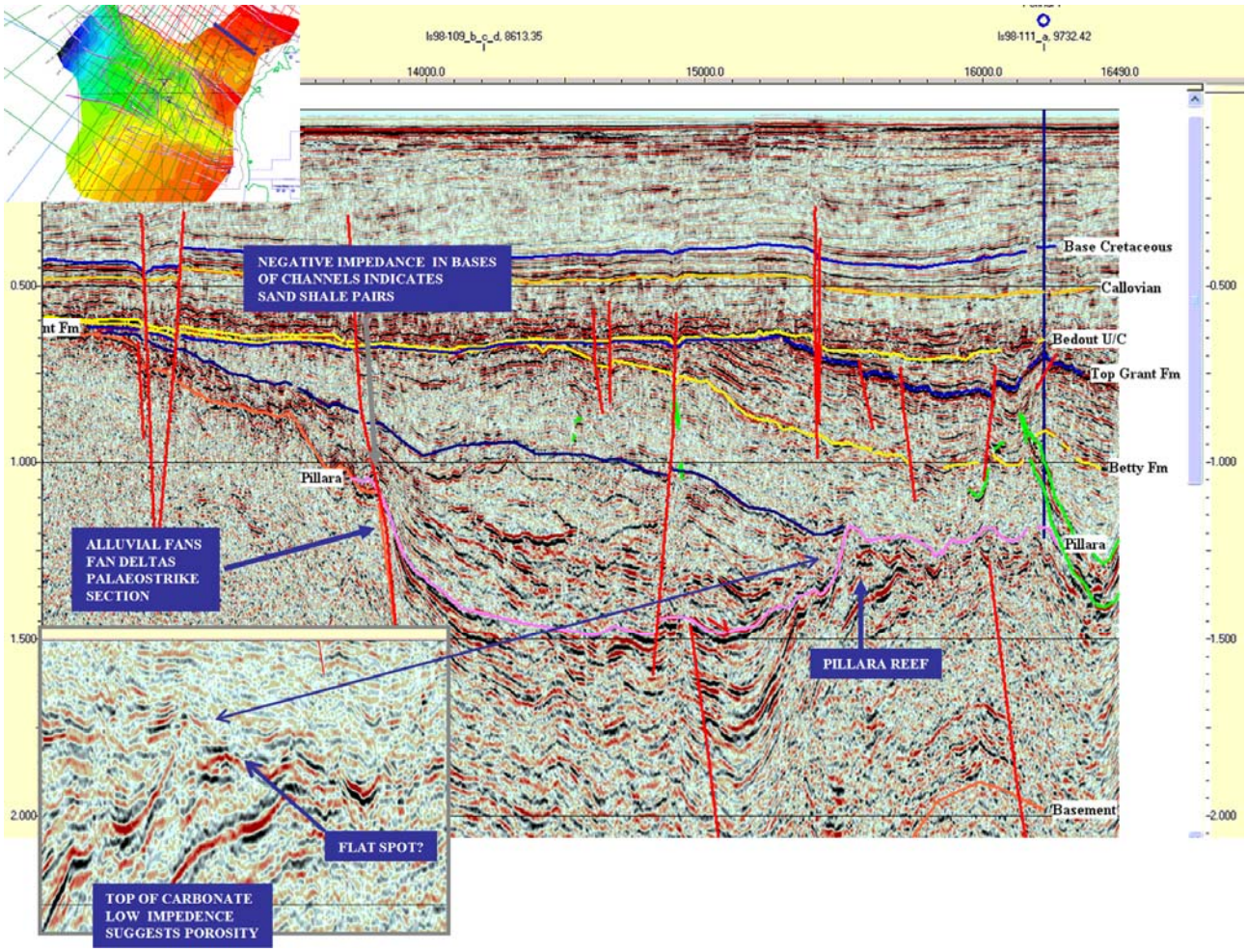

Figure 44 Line LS98-198 Devonian Reef and Alluvial Fan Fandelta

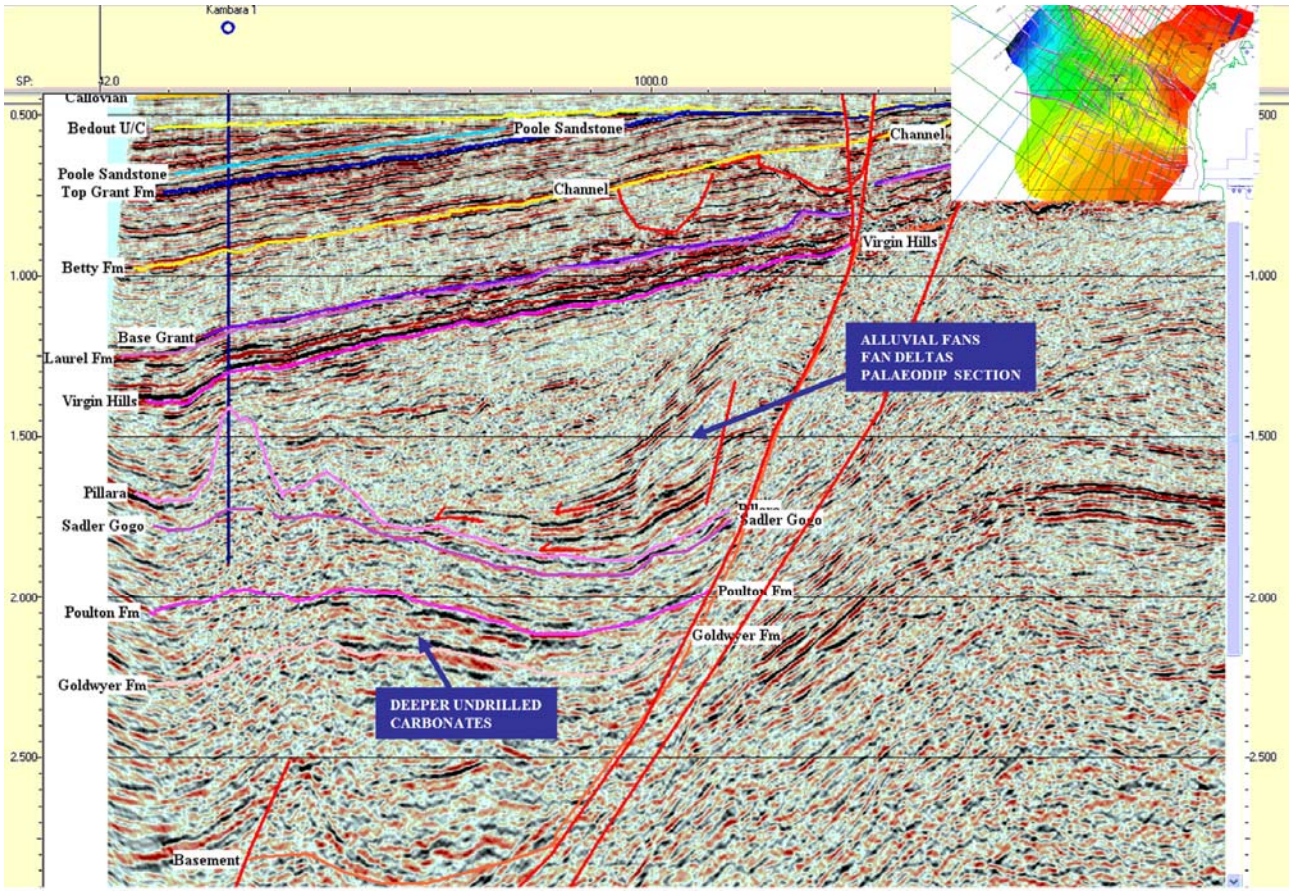

Figure 45 Line LS98-113 mid? Devonian Carbonates and Alluvial Fan Fandelta

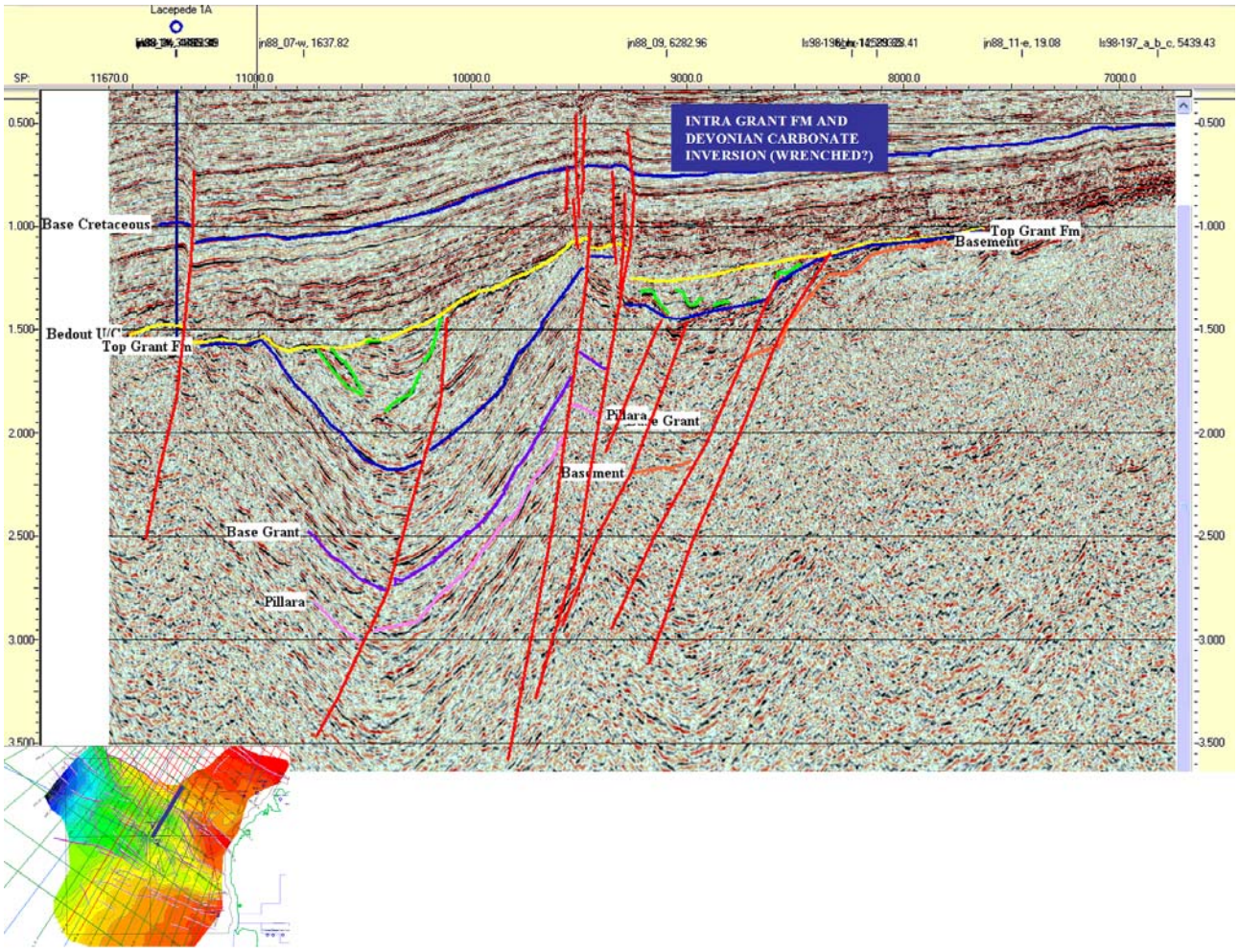

Figure 46 Line LS98-106 Intra Grant Fm siliciclastics and Devonian Carbonates

Block W07-13

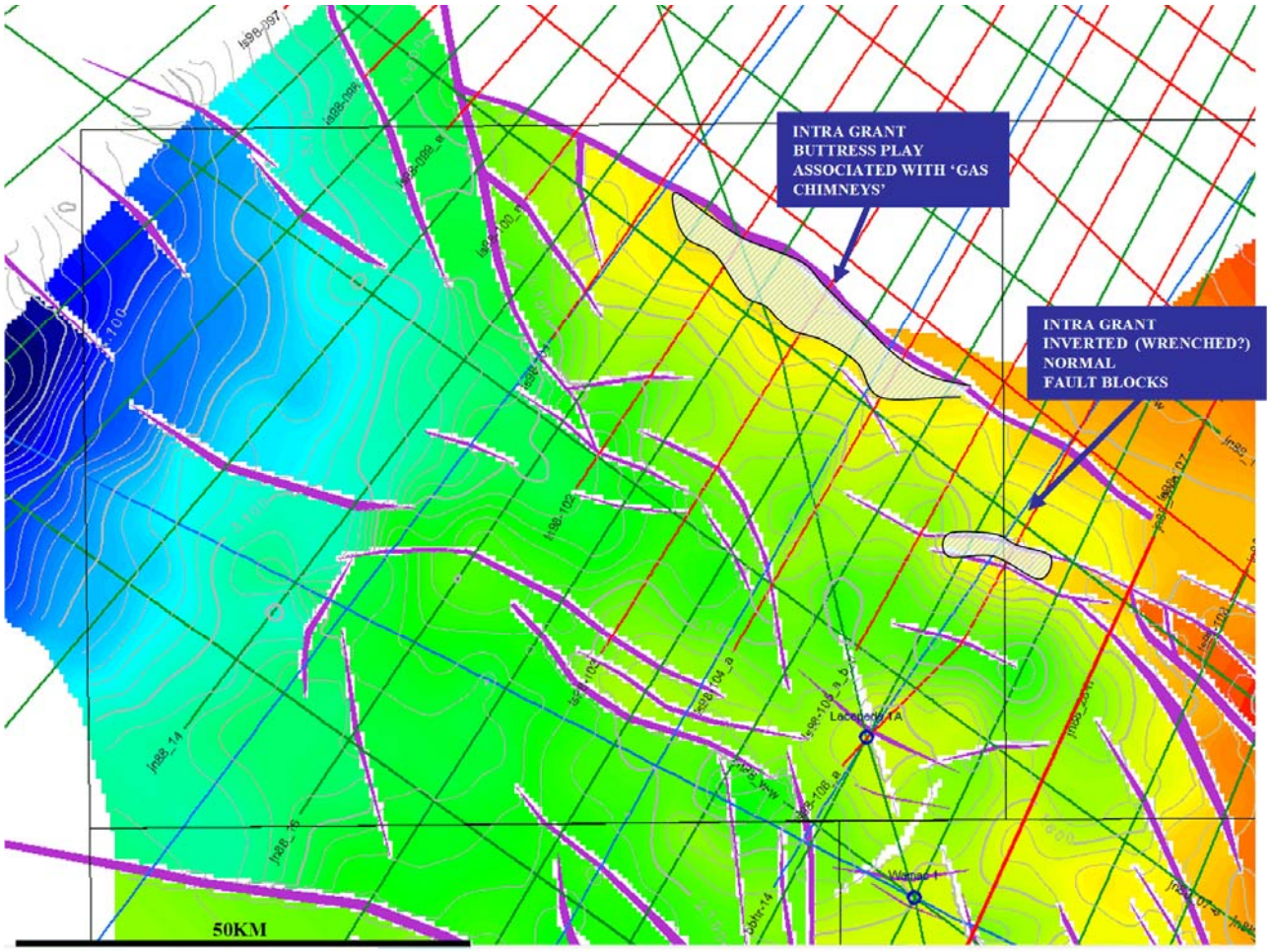

Figure 47 Block W07-13 Play Types (top Grant structure)

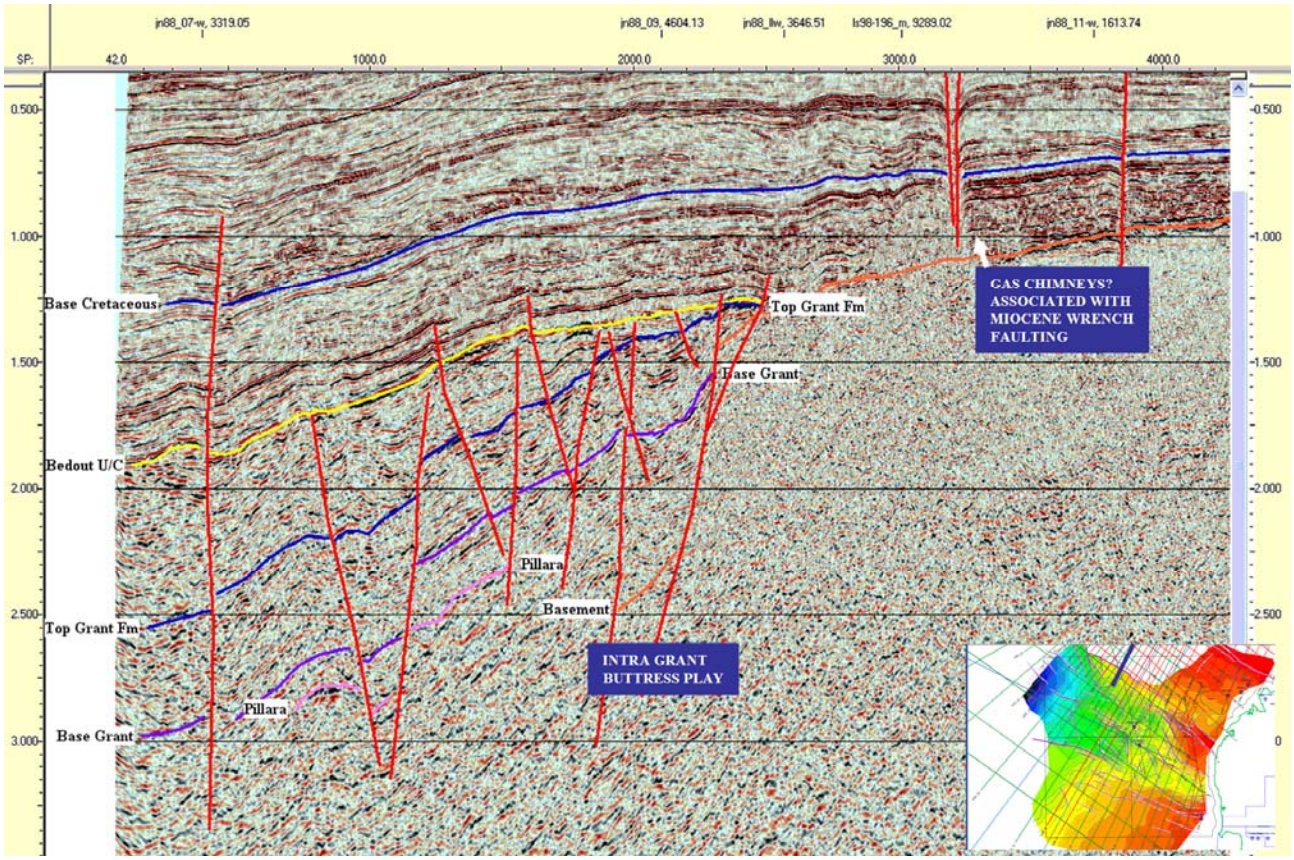

Figure 48 Line LS98-102 Carboniferous Intra-Grant Fm Buttress

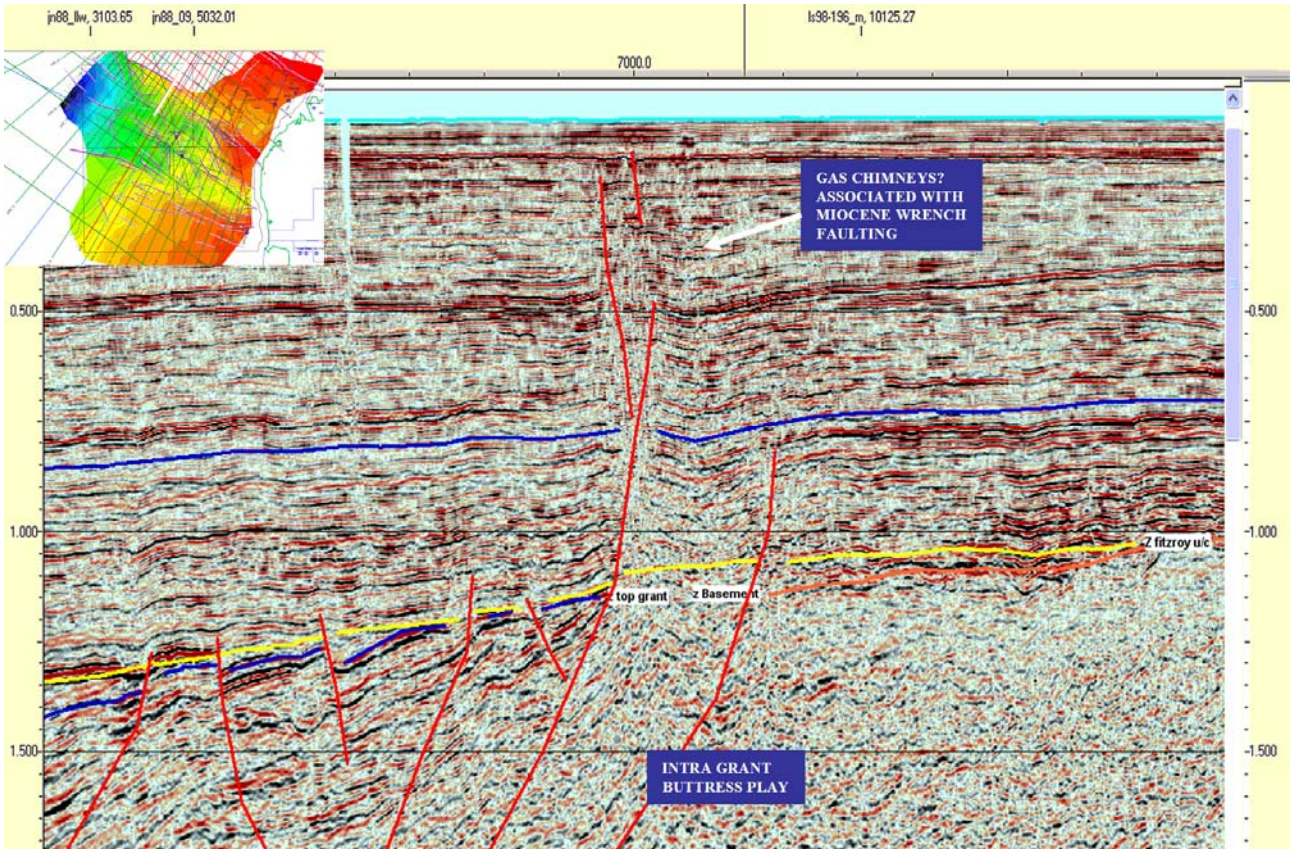

Figure 49 Line LS98-103 Carboniferous Intra-Grant Fm Buttress

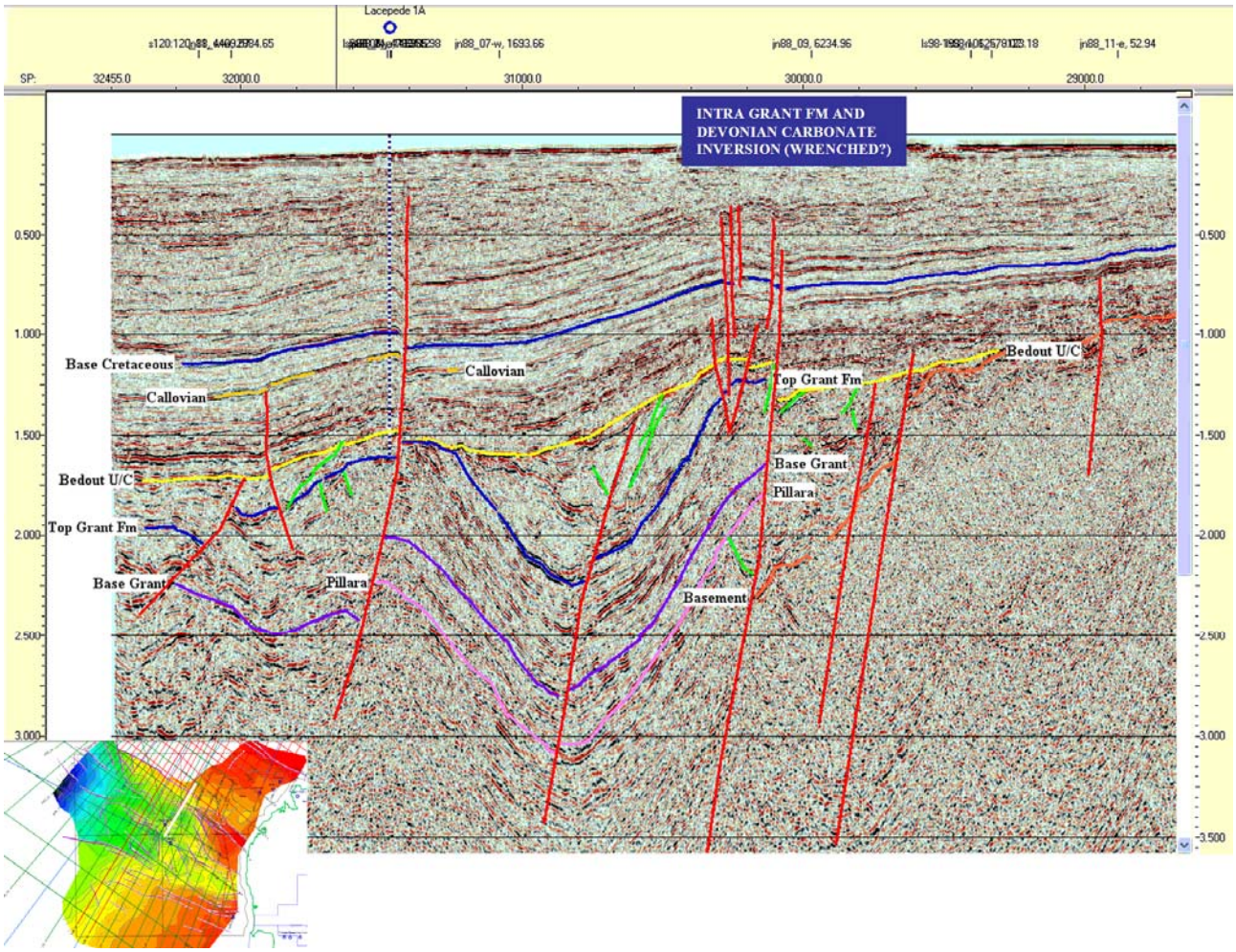

Figure 50 Line BBHR-14 Intra Grant Fm siliciclastics and Devonian carbonates

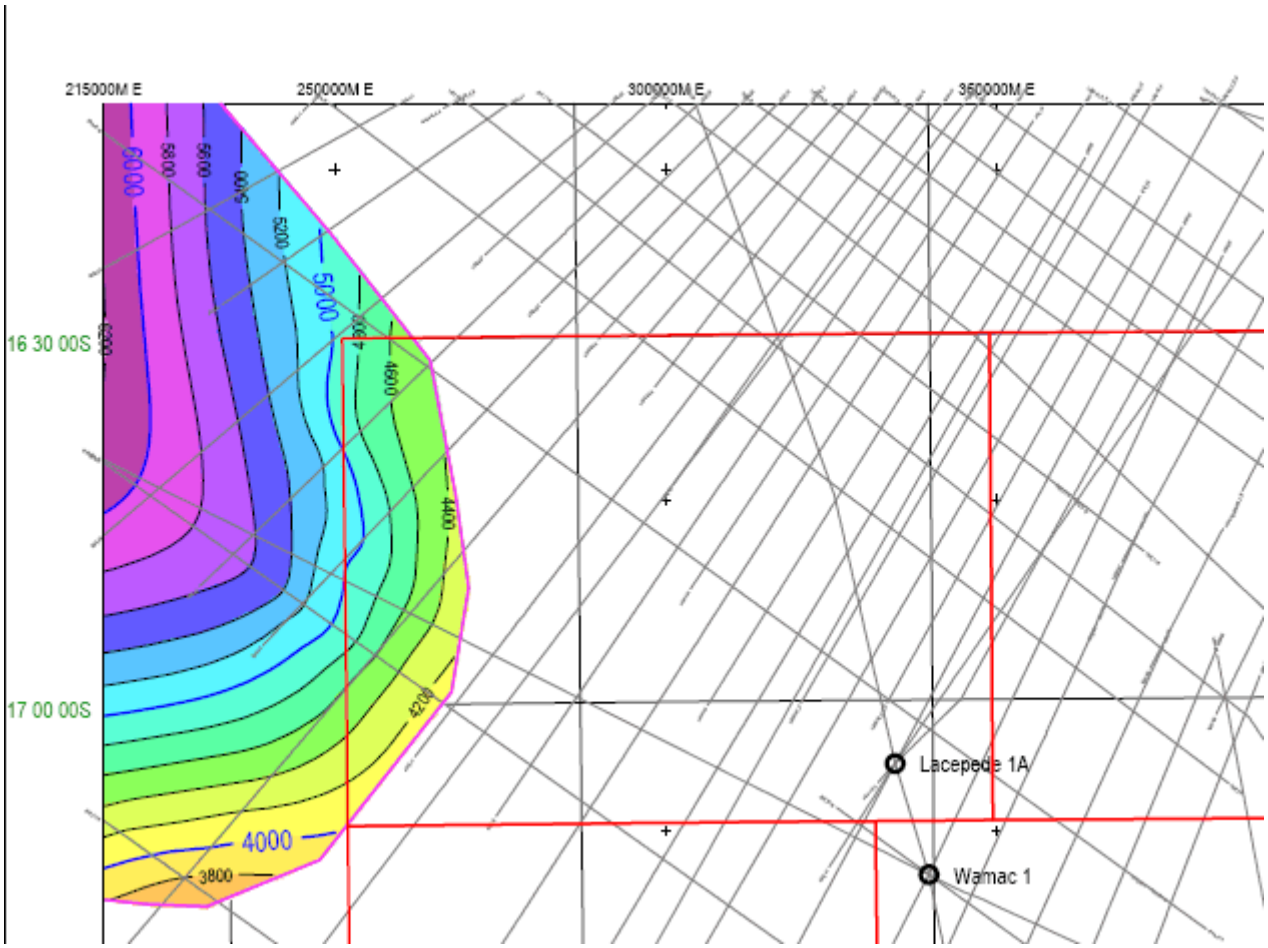

Figure 51 Block W07-13 Mid Triassic onlap

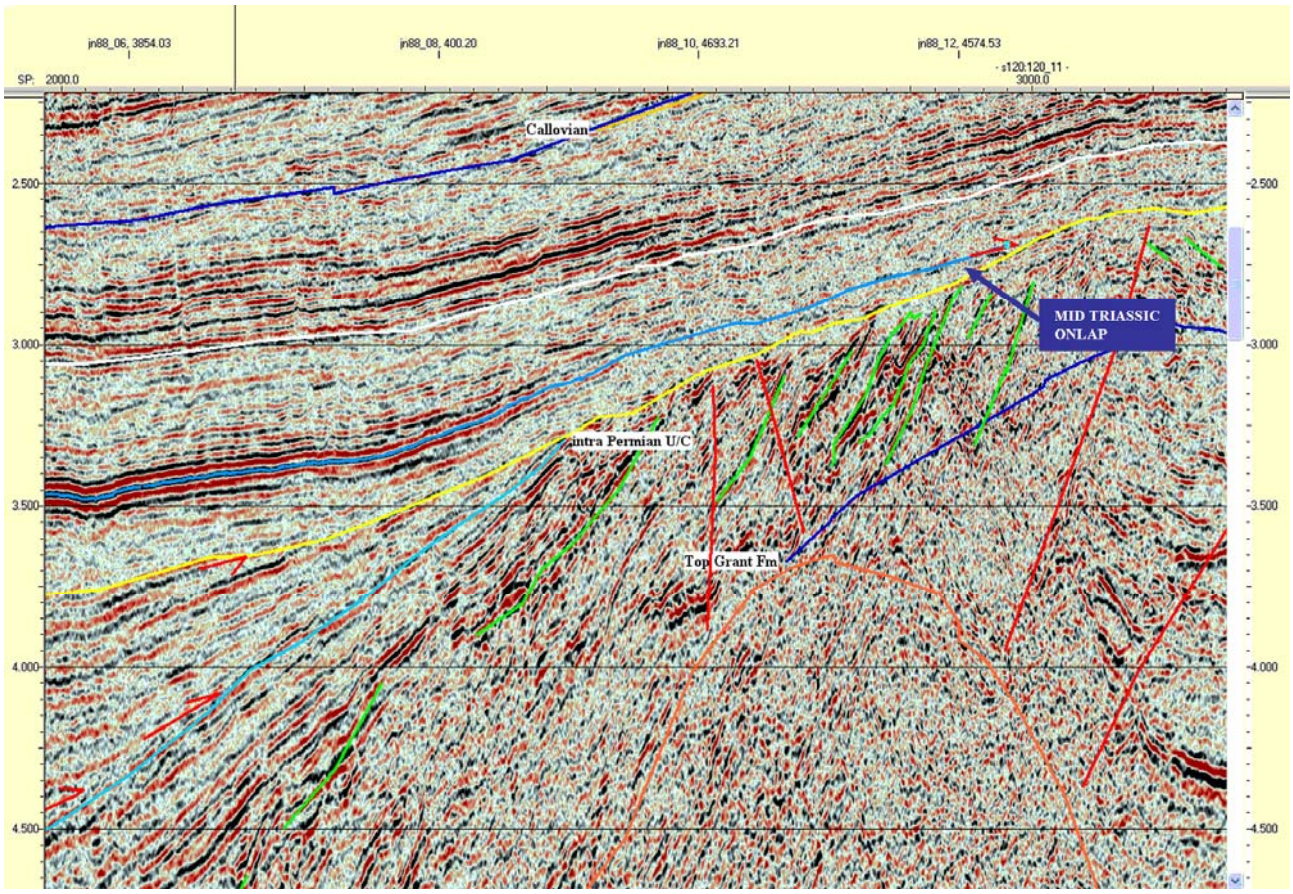

Figure 52 Line S120;120-11 Mid Triassic onlap and pinchout

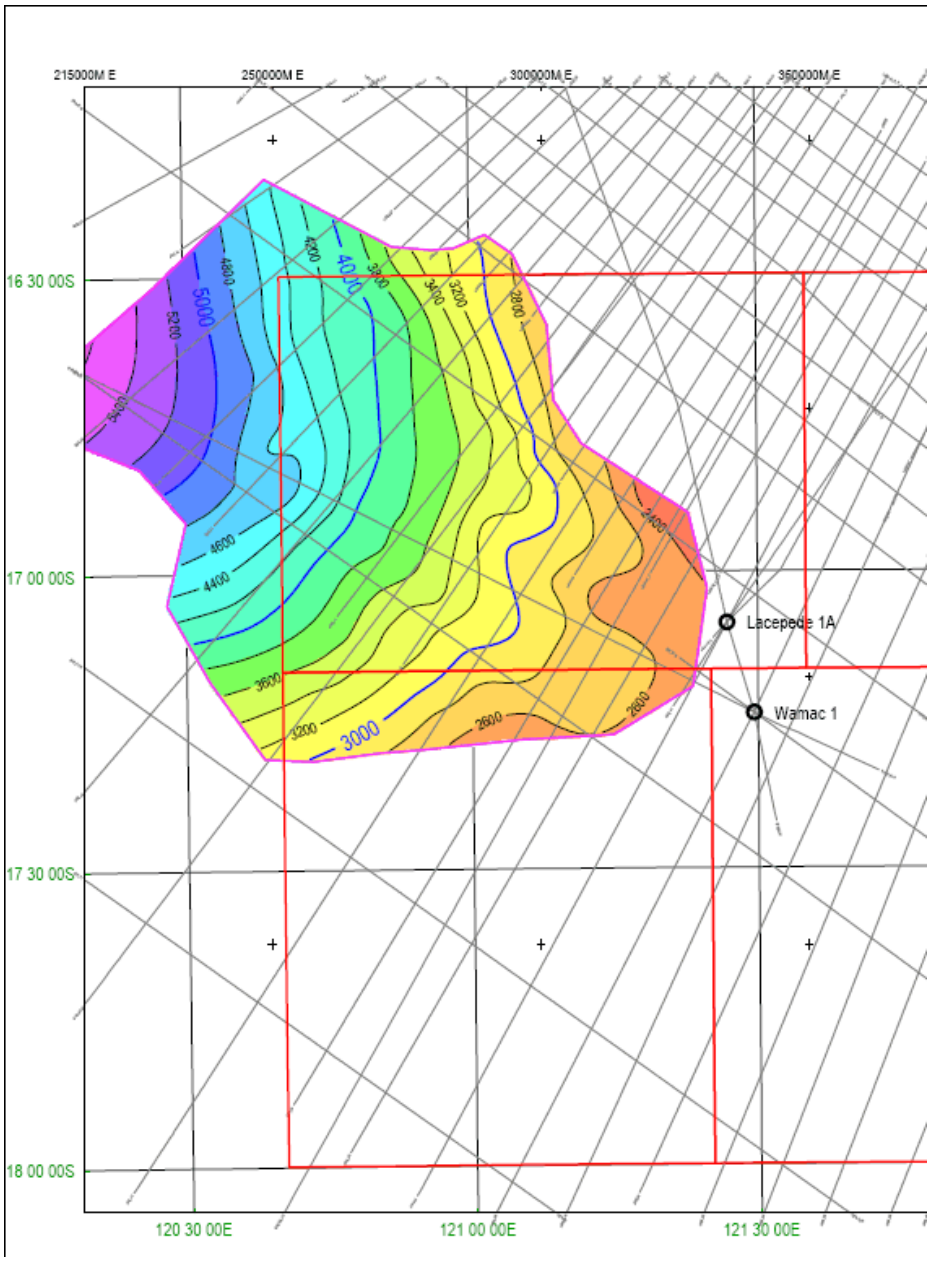

Figure 53 W07-13, 14 Base Jurassic onlap and pinchout

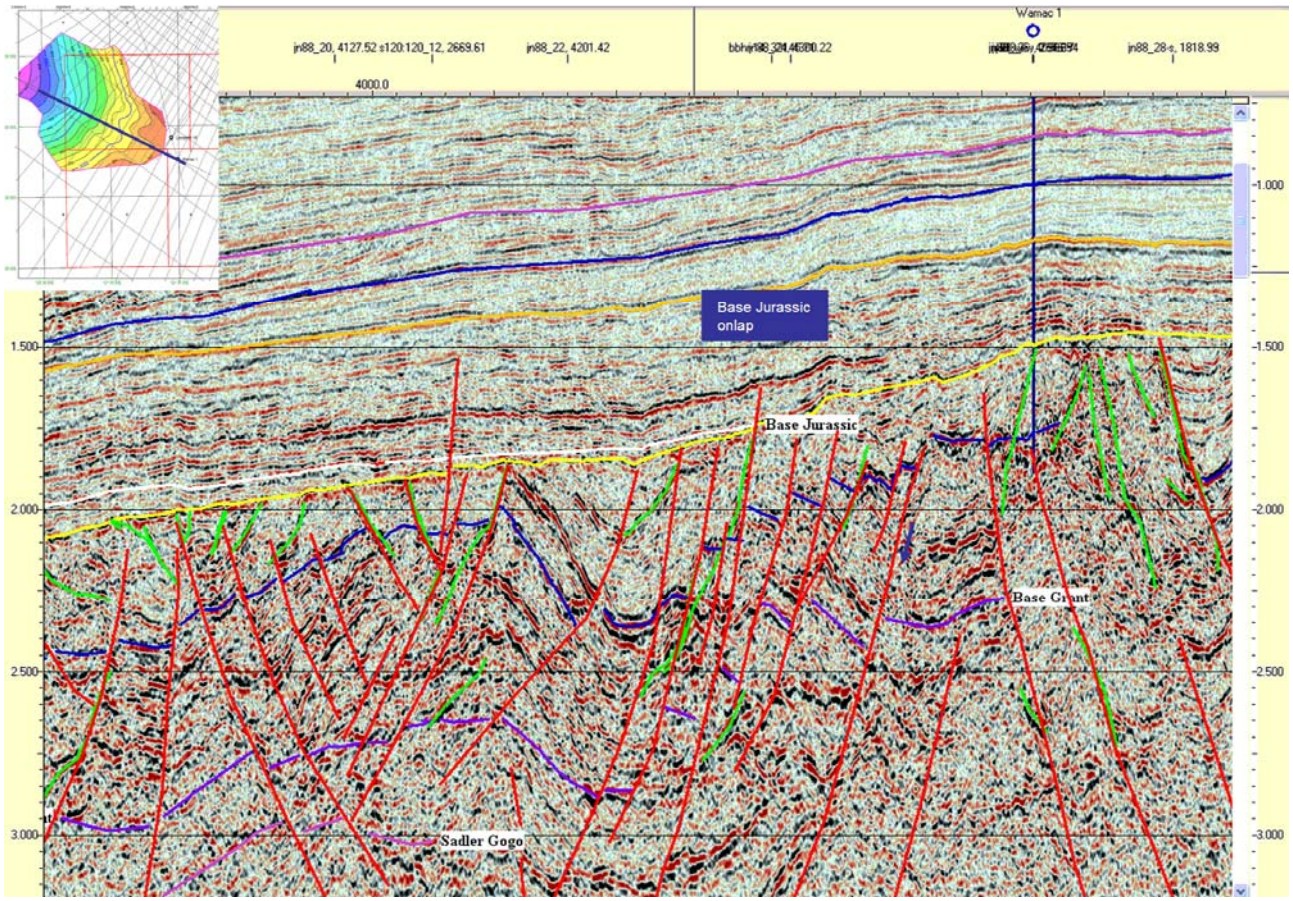

Figure 54 Line S120;120-11 Base Jurassic onlap and pinchout

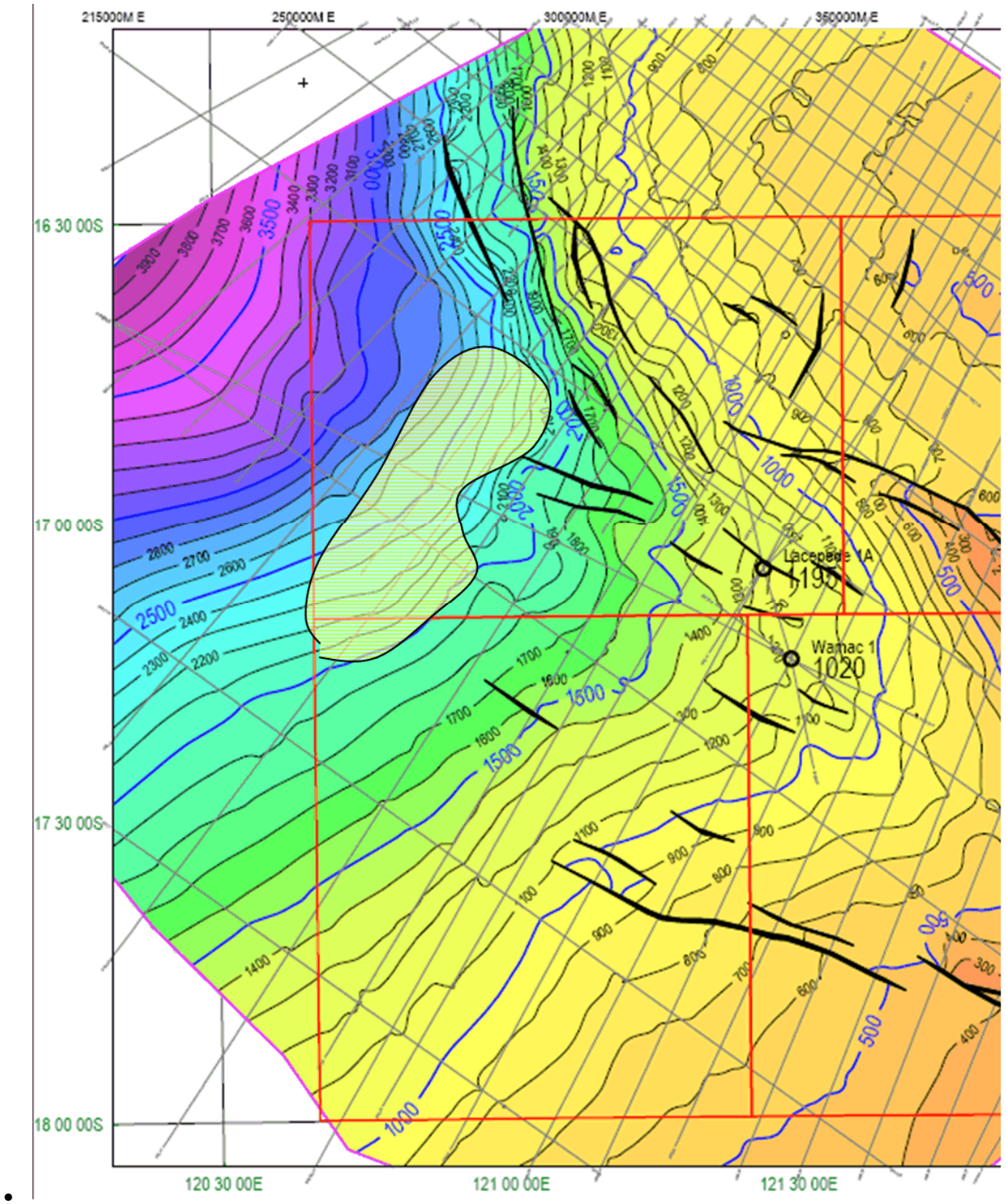

Figure 55 ?Berriasian submarine fans on base Cretaceous surface

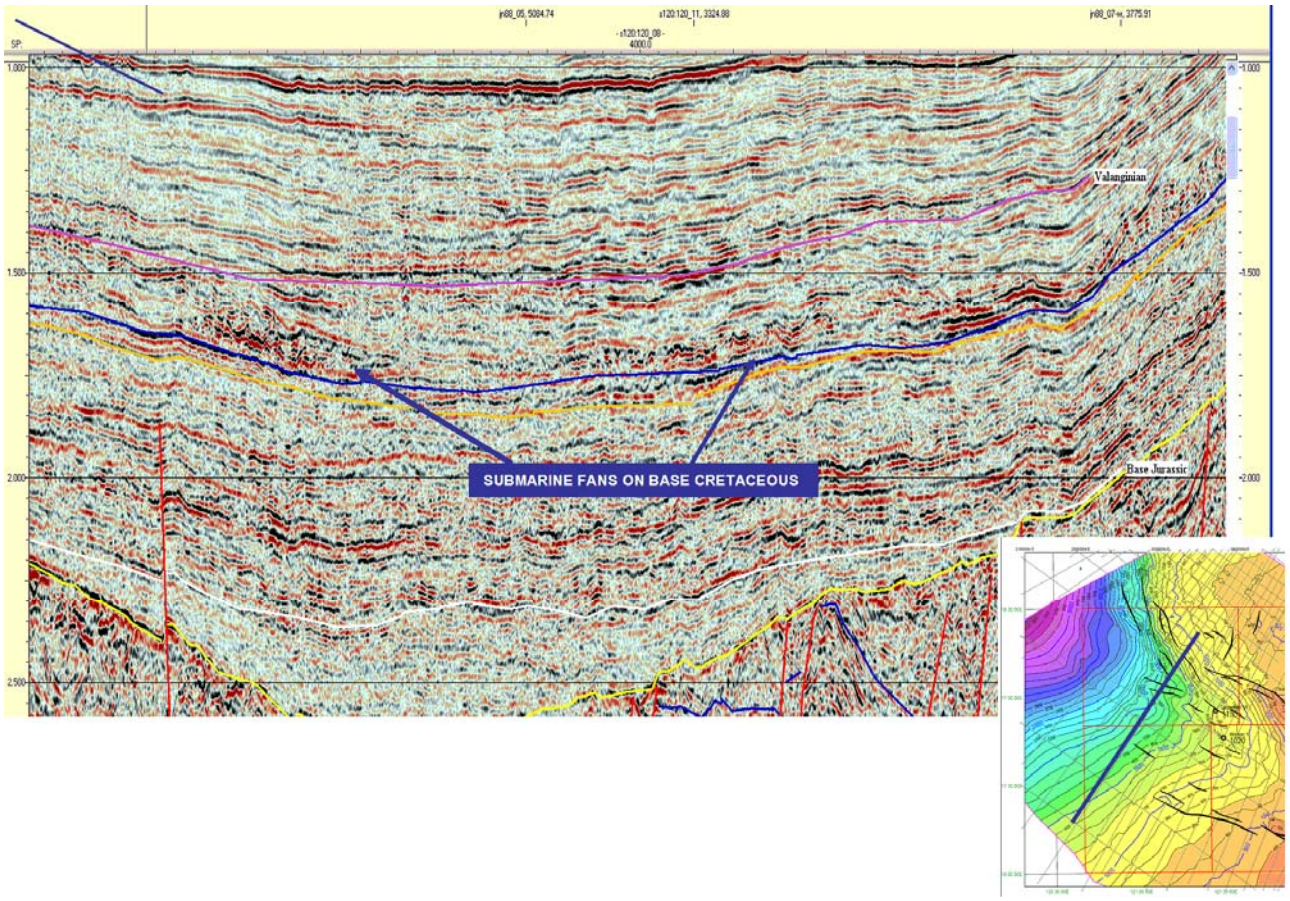

Figure 56 Line S120;120-8 ?Berriasian submarine fans

Block W07-14

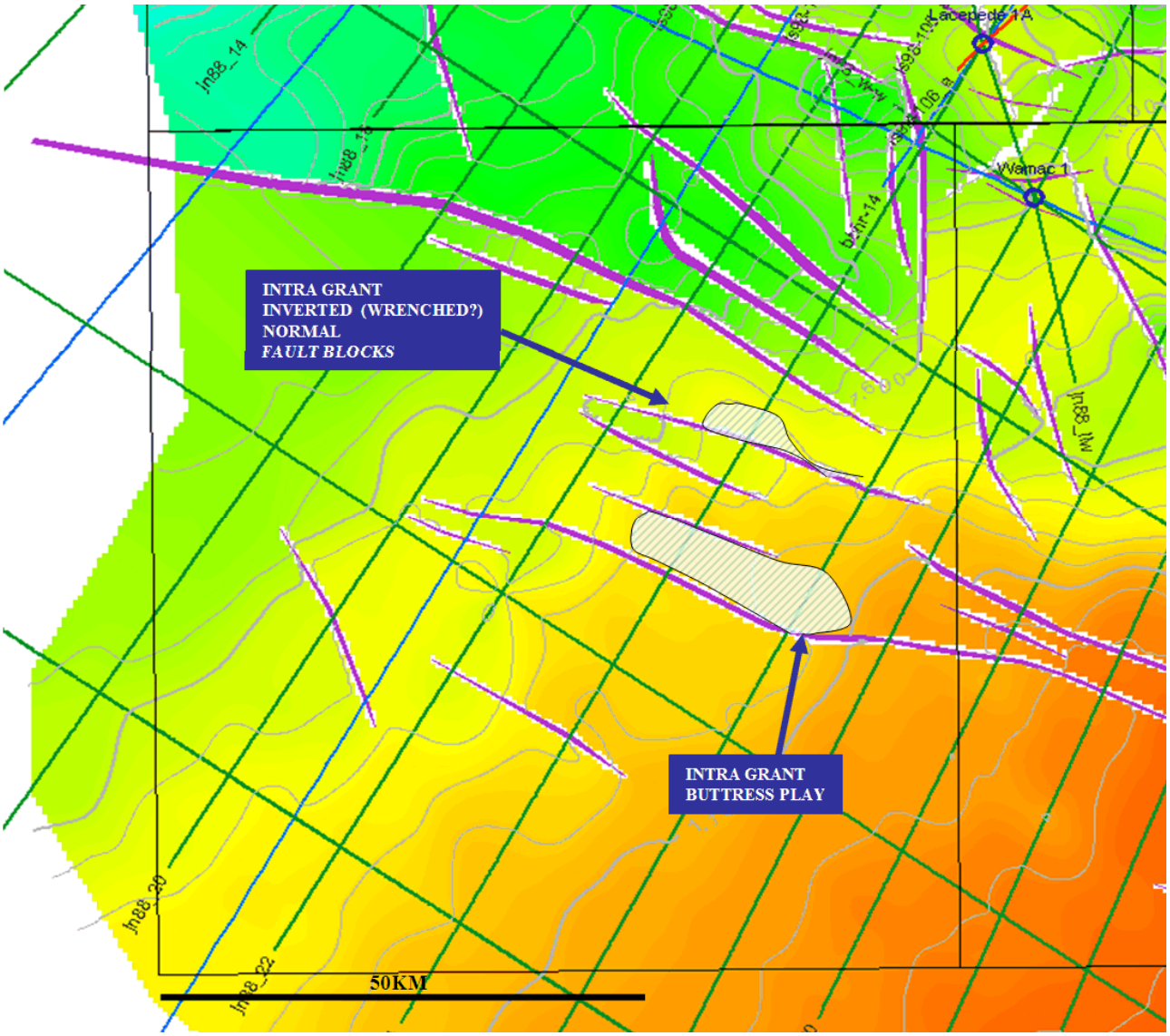

Figure 57 W07-14 Carboniferous Play Types

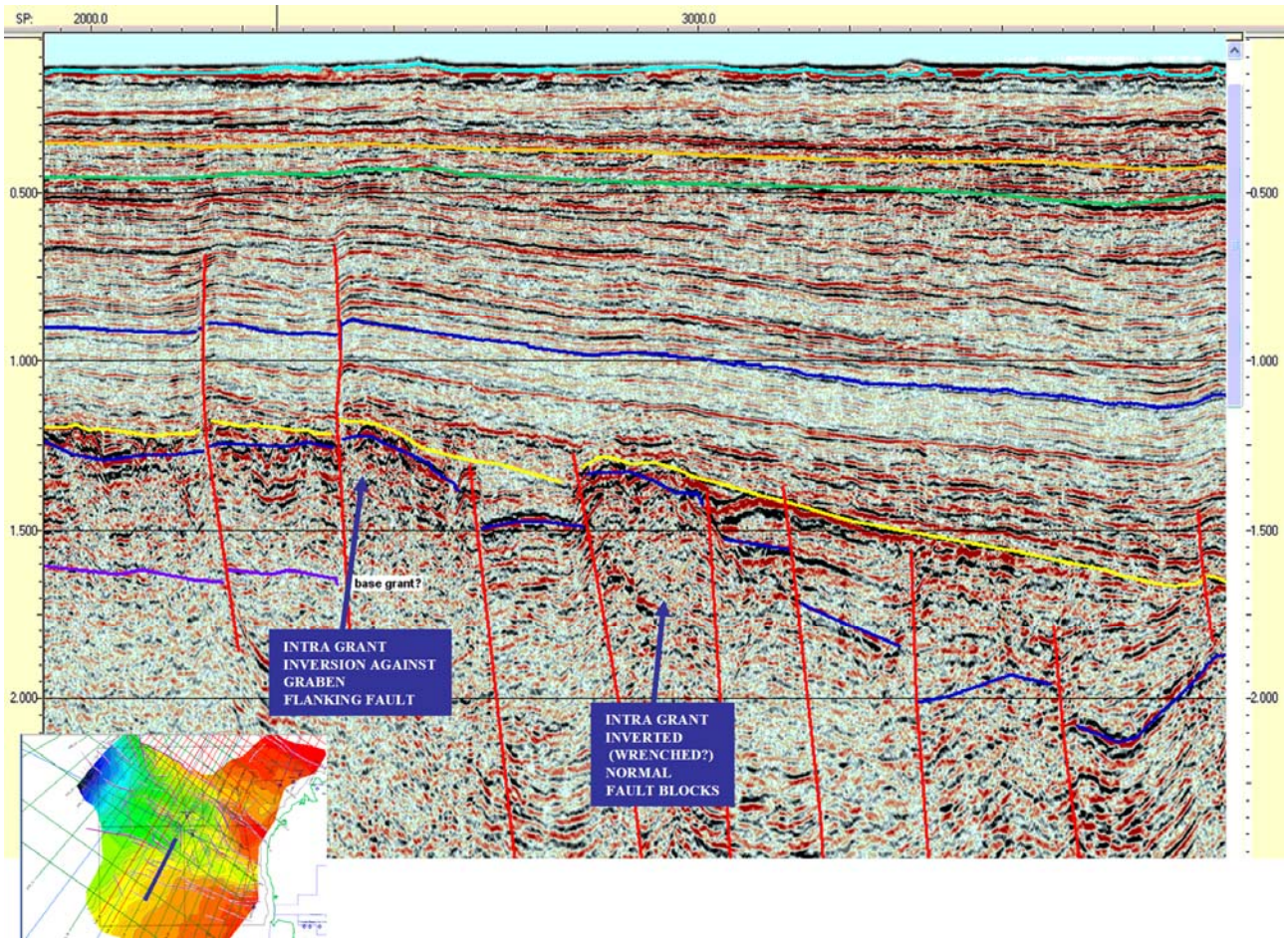

Figure 58 Line JN88-24 Carboniferous inverted/wrenched fault blocks

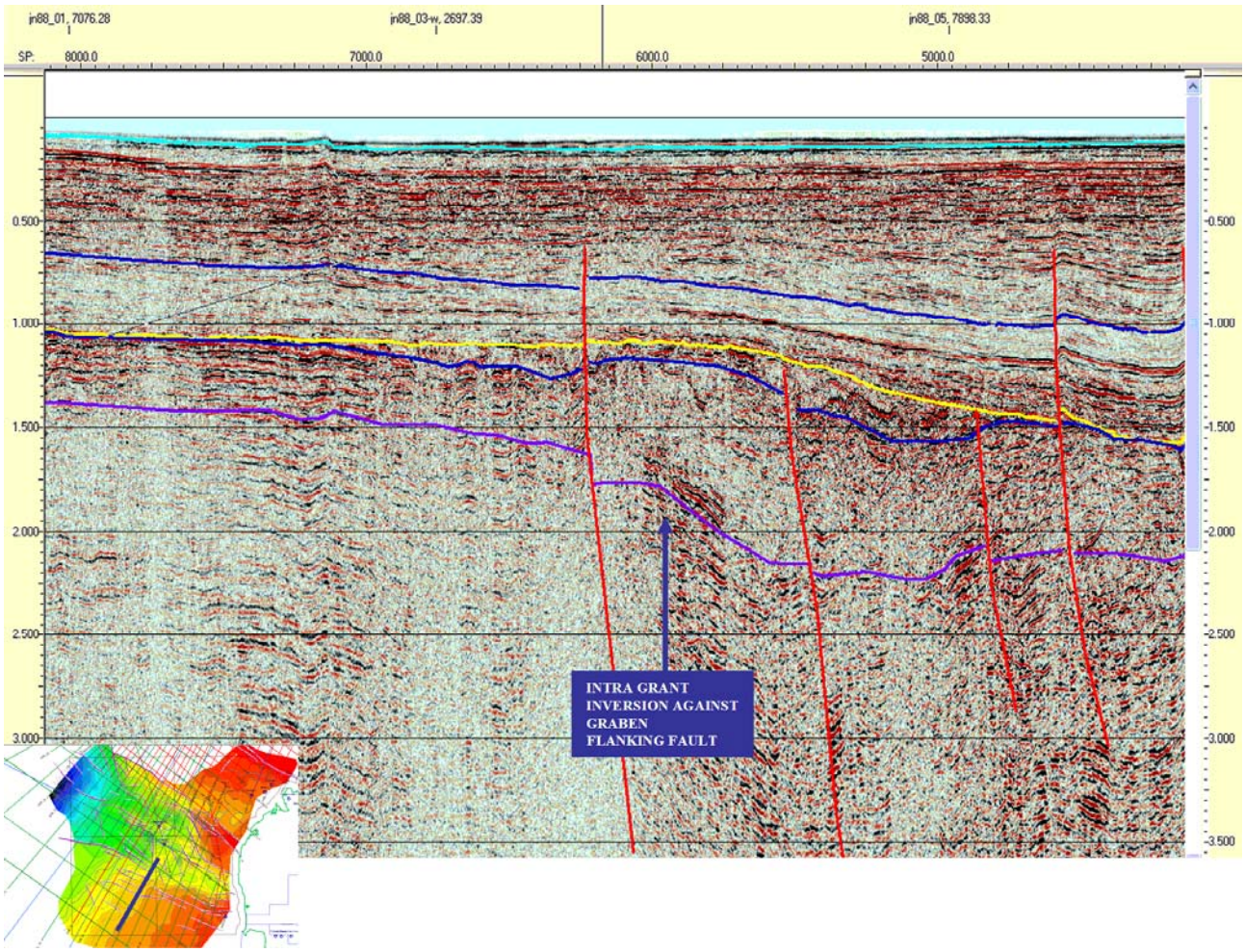

Figure 59 Line JN88-26 Carboniferous inverted/wrenched fault blocks

Block W07-15

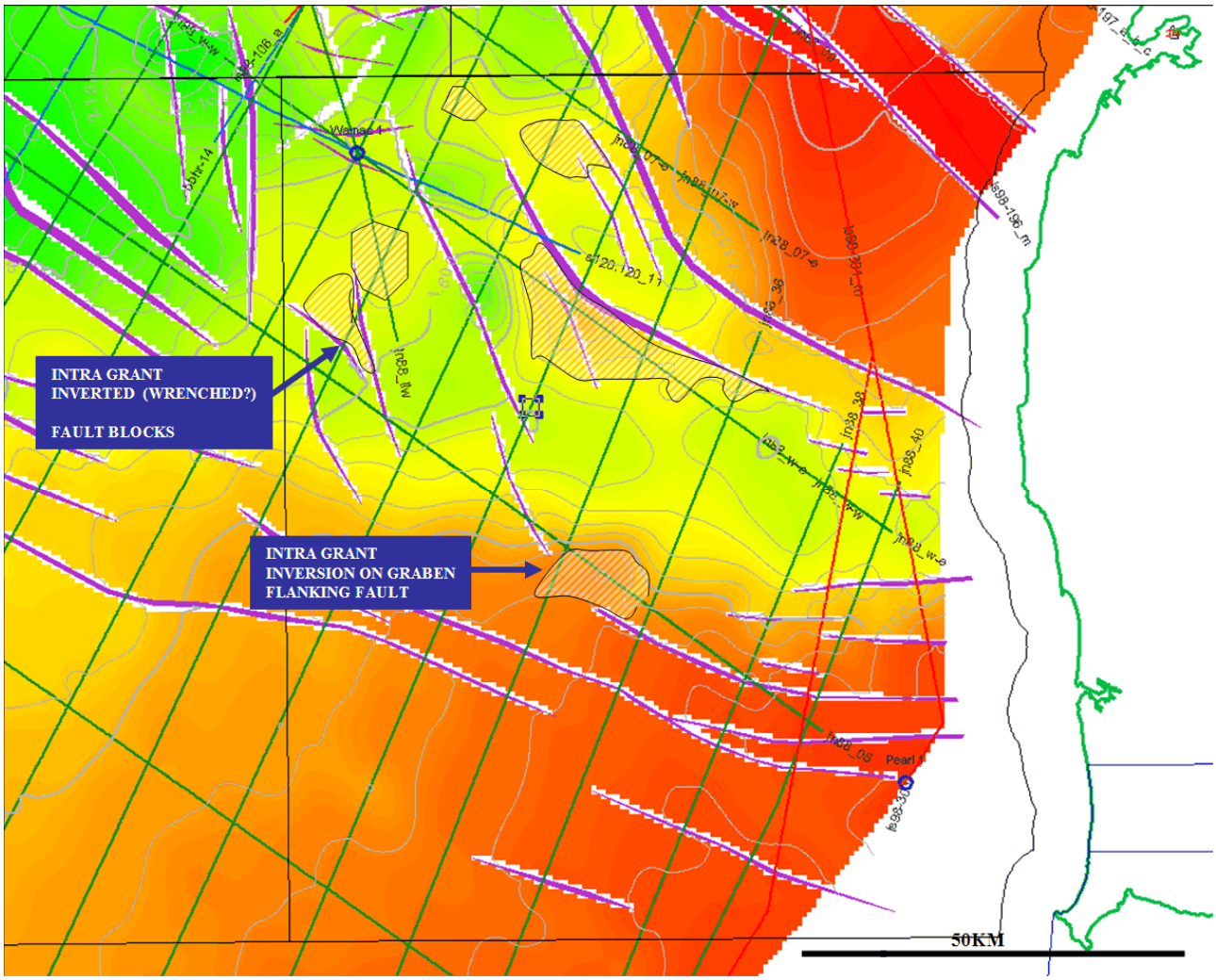

Figure 60 W07-15 Carboniferous Play Types

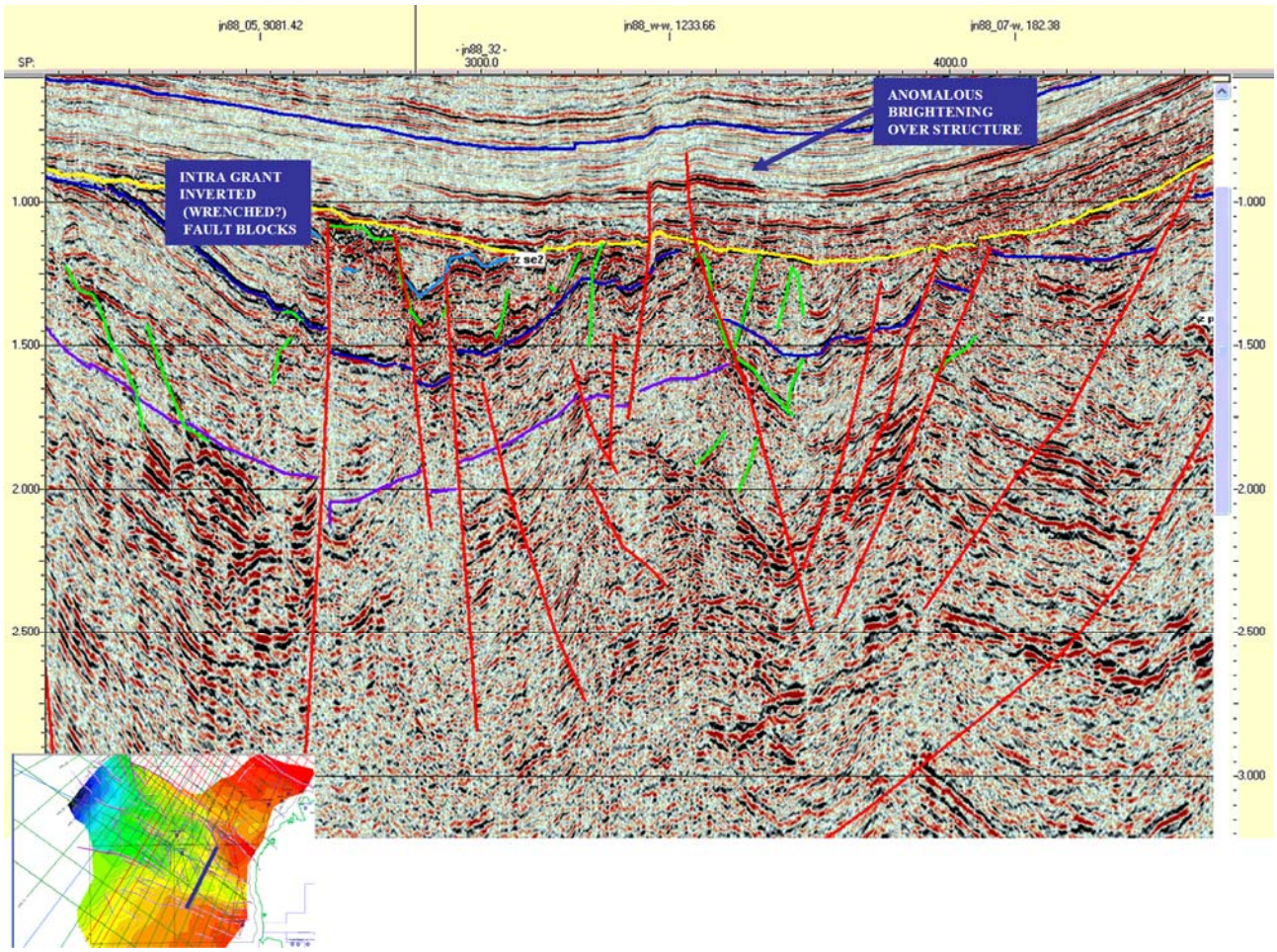

Figure 61 Line JN88-32 Inverted wrenched Carboniferous fault blocks

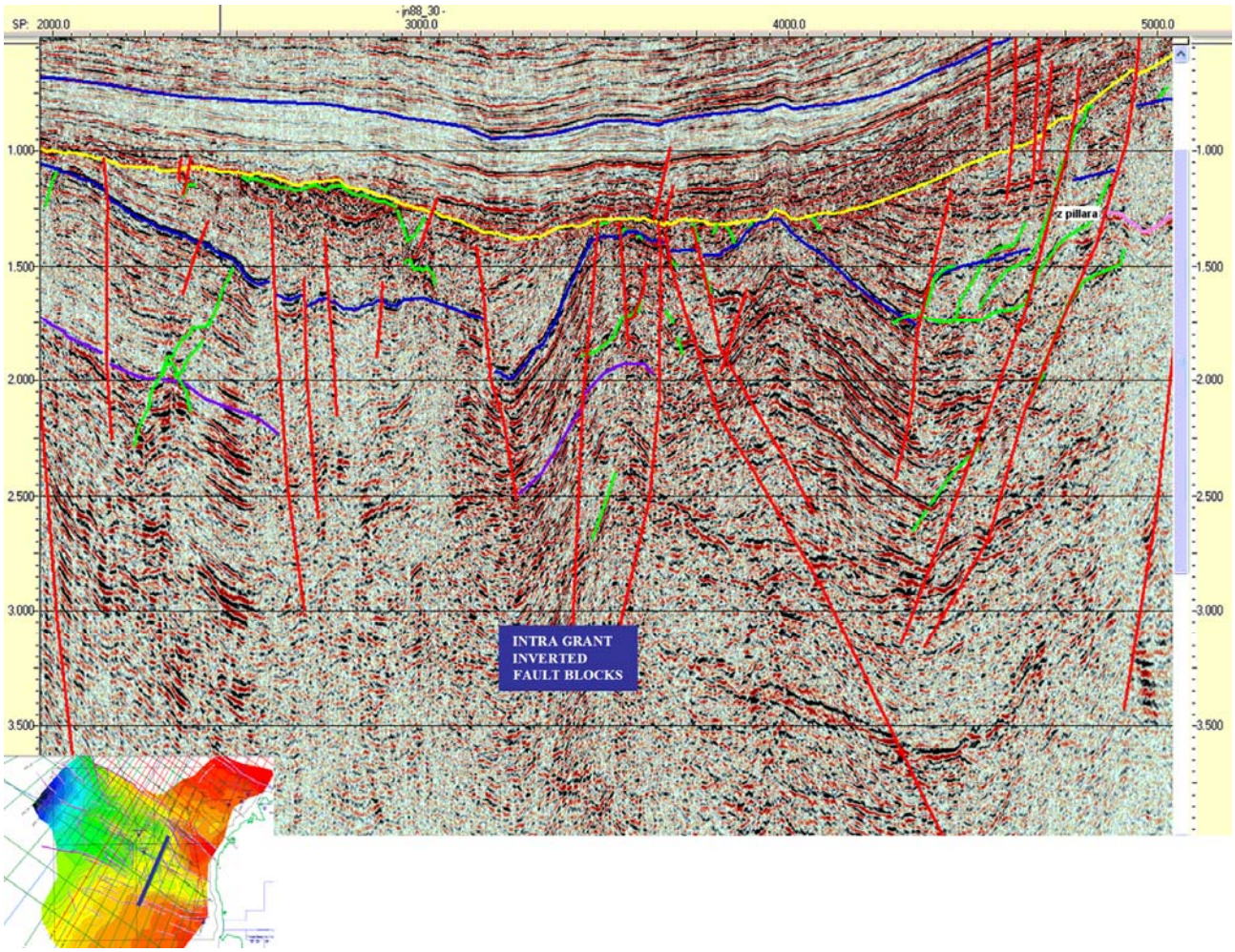

Figure 62 Line JN88-30S Inverted wrenched Carboniferous fault blocks

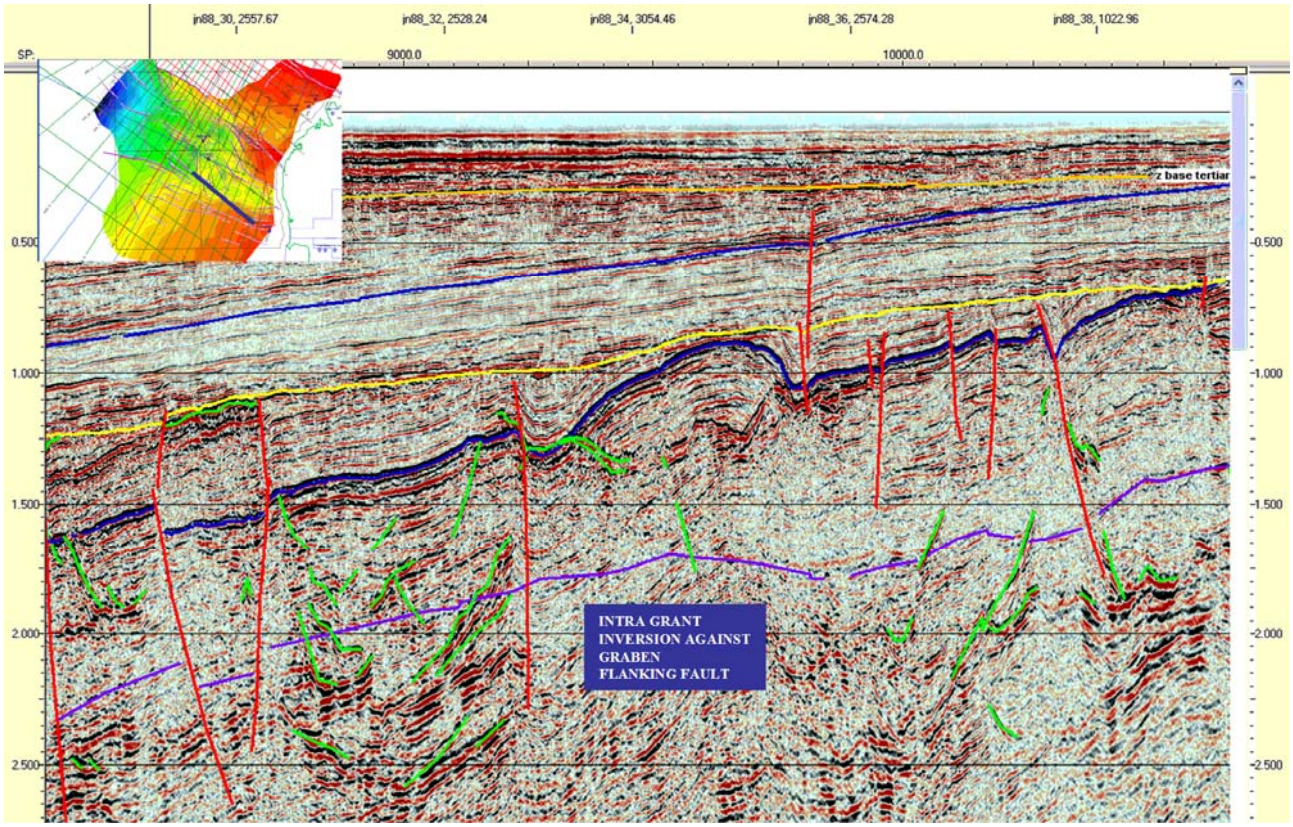

Figure 63 Line JN88-05 Inverted buttress block

Seismic Summary

These release areas occur in relatively shallow water. There are a variety of play types evident in these areas. These include Devonian carbonates including reefs as well as siliciclastic alluvial fans and fan deltas. Intense structuring in the Triassic has resulted in the formation of large scale folding, inversion and wrenching of the Palaeozoicresulting in numerous plays in the Early Permian/Late Carboniferous. In the outboard areas onlapping Mesozoics provide opportunity for stratigraphic plays. Mesozoic submarine fans also appear to be present in these areas.

Acknowledgements

Acknowledgement for the seismic part of the interpretation goes to Henk van Paridon of Geosolve Pty Ltd for promptly providing depth analysis of the seismic data set and producing very high quality depth structure maps. Acknowledgement also to Dr John Kennard of Geoscience Australia who provided his valuable knowledge and ensured the timely flow of data required to complete this analysis.

Integration of Seismic and Magnetic Interpretations

Seismic and magnetic methods generally provide quite different views of the subsurface, but joint interpretations of both data sets should be internally consistent. Consistent integrated interpretations provide more reliable information than the sum of both methods independently.

The expectation for the magnetic field study was that anomalies would predominantly be sourced in basement, and that interpretation of the magnetic field data would provide extrapolation of the basement surface away from those regions where it is reliably imaged on seismic. However, it has been found that much of the magnetic signal is generated by intrusives within the sedimentary section. Across much of the survey area these shallow-sourced anomalies mask magnetic field variations from deeper basement, but do provide independent information about structures within the sedimentary section, to complement the seismic interpretation.

As discussed previously, igneous intrusions, and in some cases possibly flows, are visible quite extensively on the seismic data as bright events due to high seismic impedance contrast with the enclosing sediments. On the seismic these events appear to be confined beneath the Bedout Unconformity.

Figure 64 shows the magnetic anomaly axes and dislocations (derived from enhanced magnetic field imagery in Figure 14 and Figure 15) combined with fault traces from the seismic interpretation at the Base Cretaceous (Figure 32) and Bedout Unconformity levels (Figure 29). The correspondence between the two independently derived feature sets is very strong. In many cases features are coincident, or extrapolate smoothly between the magnetic and seismic interpretations, which is consistent with the recognition that the magnetic anomalies are predominantly due to igneous bodies within the sedimentary section and their emplacement was controlled by the main faulting patterns within the sediments. In many cases faults mapped from the seismic data terminate against anomalies or dislocations mapped from the magnetic field data. In this case the magnetic features appear to map faults which may not have been recognised as significant in interpretation of the sparse seismic coverage. From the pattern of the faulting it appears that many of these faults may have predominant strike-slip movement, which has only a weak expression on the 2D seismic coverage.

Because the faults mapped from seismic generally have steep dips, it is not feasible to exactly correlate seismic and magnetic features and thereby attribute magnetic features to specific seismic surfaces. A plot of the magnetic source depth estimates together with the magnetic anomaly axes (Figure 65) shows that while in plan view many of the modelled sources coincide with the mapped anomaly axes, there is considerable depth variation along individual linear features. This is consistent with the interpretation that faults through the sedimentary section acted as conduits for the magnetic intrusives, and that those intrusive bodies are liable to have disruptions, deflections and terminations at many levels within the section.

The conceptual model for many of the magnetic source bodies as being somewhat irregular intrusives, possibly terminated at specific unconformities within the section, but also with changes or terminations at intermediate levels, increases the expected error on individual depth estimates (because required source geometry assumptions may be violated). It also makes it significantly more difficult to attribute those depth estimates to a specific geological surface. This is particularly true in the south and north of the area, over basement highs, where condensed and missing section allows little margin of error in tying magnetic source depths to a stratigraphic event.

There appears to be no systematic characteristics of the magnetic source bodies (other than possibly those bodies of reverse remanent magnetization) which might allow the magnetic sources to be allocated to specific event surfaces. In this respect it is important to realise that only very speculative interpretation of the magnetic field data can be supported without reference to the seismic interpretation.

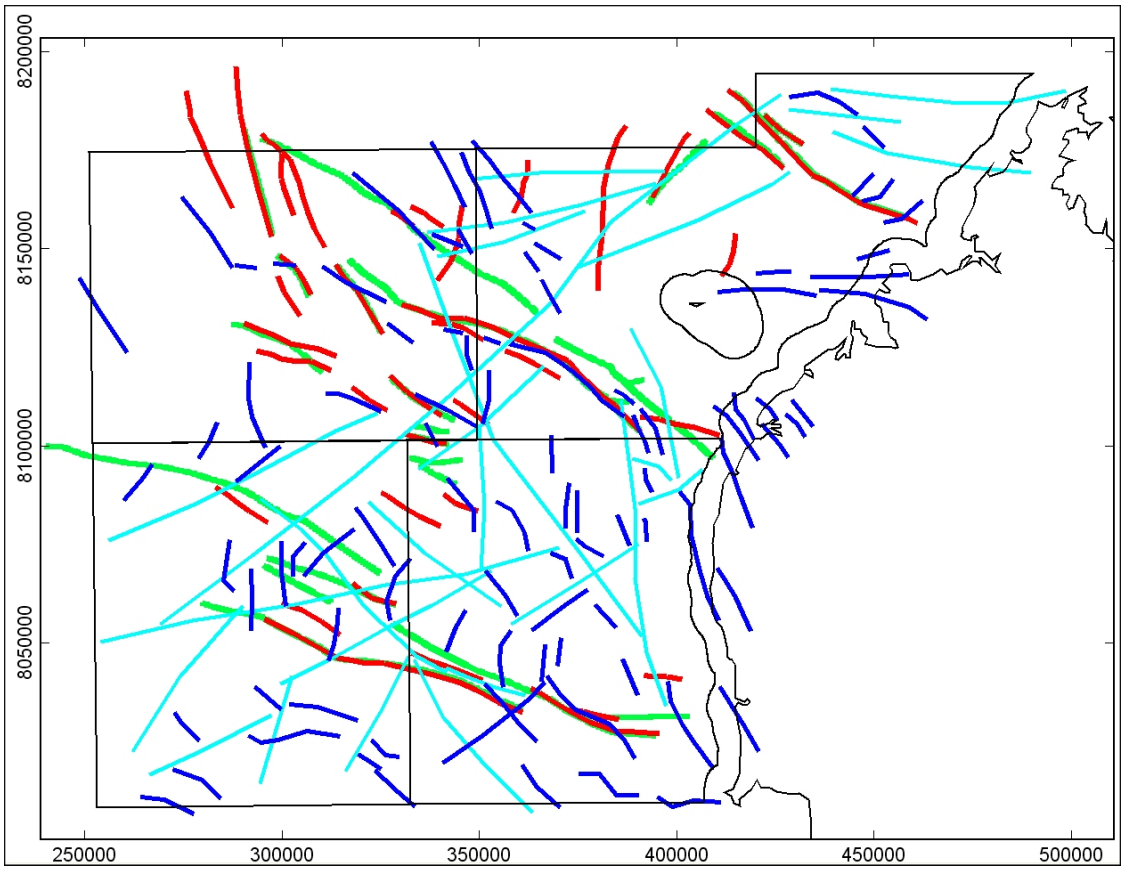

Figure 64 Magnetic anomaly axes (dark blue) and dislocations (light blue) with sesmic fault traces at Base Cretaceous (red) and the Bedout Unconformity (green)

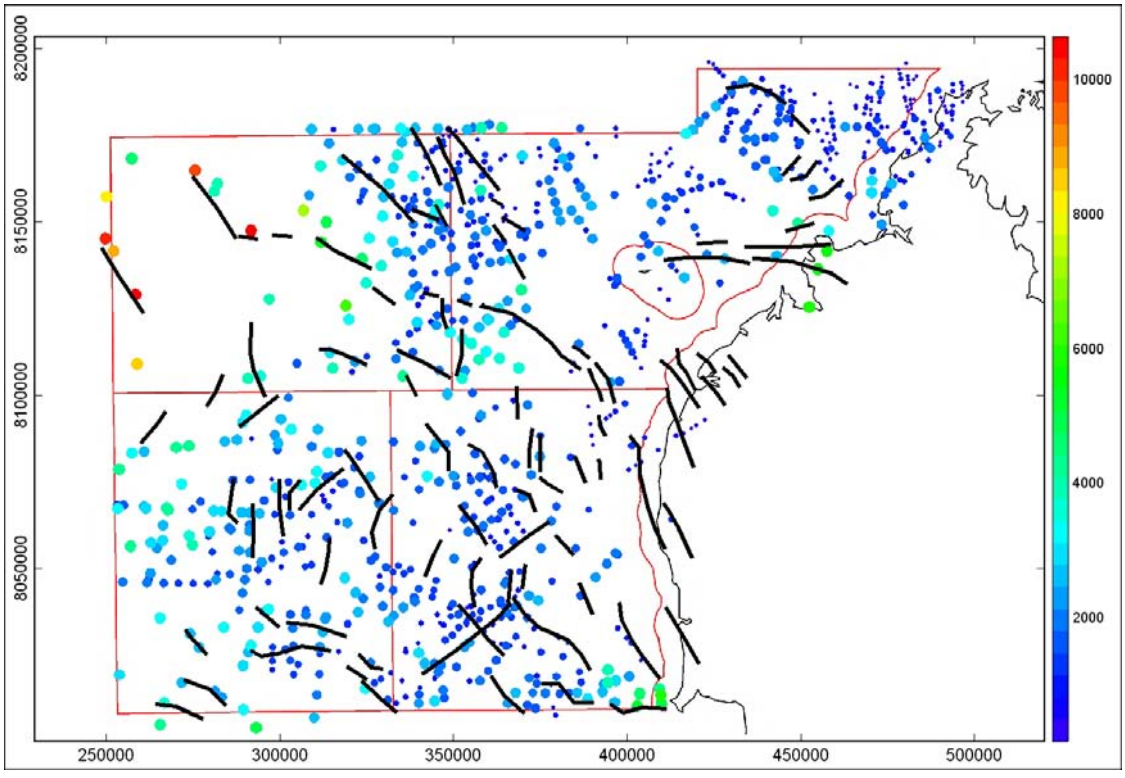

Figure 65 Magnetic anomaly axes with source estimate locations size and colour coded by depth

Figure 66 shows all magnetic source depth models, colour coded according to their attributed geological sources. In many cases this geological attribution was only possible with reference to the surfaces defined from the seismic interpretation, and could not have been made independently of the seismic interpretation.

The igneous bodies occupy a smaller volume than indicated in Figure 66. In many cases the modelling is unable to resolve several small, adjacent bodies, and therefore represents them as a single, larger body of lower magnetization. The bodies in Figure 66 are shown with a constant depth extent, to reduce distortion due to the strong vertical exaggeration of the figure. (The modelling provides an estimate of depth extent of each body, but because the lower parts of a body contribute so small a proportion of the anomaly, these depth extent estimates have low reliability).

Figure 67 shows the magnetic source bodies which lie above the Bedout unconformity. These bodies have no clear expression in the sparse seismic data. Individual bodies could be explained as due to errors in the depth estimation, but these bodies represent 30% of the intra-sedimentary sources (18% of all sources), and mostly occur within a broad geographic grouping.

The sources may be due to iron minerals redistributed within the section from alteration and decay of deeper igneous material, igneous activity younger than previously recognised in the area, or possibly unrecognised seismic velocity anomalies which have caused over-estimation of depth to the Bedout event in the region of these anomalies.

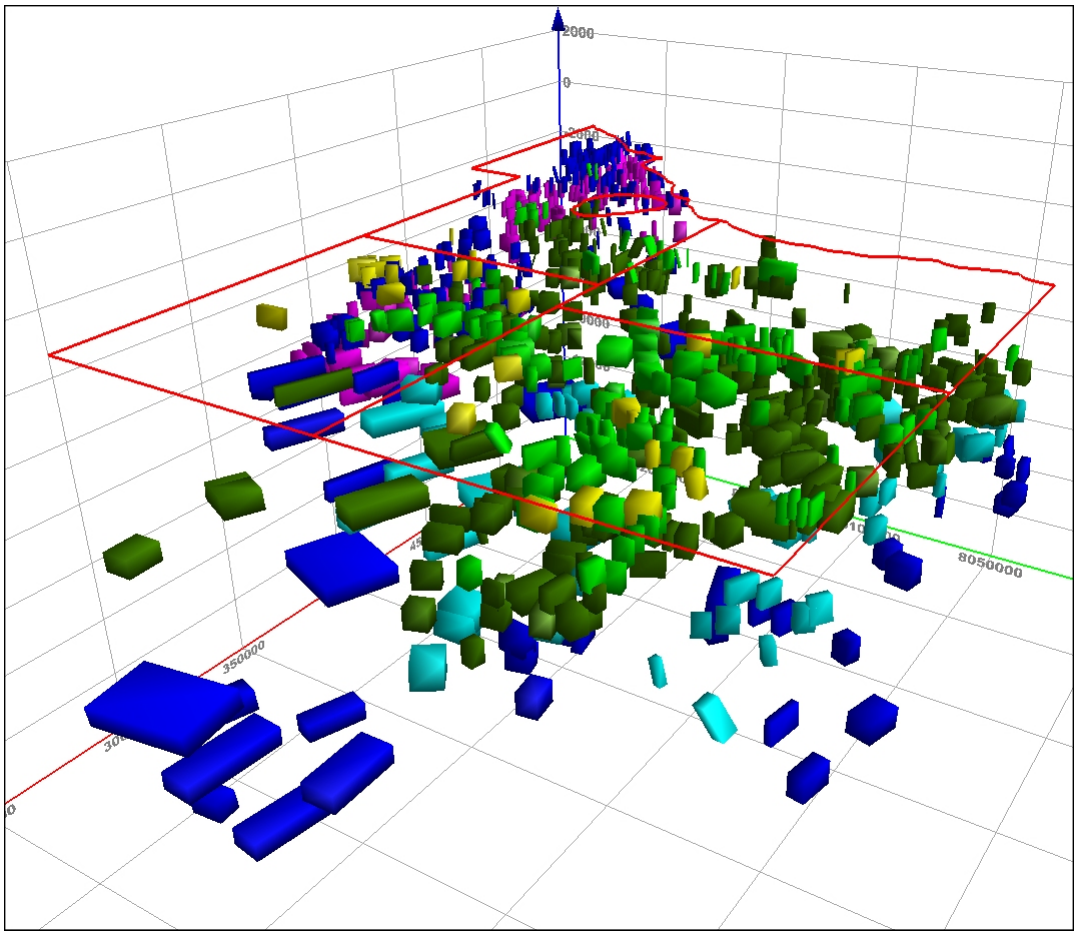

Figure 66 Magnetic source depth models (yellow – Base Cretaceous, light green – above Bedout, dark green – below Bedout, light blue – below Grant, dark blue – basement, purple – possible deeper basement.

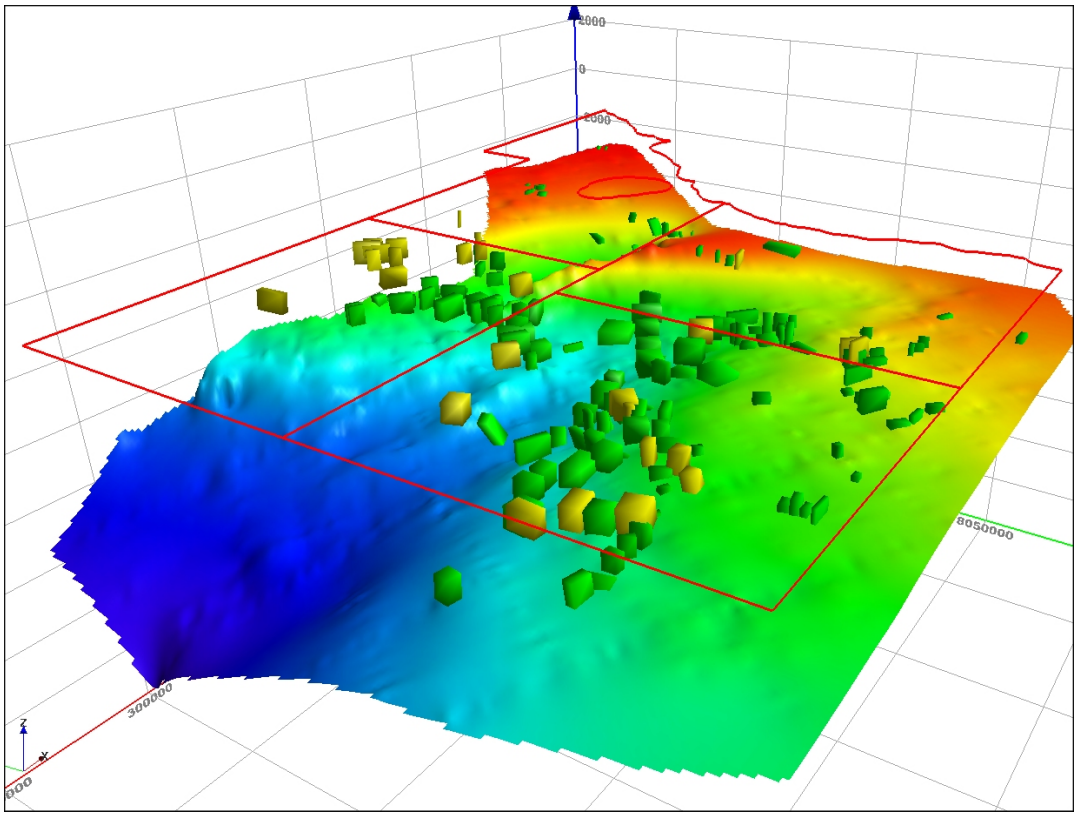

Figure 67 Bedout unconformity from seismic interpretation, with shallower magnetic sources (colour coded as in Figure 18).

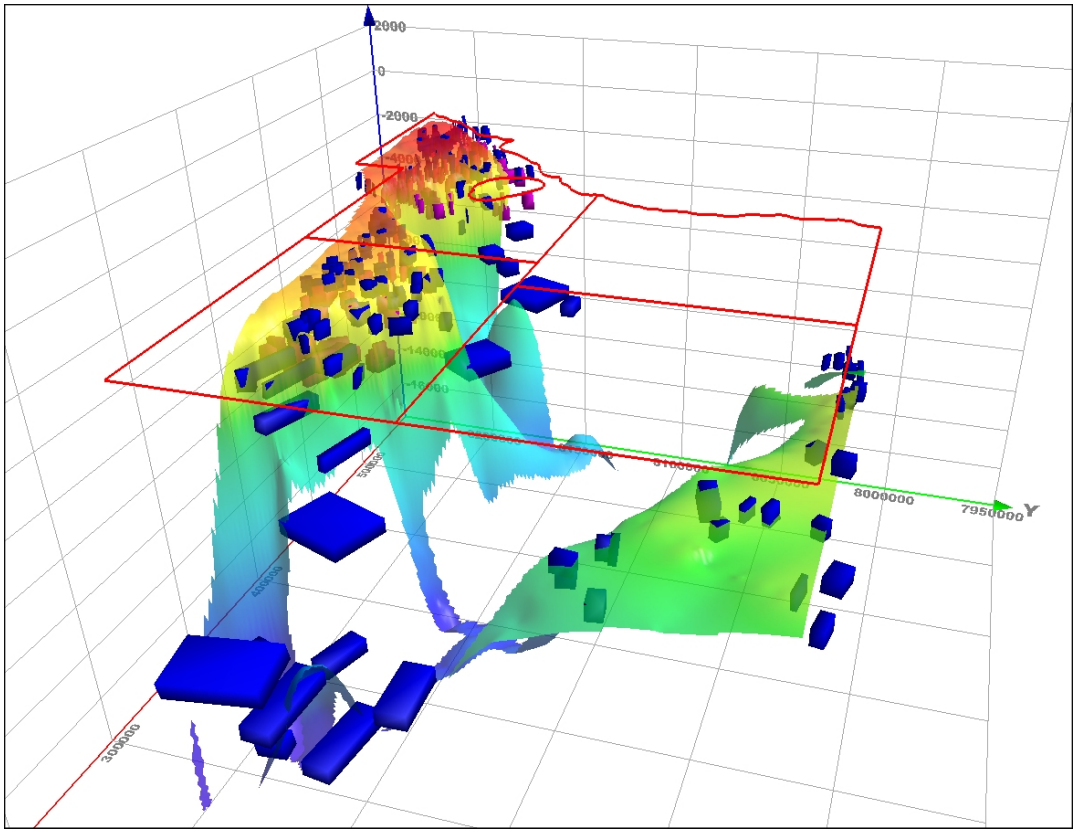

Figure 68 Magnetic source bodies interpreted to be sourced within basement, with basement surface interpreted from the seismic data.

Figure 68 shows magnetic bodies interpreted to be sourced within basement, together with a grid of basement interpreted from the seismic data.

For the shallow, small bodies, the seismic interpretation of basement has been used to guide which bodies are classified as basement sources, since it is difficult to discriminate between small bodies within basement and intra-sedimentary igneous sources on the results of the magnetic modelling. The much larger, deeper bodies are more distinctive, and can confidently be assigned as basement sources.

An integrated interpretation of basement depth was generated from the combined seismic and magnetic interpretations. Interpreted depth to basement across the survey area is shown in Figure 69. Maximum basement depths of approximately 15 kilometres are consistent between both seismic and magnetic modelling interpretations.

The definition of the basement surface over the north-easterly block WO7-12 is predominantly due to the seismic interpretation, because it was over this block that it was most difficult to discriminate between basement and intra-sedimentary magnetic bodies.

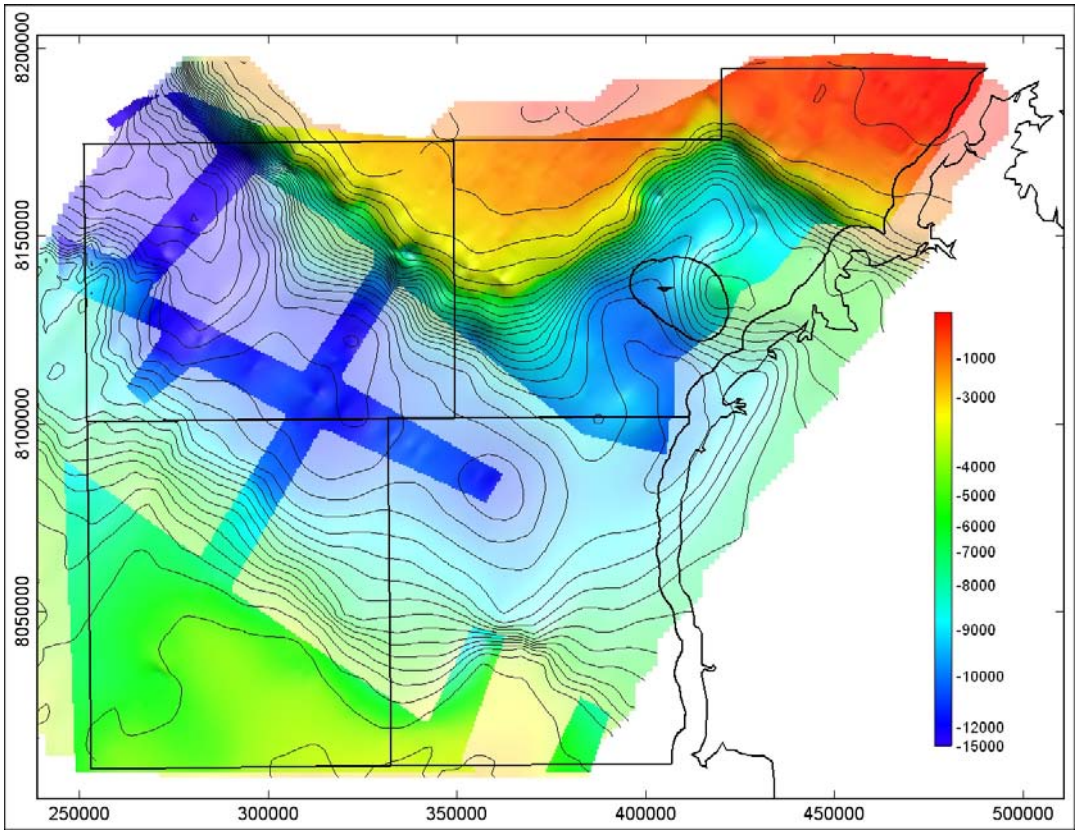

Figure 69 Integrated interpretation of basement depth (the image is of full intensity where constrained by seismic).

Figure 70 shows a plan of the magnetic bodies interpreted as being sourced within basement, plotted on the basement depth image. The small bodies over the shallow basement in Block WO7-12 are consistent with the short wavelength anomalies which continue over the onshore basement outcrops to the east. Many of these bodies cluster about the depth picked for basement on the seismic interpretation, but there is also another clustering of bodies at a greater depth This suggests that there may be another surface which is older still beneath that basement.

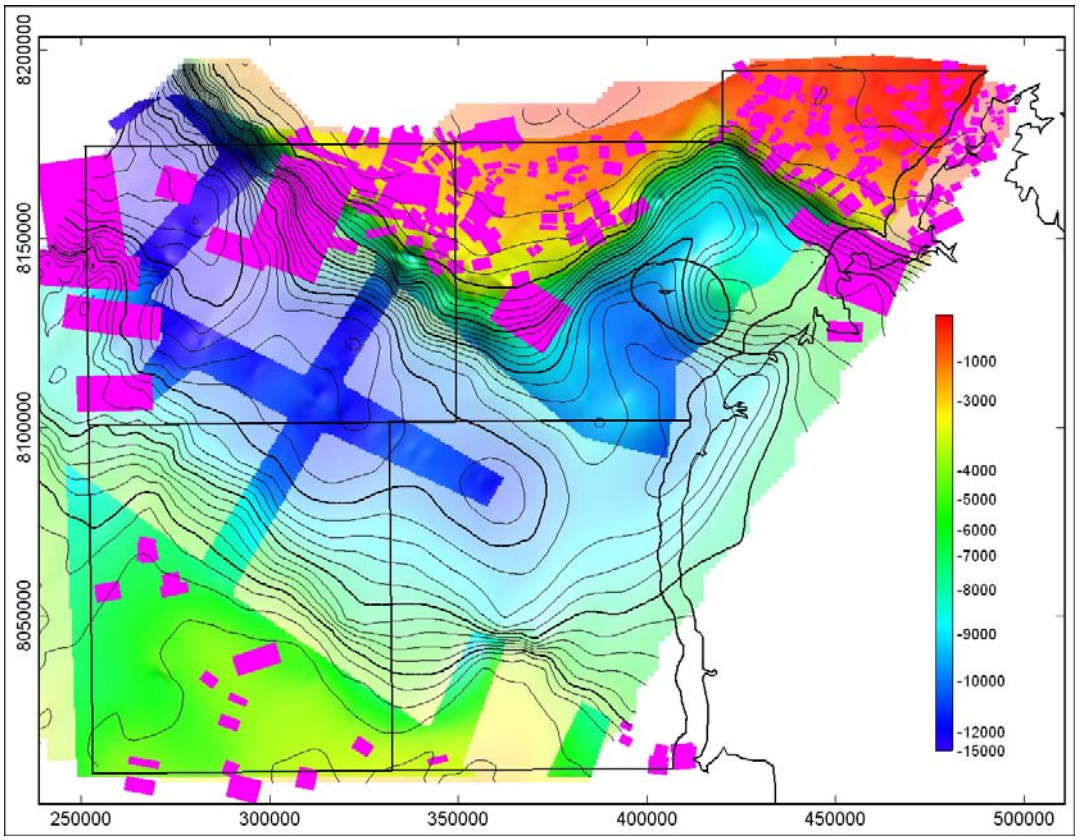

Figure 70 Basement surface with overlay of magnetic source bodies interpreted to be sourced within basement.

The basement is not evident on either the seismic imaging or magnetic modelling over the south-easterly block WO7-15. The basement surface in this region appears to be rising towards the coast, consistent with the change in trend at the coast recognised in the regional gravity data. The basement surface was interpreted in perspective view to honour both the gridded seismic basement depths and the magnetic bodies interpreted as being sourced in basement.

A faceted 3D vector representation of the surface is shown in Figure 71, and a grid generated from the vector nodes is imaged in Figure 72.

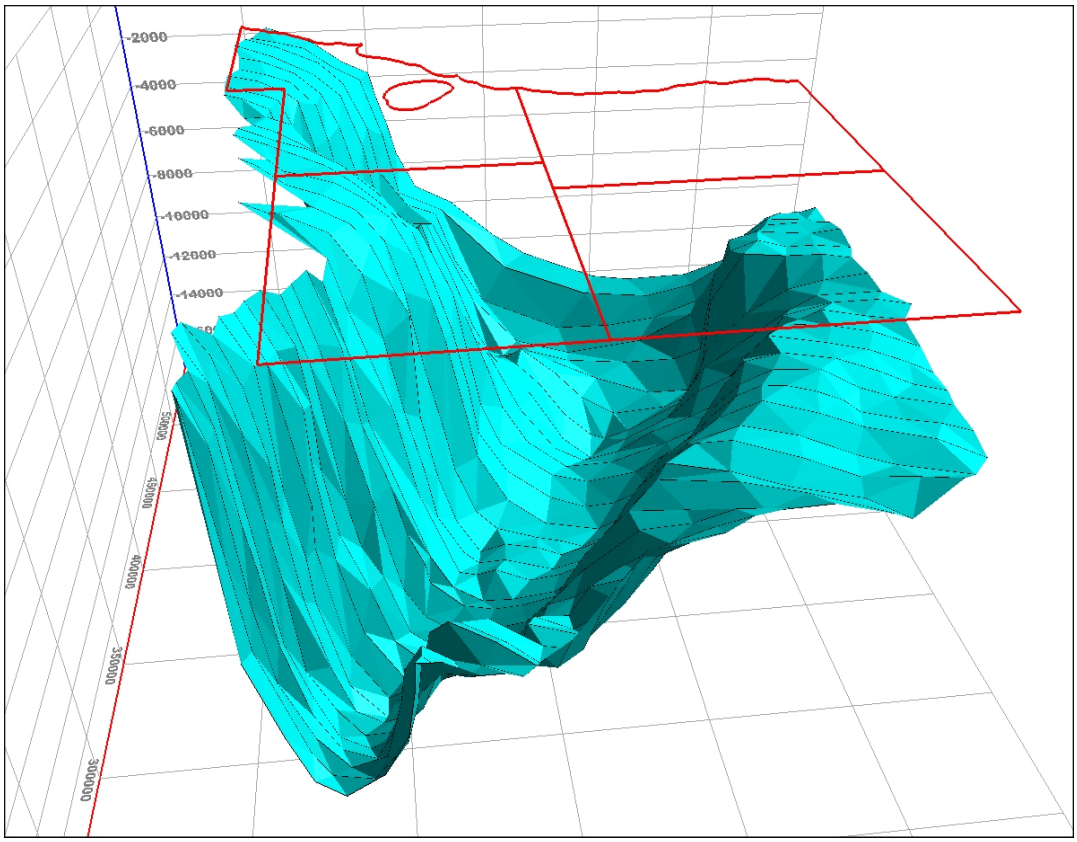

Figure 71 Faceted display of interpreted basement surface.

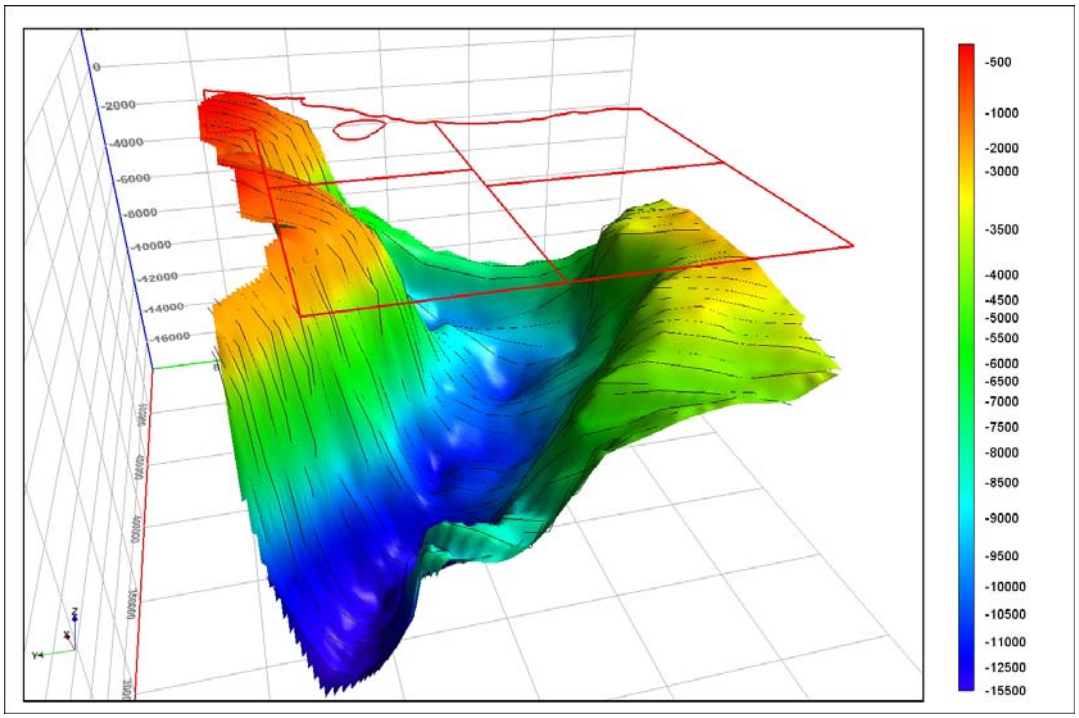

Figure 72 Image of basement surface grid derived from the faceted surface shown in Figure 23.

References

Department of Resources, Energy and Tourism, 2007- Release of Offshore Petroleum Areas 2007. www.ret.gov.au/petexp
(Formerly Department of Industry Tourism and Resources)

Drummond,B.J., Sexton,M.J., Barton,T.J., and Shaw,R.D., 1991, The Nature of Faulting Along the Margins of the Fitzroy Trough, Canning Basin, and Implications for the Tectonic Development of the Trough, Exploration Geophysics, vol. 22, pp. 111-116.

Gorter,J.D. and Glikson,A.Y., 2002, Fohn Lamproite and a possible Late Eocene - pre-Miocene diatreme field, Northern Bonaparte Basin, Timor Sea. Australian Journal of Earth Sciences vol 49:5, pp. 847-868

Jaques,A.L. and Milligan,P.R., 2004, Patterns and control on the distribution of diamondiferous intrusions in Australia. Lithos vol 77, pp. 783-802

Shaw,R.D., Sexton,M.J. and Zellinger,I., 1994, The Tectonic Framework of the Canning Basin, WA, Including 1:2 million Structural Elements Map of the Canning Basin. Geoscience Australia, Record 1994/48.

Appendix 1 - Interpretation of the Magnetic Anomalies Dominated by Remanent Magnetization

Within the survey area there are many magnetic anomalies which are evident as local reductions in magnetic field strength. In the moderate to steep geomagnetic inclination of the area (-48°) these anomalies are interpreted to be due to bodies with strong reverse remanent magnetization. The conditions to generate these anomalies are that the bodies were emplaced and cooled during a period when the earth's magnetic field was of reverse polarity, and that the stable reverse remanent magnetization of the rocks exceeds the induced and any soft remanent magnetizations, to give a resultant with reverse polarity.

A map showing the distribution of the negative magnetic anomalies is shown in Figure A1_1. The anomalies occur both as linear features, and as elliptic anomalies. The anomalies show several geographic clusterings, and in some places linear distributions, suggesting that individual intrusions have been emplaced along a single fault. There is one large and very high amplitude anomaly in the centre of Block WO7-12, which is the most prominent single magnetic anomaly within the survey area. This anomaly is shown in Figure A1_2 in both TMI and modulus of the analytic signal images. The analytic signal image is generally useful in locating sources of anomalies dominated by remanence, but in the case of these anomalies it is less required, because the anomalies have mostly the simple form of purely negative anomalies. The main anomaly and its satellite bodies have minor positive lobes to the south, suggesting an almost exact reversal of the current field direction, which in the survey area induces predominantly positive anomalies with a minor flanking low to the south. Some of the anomalies have no associated minor positive lobe, or have the lobe to different sides. While this can in part be controlled by the shape and plunge of the body, the changes in anomaly shape appear to mostly reflect changes in resultant magnetization direction. This may be in part due to different remanent magnetization directions of various bodies, and in part due to different ratios of induced to remanent magnetization, resulting in divergence of the resultant magnetization directions.

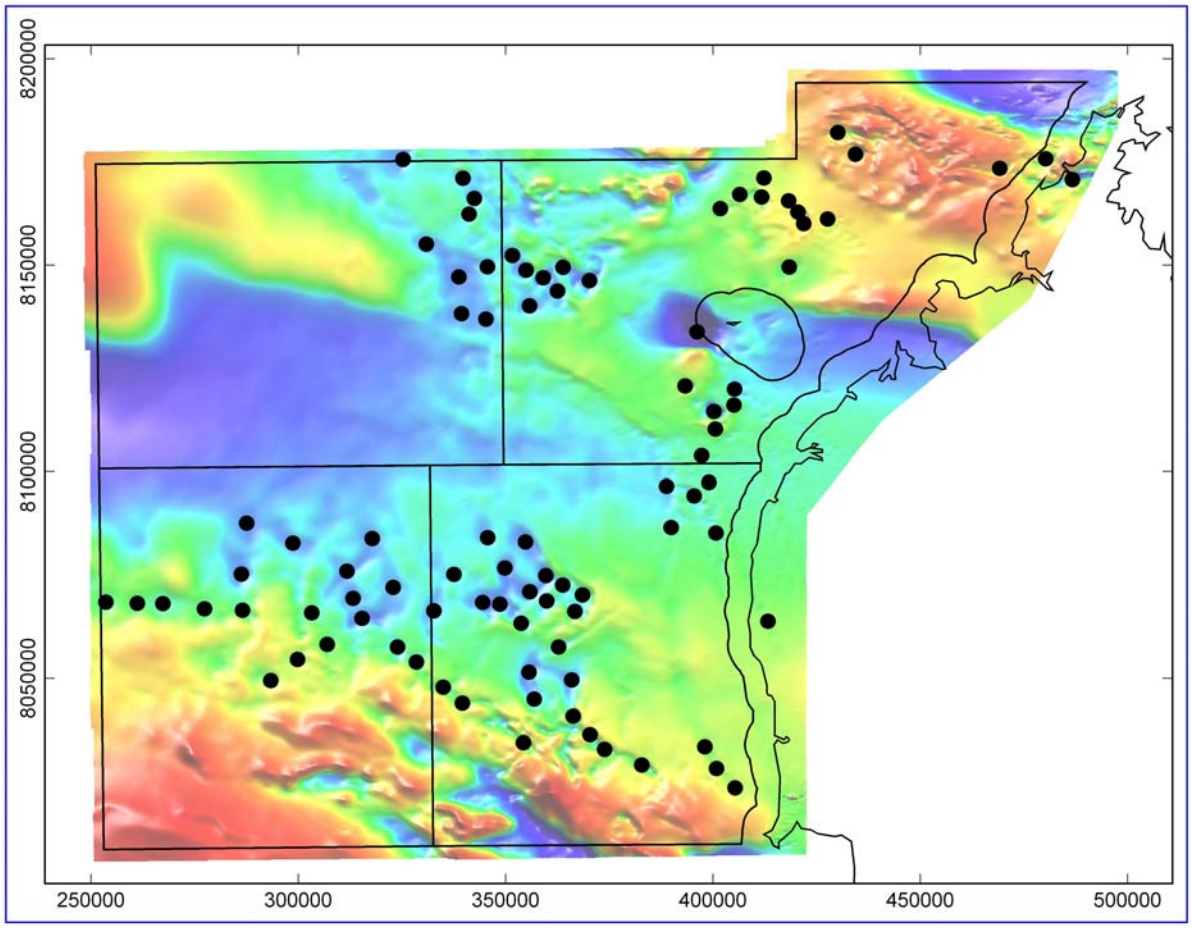

Figure A1_1 Distribution of clearly remanence-dominated anomalies.

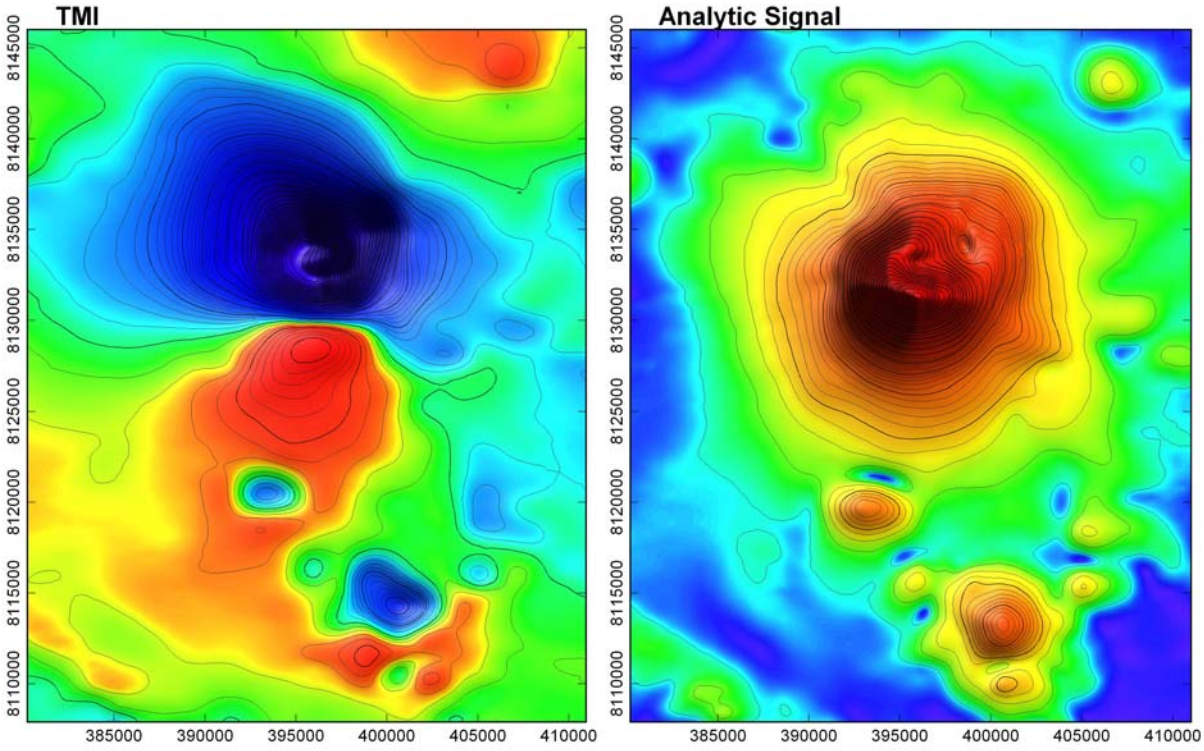

Figure A1_2 TMI and modulus of the analytic signal images over the main remanent magnetization source and its satellites.

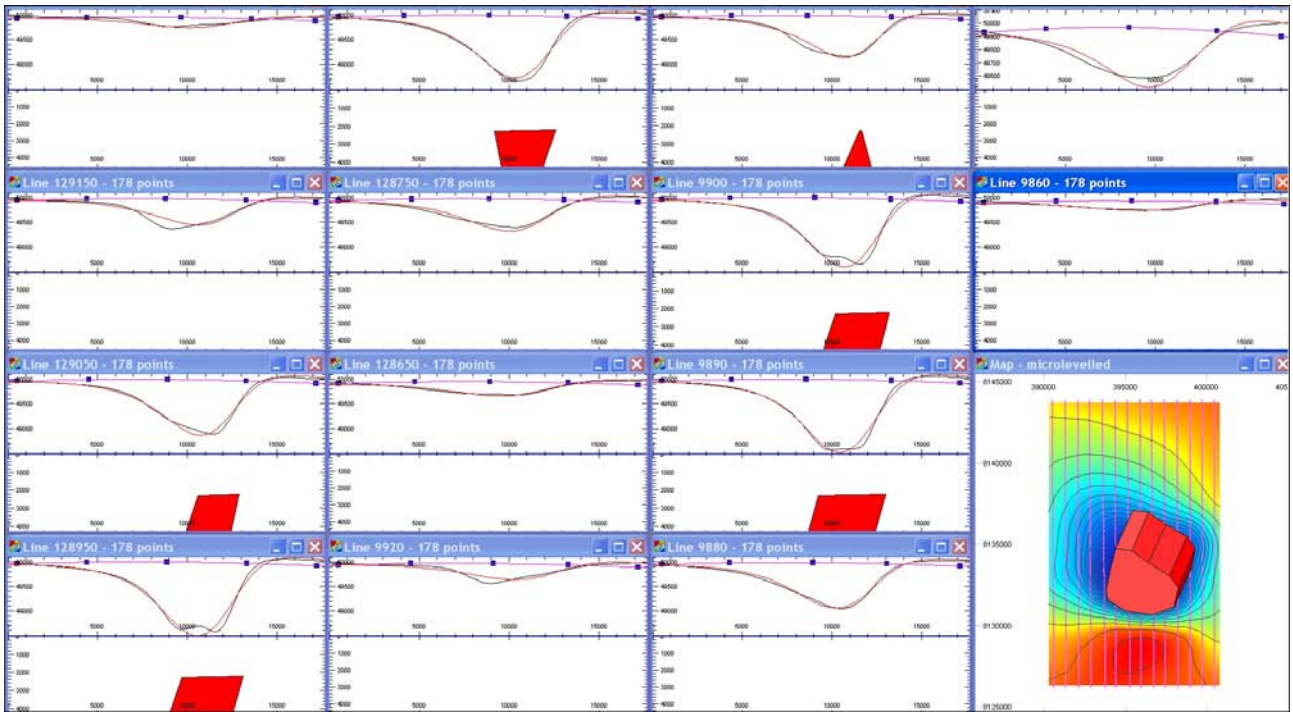

Figure A1_3 Modelled sections over the major remanent magnetization anomaly.

The analytic signal image in Figure A1_2 highlights an increase in curvature at the centre of the magnetic anomaly. This might be due to a shallower offshoot of the body, or higher magnetization bodies within the main intrusive, as are common in kimberlites, carbonatitites and other associated plug-type bodies.

This large anomaly was modelled by an inversion of the profile data. The model sections are shown in Figure A1_3. Initially a vertical elliptic pipe body was located over the analytic signal image. This image approximately positions the body because the modulus of the analytic signal has little sensitivity to magnetization direction. The body was then inverted for magnetization strength and direction, and for depth. The result of this first inversion is to produce a body of approximately correct position and magnetization. From that starting point a simultaneous inversion of magnetization, position and depth allowed optimisation of those values. Finally the shape restrictions of the body were relaxed from having an elliptic section and vertical plunge, to having an arbitrary polygonal section and arbitrary plunge. The final resultant magnetization has an inclination of +68° and a declination of 035°. Some of the individual profiles show the sharper curvature features over the centre of the anomaly, but there is insufficient definition of these features to justify adding further complexity to the model to match them. 28 remanently magnetized bodies were modelled, all had resultant magnetizations of moderate to steep positive inclination, and all but one were at depths at or below the Top of Grant unconformity.

Figure A1_4 and Figure A1_5 show TMI and modulus of the analytic signal images over two of the groups of remanence dominated anomalies. The analytic signal images highlight the structural controls on the anomalies, which are evident as rectilinear patterns. The analytic signal images suggest that the anomalies are due to a combination of circular pipe-like bodies, and more linear sheets and dykes. These patterns are common in intrusions into sediments, with pipe necks and subsidiary sheets in cone and funnel forms. Modelling these anomalies to derive depths and magnetizations is difficult because the overlap of the anomalies makes it difficult to separate them and to resolve the background field.

Figure A1_6 shows a string of negative TMI anomalies along a linear trend. Similar patterns occur where linear anomalies have too high a curvature to be properly sampled at the survey line spacing, but these circular anomalies are sufficiently sampled and are due to distributed intrusions along the linear trend.

Further study could be applied to research the possible age of the remanent magnetizations, and to investigate any geographic control on the spread of resultant magnetization directions, but such studies were beyond the scope of this project, and are unlikely to be relevant to petroleum prospectivity of the area.

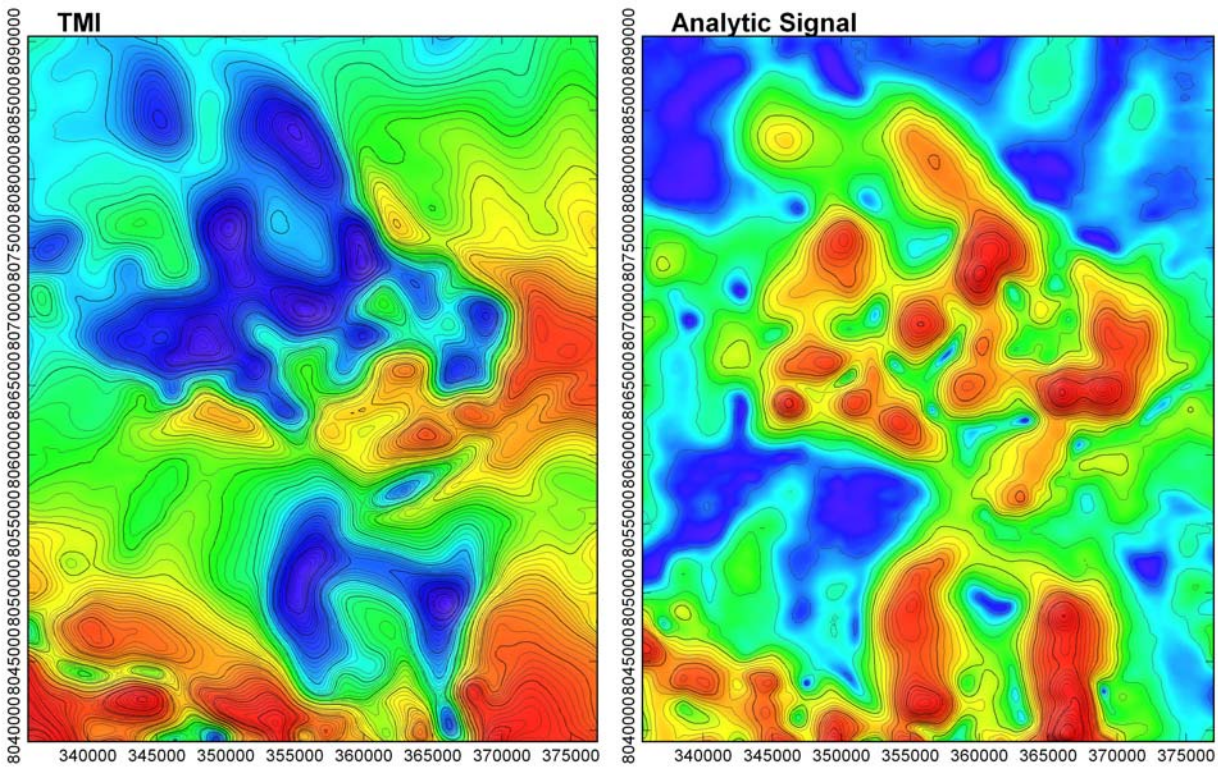

Figure A1_4 rectilinear patterns of multiple, overlapping remanent magnetization anomalies.

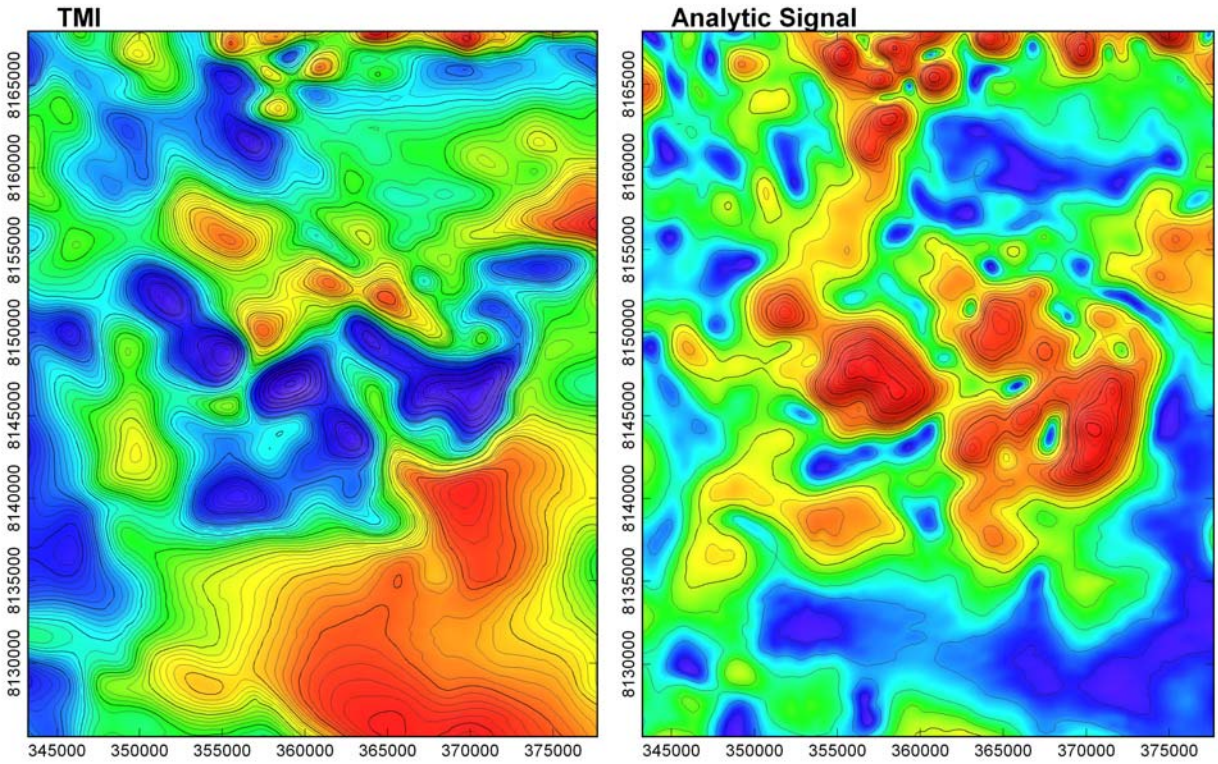

Figure A1_5 rectilinear patterns of multiple, overlapping remanent magnetization anomalies.

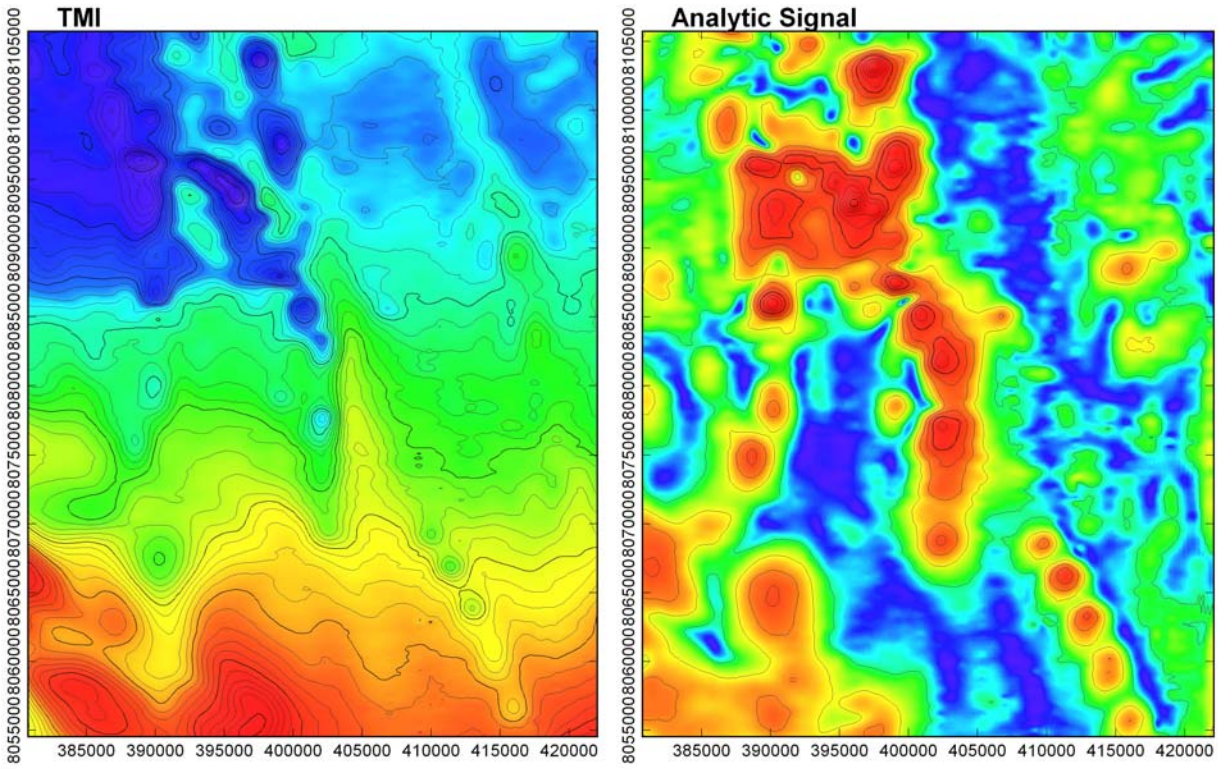

Figure A1_6 string of negative TMI anomalies in a linear trend (in the SE of the image).